

A PETROLOGIC STUDY OF THE
HYDROTHERMAL ALTERATION AND ORE MINERAL DEPOSITION
IN DRILL CORE SAMPLES FROM AGROKIPIA, CYPRUS

by

MONA BOTROS



DALHOUSIE UNIVERSITY

Department of Geology

Halifax, N.S. Canada B3H 3J5

Telephone (902) 424-2358 Telex: 019-21863

DALHOUSIE UNIVERSITY, DEPARTMENT OF GEOLOGY

B.Sc. HONOURS THESIS

Author: Mona BOTROS

Title: A PETROLOGIC STUDY OF THE HYDROTHERMAL ALTERATION AND ORE MINERAL DEPOSITION IN DRILL CORE SAMPLES FROM AGROKIPIA, CYPRUS

Permission is herewith granted to the Department of Geology, Dalhousie University to circulate and have copied for non-commercial purposes, at its discretion, the above title at the request of individuals or institutions. The quotation of data or conclusions in this thesis within 5 years of the date of completion is prohibited without permission of the Department of Geology, Dalhousie University, or the author.

The author reserves other publication rights, and neither the thesis nor extensive extracts from it may be printed or otherwise reproduced without the authors written permission.

Signature of author

Date:

April, 1983

COPYRIGHT 1983

Distribution License

DalSpace requires agreement to this non-exclusive distribution license before your item can appear on DalSpace.

NON-EXCLUSIVE DISTRIBUTION LICENSE

You (the author(s) or copyright owner) grant to Dalhousie University the non-exclusive right to reproduce and distribute your submission worldwide in any medium.

You agree that Dalhousie University may, without changing the content, reformat the submission for the purpose of preservation.

You also agree that Dalhousie University may keep more than one copy of this submission for purposes of security, back-up and preservation.

You agree that the submission is your original work, and that you have the right to grant the rights contained in this license. You also agree that your submission does not, to the best of your knowledge, infringe upon anyone's copyright.

If the submission contains material for which you do not hold copyright, you agree that you have obtained the unrestricted permission of the copyright owner to grant Dalhousie University the rights required by this license, and that such third-party owned material is clearly identified and acknowledged within the text or content of the submission.

If the submission is based upon work that has been sponsored or supported by an agency or organization other than Dalhousie University, you assert that you have fulfilled any right of review or other obligations required by such contract or agreement.

Dalhousie University will clearly identify your name(s) as the author(s) or owner(s) of the submission, and will not make any alteration to the content of the files that you have submitted.

If you have questions regarding this license please contact the repository manager at dalspace@dal.ca.

Grant the distribution license by signing and dating below.

Name of signatory

Date

TABLE OF CONTENTS

	Page
ABSTRACT	iii
ACKNOWLEDGEMENTS	v
CHAPTER 1: INTRODUCTION	1
1.1 Location of Study	1
1.2 Purpose of the Thesis	2
CHAPTER 2: GEOLOGIC SETTING	4
2.1 Regional Geology	4
2.2 Geology of the Agrokipia Area	6
2.3 History of Mining in the Agrokipia Area	8
CHAPTER 3: PETROLOGY/PETROGRAPHY	10
3.1 Summary of the Rock Sequence	10
a) CY-2 Core Summary	10
b) CY-2A Core Summary	11
3.2 Hand Specimen/Thin Section Study	13
a) CY-2 Samples	14
i) Relatively Fresh Basalt	14
ii) Partly Altered Basalt	15
iii) Pervasively Altered and Partly Mineralized Basalt	16
b) CY-2A Samples	17
i) Relatively Fresh Basalt	17
ii) Partly to Highly Altered and Highly Mineralized Basalt	19

	Page
iii) Pervasively Altered and Highly to Pervasively Mineralized Basalt	20
iv) Highly to Pervasively Altered and Partly Mineralized Basalt	22
3.3 Ore Mineralogy	24
CHAPTER 4: X-RAY DIFFRACTION ANALYSES	29
CHAPTER 5: MICROPROBE STUDIES	31
CHAPTER 6: DISCUSSION	35
6.1 Downhole Distribution of Primary and Secondary Minerals	35
a) CY-2 Core	35
b) CY-2A Core	37
6.2 Paragenetic Sequence of the Secondary Minerals	41
a) Paragenesis of the Clays, Chlorites and Micas in CY-2 and CY-2A	41
b) Paragenesis of the Ore Minerals in CY-2 and CY-2A	44
6.3 Probable Relative Temperatures of Alteration of a Number of Samples from Different Levels in the Cores	47
CHAPTER 7: SUMMARY	49
REFERENCES	52
APPENDIX 1: CY-2 Sample Descriptions	
APPENDIX 2: CY-2A Sample Descriptions	

ABSTRACT

The effects of hydrothermal alteration and ore mineralization were studied in 34 basalt drill core samples from the Agrokipia Cretaceous seafloor hydrothermal system in Cyprus. Transmitted and reflected light microscope, X-ray diffraction and electron microprobe techniques were employed to determine the variation of secondary minerals and textures with depth. The depth intervals examined were the 24.00 m to 92.85 m interval in hole CY-2 and the 136.70 m to 406.85 m interval in hole CY-2A. These intervals represent the most altered sequences of the cores.

The four stable secondary mineral assemblages which occur in the samples studied are:

- 1) smectite + green chlorite + minor quartz + hematite in relatively fresh to partly altered basalt (in CY-2 samples and in CY-2A between 136.70 m and 150 m)
- 2) chlorite (green and brown) + smectite + pyrite + sphalerite + chalcopyrite in highly mineralized and partly to highly altered basalt (CY-2A 150 m to 170 m)
- 3) illite + quartz + sphene + pyrite + hematite in highly to pervasively mineralized and pervasively altered basalt (CY-2A 170 m to 300 m)
- 4) abundant green and brown chlorite + albite + epidote + minor pyrite + trace sphalerite in partly mineralized and highly to pervasively altered basalt (CY-2A 300 m to 406.85 m)

With the exception of the 30 m to 60 m interval, it appears that hole CY-2 did not penetrate any hydrothermally altered basalts while the 150 m to 300 m interval in hole CY-2A represents the most intense hydrothermal activity.

Microprobe analyses revealed the occurrence of Mn-rich chlorite and calcite with the highest Mn content in the chlorite of sample CY-2 92.85 and the calcite of sample CY-2A 153.25. The MnO values of the chlorites in hole CY-2A appear to increase with depth while those of calcite decrease with depth. In all cases, the vesicle chlorites contained higher levels of MnO than the matrix chlorites.

ACKNOWLEDGEMENTS

I would like to express my gratitude to Dr. J.M. Hall for his valuable advice, encouragement and enthusiasm. Thanks are due to Dr. P.T. Robinson for providing samples at such short notice and for his help with some of the petrological aspects of the thesis.

Many of the XRD analyses were carried out by G. Lechiment and Dr. J. Lydon at the Geological Survey of Canada in Ottawa.

I benefitted greatly from discussions with K. Gillis, Dr. M. Zentilli, Dr. D.B. Clarke and Dr. J. Lydon.

Thanks are also due to G. Brown and M. Justino for thin section preparation, and to R. Mackay for guidance in the use of the electron microprobe. I would like to express my gratitude to D. Matheson for the drafting work, and to J. Barrett for typing the thesis at such short notice.

on the ancient sea floor (Constantinou and Govett, 1973). Fluid inclusion and strontium isotope studies have confirmed that modified seawater was the main ore-bearing fluid and that the hydrothermal alteration involved seawater-rock interaction (Spooner and Bray, 1977; Spooner et. al., 1977).

Recovery of drill core from the stockwork zone of a Cyprus massive sulphide deposit will permit a three-dimensional study of a convective hydrothermal system to determine the geological, chemical, and physical characteristics and parameters of a single circulation cell. The Agrokipia A ore deposit was chosen as the drilling site for CY-2 (figure 1, inset) because the massive sulphides had already been mined out so that the hole would start at the top of the stockwork zone and pass downward into the hydrothermally altered basalts. However, CY-2 did not penetrate extensively altered and mineralized basalts and therefore another attempt was made to intersect a stockwork zone, this time at the Agrokipia B deposit where hole CY-2A was drilled (figure 1, inset). CY-2A recovered approximately 550 m of hydrothermally altered basalts as evidenced by the pervasive alteration and mineralization of the CY-2A samples below 150 m depth.

1.2 Purpose of the Thesis

This thesis describes a petrologic study of drill core samples from the Agrokipia paleohydrothermal system using transmitted and reflected light microscopy, X-ray diffraction and electron microprobe

techniques. The study concentrates on the highly altered sequences of both CY-2 and CY-2A.

The variation of the alteration minerals and textures with depth will be examined to determine the paragenetic sequence of the secondary minerals, as well as stable secondary mineral assemblages.

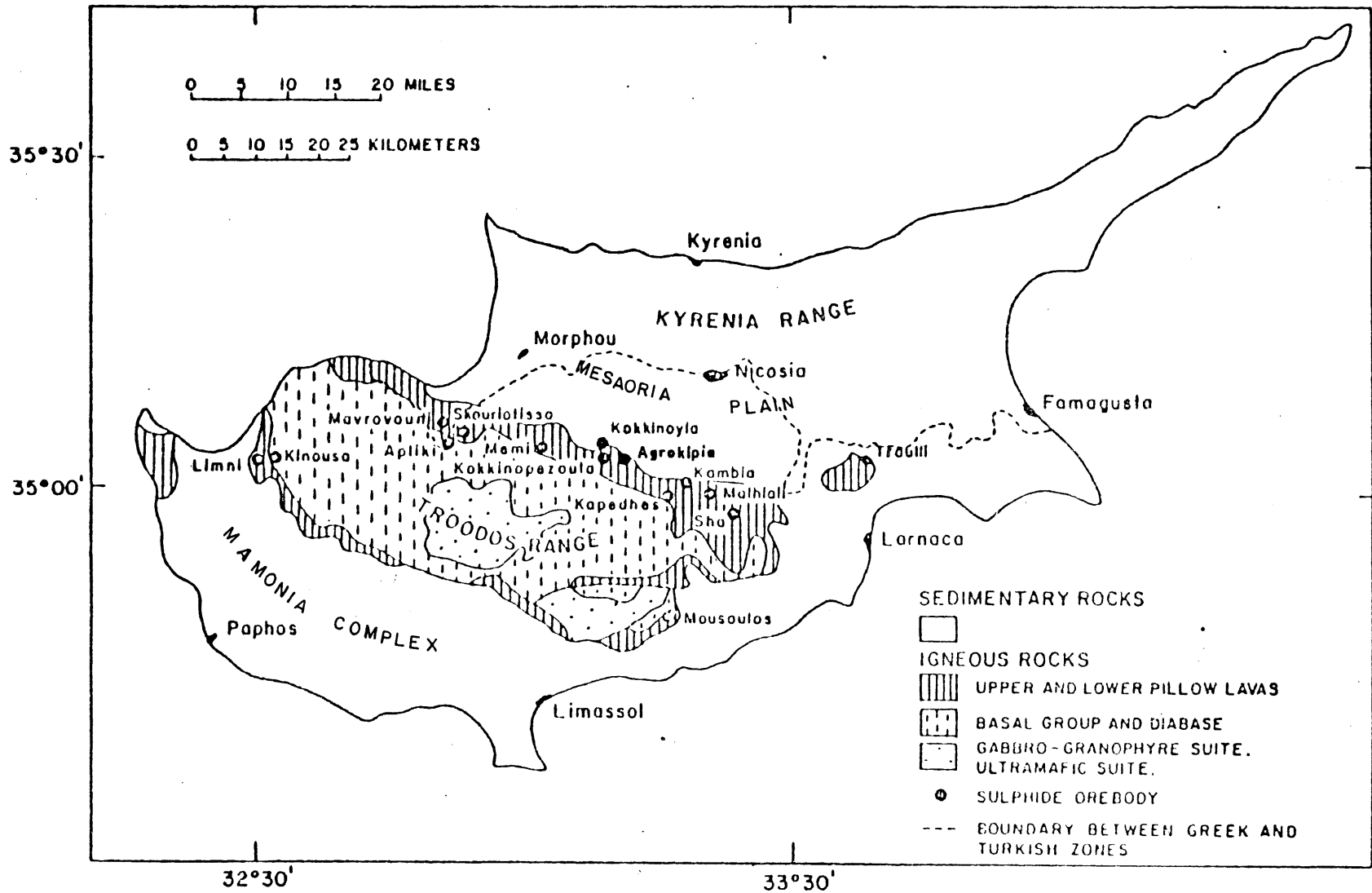


Figure 2. Index map of the Troodos massif, Cyprus.

Troodos Massif

The Troodos Massif occupies a roughly 3000 km² oval area in the southern part of Cyprus. A complete and relatively undeformed ophiolite sequence ranging upward from harzburgite tectonite to pyroxenites and dunites to cumulate gabbros, followed by a sheeted dyke complex, and finally pillow lavas overlain locally by manganoan sediments, is present (figure 3). A differential uplift of some 2000 m (DeVaumas, 1959, 1961; Gass and Masson Smith, 1963; Robertson, 1977) caused by a serpentinite diapir intrusion in the late Tertiary and subsequent erosion is responsible for the present outcrop pattern and domal structure of the Troodos complex. The original upward ophiolite sequence is now arranged in an outward succession (figure 2). The core of the plutonic complex is primarily occupied by harzburgite tectonite and minor lherzolite, mostly serpentized. They are either separated from gabbros by dunite or pyroxenite, or are faulted against them. The gabbroic rocks are extensively exposed and completely surround the ultra mafic core. They include olivine gabbros, pyroxene gabbros and uralite gabbros. Plagiogranites outcrop locally in some areas between gabbros and the sheeted dyke complex which covers the largest part of the surface area of the massif. This complex consists of a dense linear dike swarm often made up of virtually 100% diabase dikes displaying several phases of intrusion (Constantinou, 1980). The pillow lavas outcrop in the periphery of the Troodos massif and were divided into three groups by early workers of the Cyprus Geological Survey based on field relationships, local unconformable contacts and primary and secondary

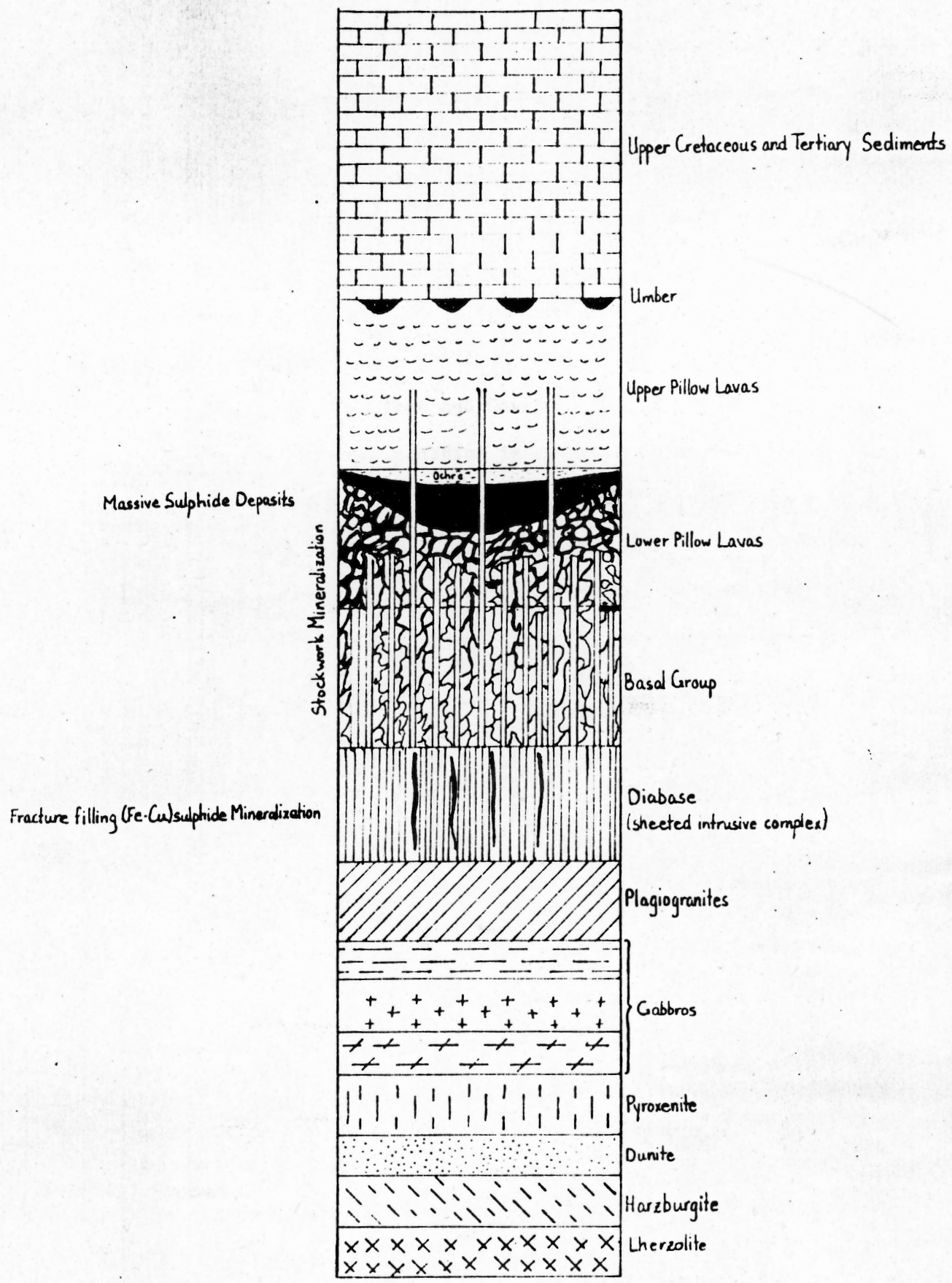


FIGURE 3. Stratigraphy of the Troodos ophiolite massif in the area of a locally occurring, typical massive sulphide deposit(modified after Constantinou, 1980).

petrological and chemical differences. In upward succession, the three pillow lava groups are the Basal Group (B.G.), the Lower Pillow Lavas (L.P.L.) and the Upper Pillow Lavas (U.P.L.).

The massive cupriferous sulphide deposits often occur at the contact between the L.P.L. and the U.P.L., but may also be found higher or lower in the sequence (figure 3). The ore bodies are generally lenticular in shape suggesting formation in fault controlled basins on the sea floor (Constantinou and Govett, 1973; Adamides, 1975).

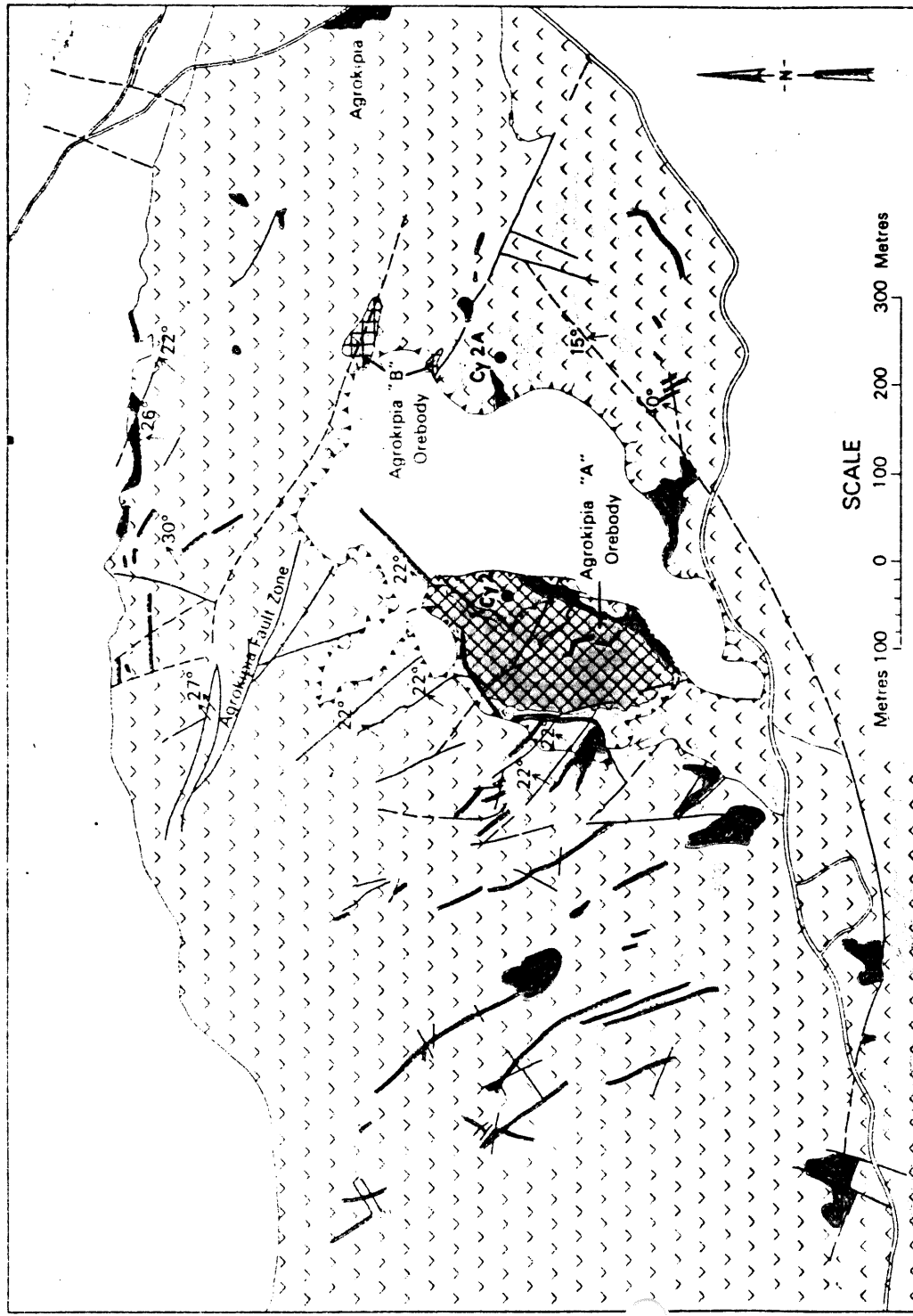
A general vertical zonation is apparent in the ore bodies and is characterized by massive ore with more than 40% S, underlain by a sulphide-silica zone with 30-40% S, and followed by a stockwork zone containing less than 30% S (Constantinou, 1980). Many cupriferous sulphide deposits are overlain by ochre, a manganese-poor, iron-rich sediment believed to have formed by sea-floor oxidation of the sulphides (Constantinou, 1980).

2.2 Geology of the Agrokipia Area

Geographically, the Agrokipia area is located 23 km southwest of Nicosia by road and, together with the adjacent Mitsero area, comprises the Tamasos Mining District, one of five mining districts in Cyprus. Of the five ore bodies occurring in this district, two, the Agrokipia A and the Agrokipia B, are located in the area (figure 4).

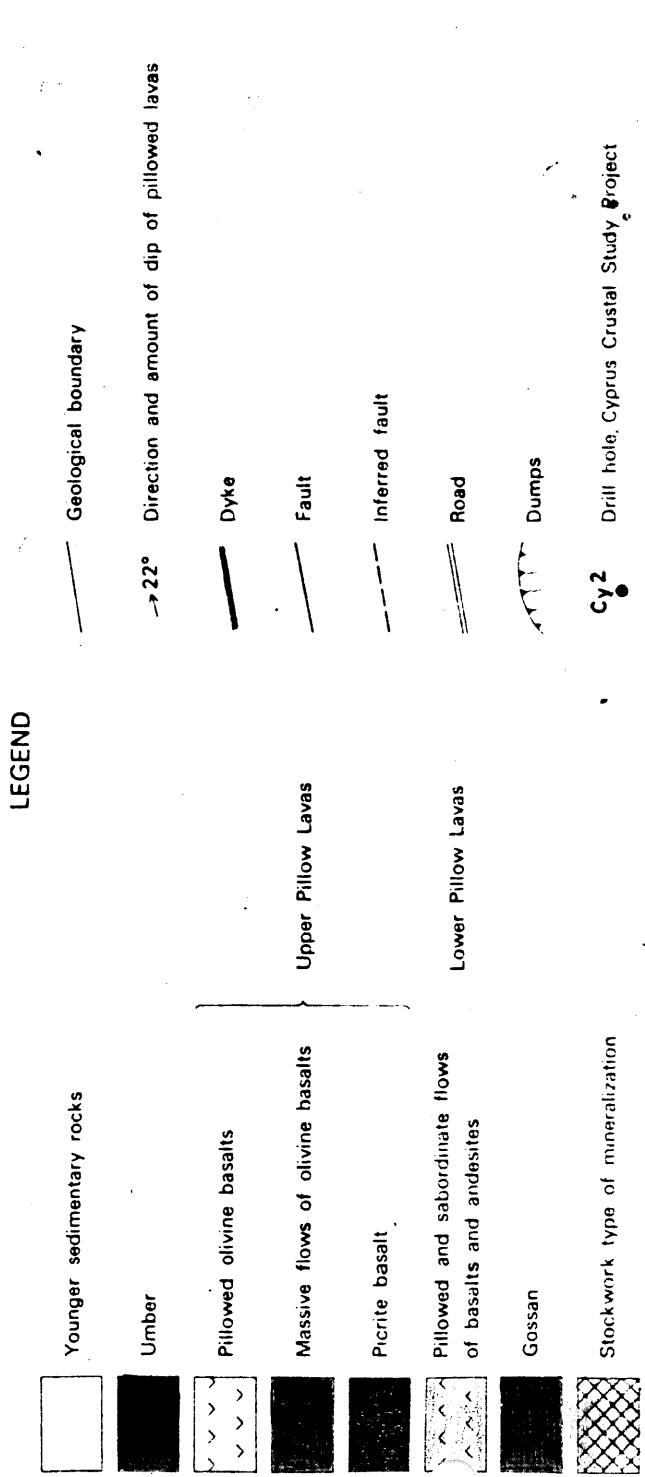
Geologically, Agrokipia is located in the pillow lava sequence close to the contact with the overlying Upper Cretaceous and Tertiary sediments. The sediments occur in unconformable contact with the

FIGURE 4. GEOLOGICAL MAP OF THE AGROKIPIA AREA



Drawn by Geological Survey Department, Cyprus 1982

After D.L. Searle and A. Pansyiotou, 1965



Upper Pillow Lavas and dip northward at 25° to 30°. The basal sediment unit is referred to as umber, a manganese-rich, iron-rich sediment which occurs as sporadic lenses in depressions on the Upper Pillow Lava surface (figures 3 and 4).

The U.P.L. are olivine-rich basalts occurring primarily as pillows with minor flows and intrusive dikes. The U.P.L. unconformably overlie the L.P.L., which are primarily oversaturated basalts and andesites with a high proportion of dikes and massive flows. Locally, but not at Agrokipia, the contact between the two pillow lava units is unconformable and is marked by a thin band of Mn-poor, Fe-rich ochre.

The Agrokipia Fault zone is the main fault structure in the area. The fault zone ranges in width between 30 and 100 m and trends about 300°. The Agrokipia B orebody is generally confined within the boundaries of the zone. The top of the mineralization occurs within the L.P.L. approximately 150 m below the contact with the U.P.L., and between 100 m and 200 m below the surface. This deposit is cut by several post-mineralization dikes which strike E-W and dip to the north at 70° (Bear, 1960). The massive ore was erratic in both grade and occurrence but had an average copper content of up to 4% and an average zinc content of up to 8% (Searle, 1972). In addition to chalcopyrite and sphalerite, the deposit contained minor amounts of tennantite and galena. The reserves at Agrokipia B are estimated to be 5.7 million tons assaying at less than 0.5% Cu and 20% S. The massive ore was mined out between 1958 and 1964.

The Agrokipia A deposit comprised two massive lenses, the northern and southern, which merged a few metres below the surface. This deposit was mined by opencast methods as the overburden ranged from a thin gossan covering the southern orebody to 30 m of U.P.L. over the northern orebody (Bear, 1963; Searle, 1972). The northern lens consisted of about 65,000 tons of sulphide ore assaying 30% sulfur, 1% copper and minor zinc. The southern, low-grade orebody consisted of 700,000 tons of ore with less than 30% sulfur and about 0.5% copper.

The contact between the Agrokipia A ore zone and the overlying massive lava flow dips to the northeast at 22°.

Two unmineralized diabase dikes cut the Agrokipia A orebody (Castaneda et.al., unpublished report, 1982). The dikes are 1.0 and 1.5 m thick and display chilled margins. Their trend of 320° and their dips of 55° and 75° to the northeast are consistent with the attitude of most dikes in the area.

2.3 History of Mining in the Agrokipia Area

Mining and smelting activities began in ancient times in the Tamasos Mining District as evident from the large accumulations of primitive slag heaps. Archaeologists believe that mining operations declined around the fourth century A.D. as a result of the fall of the Roman Empire. Serious prospecting in the Agrokipia area was not resumed until 1936. In 1950-51, results from geophysical prospecting techniques, together with drilling information, uncovered the Agrokipia A orebodies. Open-pit mining operations began in 1951 and

continued until 1960. Only about 300,000 tons of the estimated 765,000 tons of reserves were mined (Table 1, I.C.R.D.G., 1983, in press).

Table 1. Production from Agrokipia Mines

	Agrokipia A	Agrokipia B
	<u>1951-1960</u>	<u>1958-1964</u>
Ore Mined	332,838 tons	74,074 tons
Pyrite Produced	134,197 tons	65,398 tons

In 1957, drilling was carried out on a gravity anomaly to the east of the Agrokipia A deposit in an area devoid of any surface indications in the form of gossans. This revealed the presence of the Agrokipia B orebodies at depth. The orebodies were mined by sublevel stoping methods between 1958 and 1964, during which time only about 74,000 tons of the 5.7 million tons of reserves were mined.

CHAPTER 3

PETROLOGY/PETROGRAPHY

3.1 Summary of the Rock Sequence3.1a CY-2 Core Summary

Hole CY-2, drilled into the Agrokipia A pit penetrated 86 m of partly altered extrusives followed by 28 m of less altered lavas and finally by 112 m of relatively fresh basalt (figure 5, I.C.R.D.G., 1983, in press). Pillowed and massive flows occur in the first 86 m of extrusives. Pyrite is found primarily as disseminations in this interval although it was observed filling fractures in CY-2 at 48.05 m. Intense argillic alteration around 48.05 m has produced a light to medium gray coloured rock. The rest of the interval has undergone smectite-style alteration characterized by the occurrence of smectite- and zeolite-group alteration minerals.

The underlying, less altered interval consists primarily of massive flows with some pillows. Smectite-style alteration is present in the upper part of this zone, grading to a celadonite-jasper style of alteration to 114 m. Pyrite as vesicle fillings in this interval marks the base of the Agrokipia A mineralization.

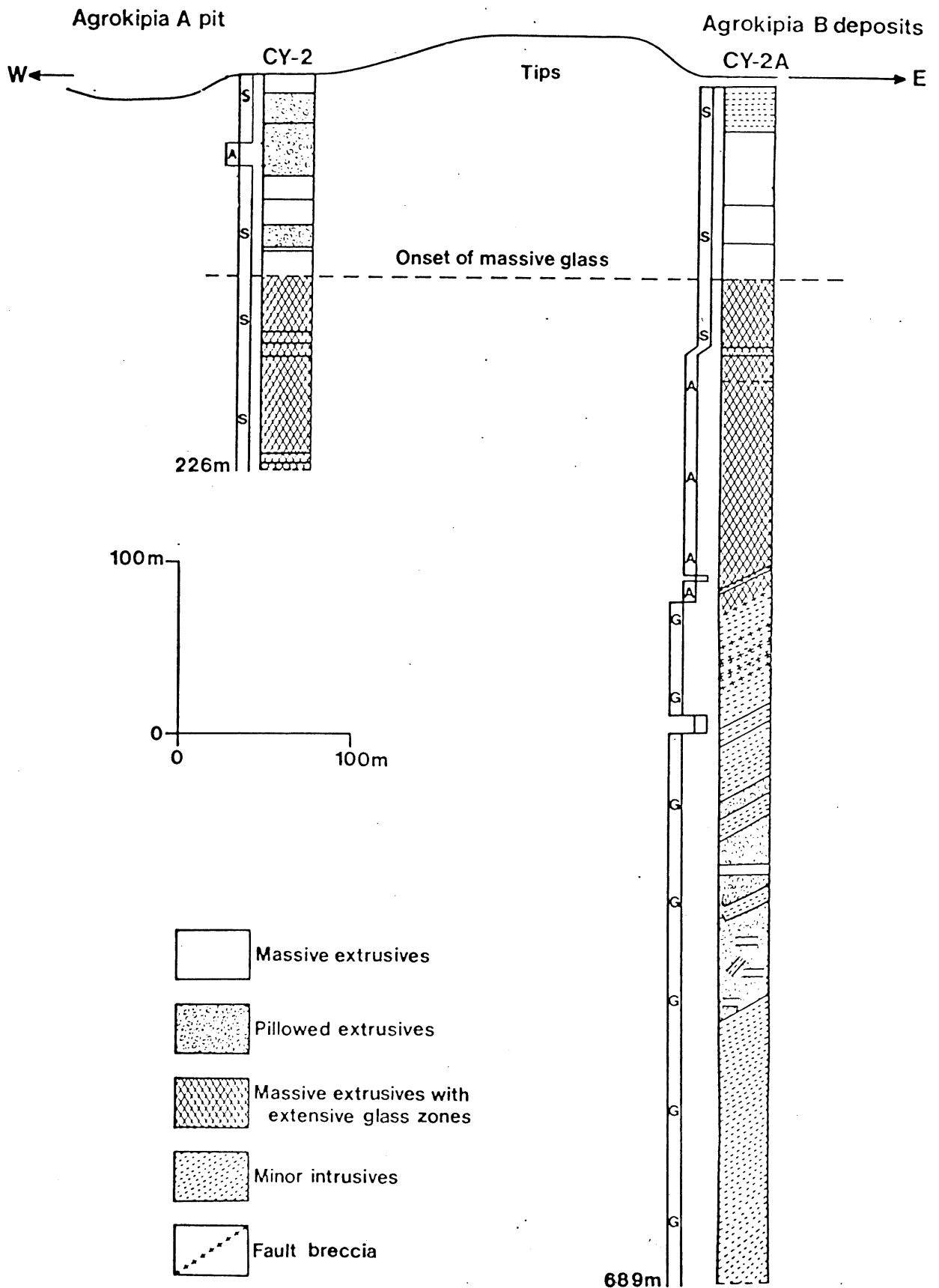


FIGURE 5. Downhole lithologies and alteration styles in drill core samples from CY-2 and CY-2A. The column to the left of the cores displays the alteration style, with greater distance from the core indicating greater temperature and pressure conditions of metamorphism. S= alteration to smectite- and zeolite-group minerals. A= argillic alteration characterized by the presence of quartz, illite and abundant pyrite. G= greenschist style alteration as indicated by abundant chlorite as well as epidote, albite and pyrite (modified from I.C.R.D.G., 1983).

The remaining 112 m of the section comprise a relatively fresh sequence of alternating grey-brown, aphyric, vesicular massive basalts and dark brown basaltic glasses. The glass zones make up 17% of this interval. The green celadonite-red jasper style of alteration characteristic of the lower part of the interval to 114 m, continues to 146 m. The basalts in the remainder of the core have been altered to clays, zeolites, and quartz.

3.1b CY-2A Core Summary

Hole CY-2A, located adjacent to the Agrokipia B deposit, penetrated 4 or 5 main lithological units on which are superimposed a range of alteration styles (figure 5). The first 109 m of the section consists of a sequence of grey-brown, thick, massive basaltic or basaltic andesite flows which are difficult to differentiate into cooling units.

At 109 m, extensive basaltic glass zones appear which are similar to those appearing in CY-2 at about this level. The glass is black or dark brown where fresh and off-white where it has undergone pervasive argillic alteration. The glass zones alternate with zones of slightly vesicular, aphyric, grey-brown basalt. The contacts between the two rock types are gradational over a distance of about 2 cm. This alternating sequence of glass and massive basalt becomes highly altered at approximately 150 m but is inferred to continue to 291 m. The first evidence of intense hydrothermal alteration appears at 153 m in the form of mineralized veins and vesicles. The intense argillic

style of alteration has produced altered basalts which are light grey in colour and physically hard relative to the glass which has become cream-coloured and very soft. Economic mineralization is most intense between 154 and 290 m. Pyrite, sphalerite and lesser chalcopyrite occur in veins, vesicles and as disseminations together with thick, vein-like masses of quartz, hematite and pyrite.

At 283 m, thin dikes appear to intrude the deepest of the altered glass lavas and by 297 m dikes have completely replaced the alternating glass-basalt sequence. Evidence of multiple dike intrusion is provided by the presence of chilled margins. These are recognizable by the replacement of glass zones by chlorite. Both medium-grained diabase dikes and aphanitic dikes are present. The dikes usually show an argillic style of alteration followed by a propylitic style which appears at about 300 m and is characterized by abundant green chlorite, albite, and epidote. More readily recognizable greenschist facies conditions prevail below this depth.

At close to 400 m, the sequence of dikes is replaced by a series of pillows and pillow breccias interrupted by dikes. The dikes constitute about one quarter of the section between 400 m and 580 m. From this depth to the base of the hole the sequence consists entirely of dikes. The propylitic alteration style which first appeared at about 368 m, continues in this interval to the base of the hole at 689 m.

3.2 Hand Specimen/Thin Section Study

The sample numbers represent the depth in metres in the core. The classification of the samples according to the level of alteration is qualitative and is based on the degree of alteration of the plagioclase microlites since most samples are aphyric. Thus in a relatively fresh basalt most microlites are euhedral and unaltered (plate 1). A partly altered basalt contains plagioclase microlites which have undergone some alteration ($\leq 60\%$) and are subhedral (plate 2). If the microlites are extensively altered ($>60\%$ alteration) then the sample is classified as a highly altered basalt (plate 3). In a pervasively altered basalt the plagioclase microlites are completely pseudomorphed by chlorite and/or smectite and/or quartz and/or illite. In most pervasively altered basalts the original outline of the microlites is retained and a relict igneous texture is still present (plate 4), however, in some cases the plagioclase habit is completely obliterated and no relict igneous texture is recognizable (plate 5).

The classification of the samples according to the degree of mineralization is also only semi-quantitative and is based on the proportion of ore minerals in the matrix and the degree of mineralization of the veins and vesicles. A partly mineralized basalt has a minor proportion of ore minerals in the matrix (5 to 10%) and minor sulphides are present in either the veins, or both the veins and the vesicles. A highly mineralized basalt contains subordinate quantities of ore minerals in the matrix ($>10\%$ to 20%) and a significant proportion of either the veins, or both the veins and the vesicles consists

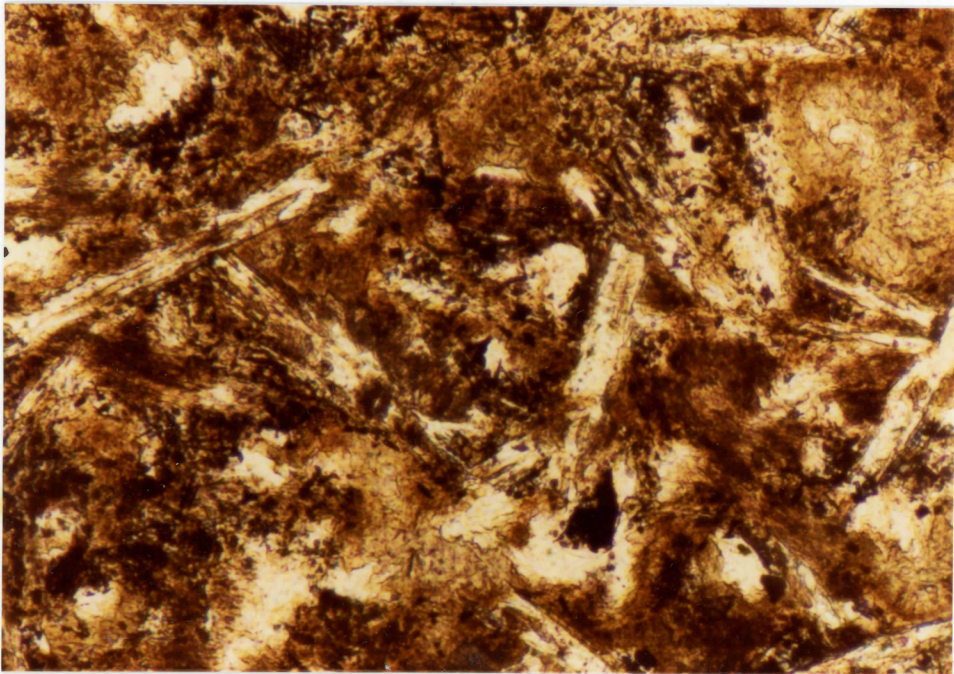
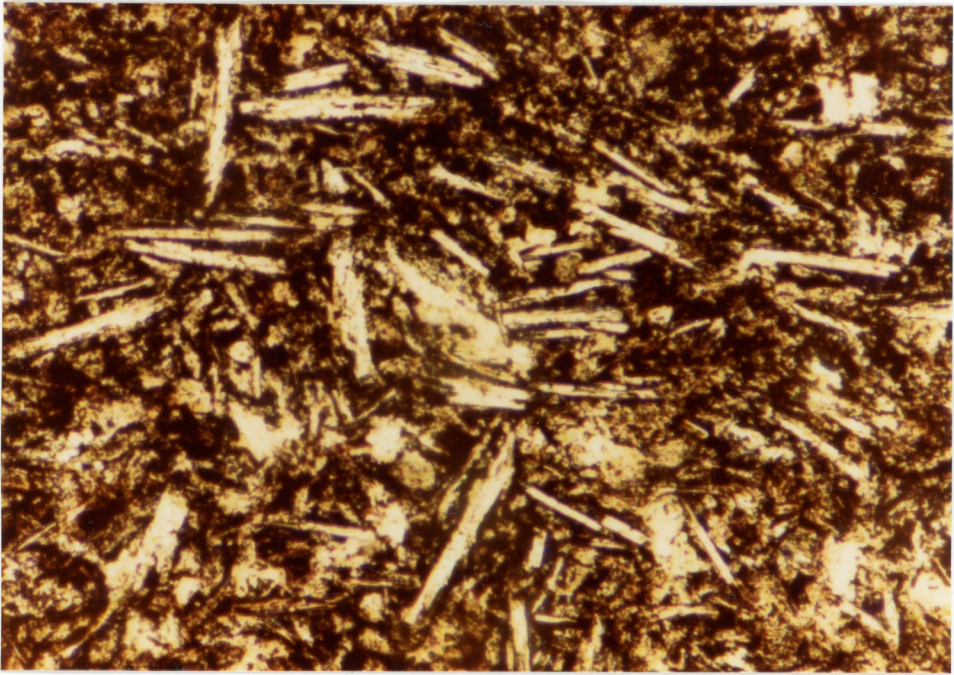


PLATE 1: CY-2 92.85 m. Relatively fresh basalt with euhedral plagioclase microlites. Magnification: 10 X 1.6 X 8.

PLATE 2: CY-2 24.00 m. Partly altered basalt with subhedral plagioclase microlites partly altered to chlorite and smectite.
Magnification: 10 X 1.6 X 8.

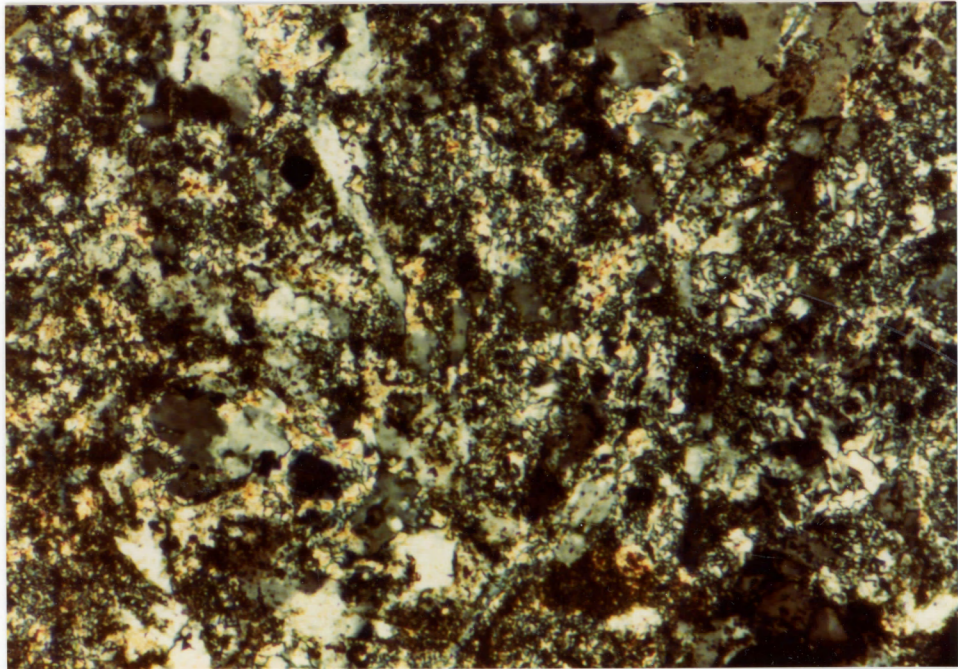


PLATE 3: CY-2A 270.15 m. Plagioclase laths highly altered to illite.
Magnification: 10 X 1.6 X 8. Crossed nicols.

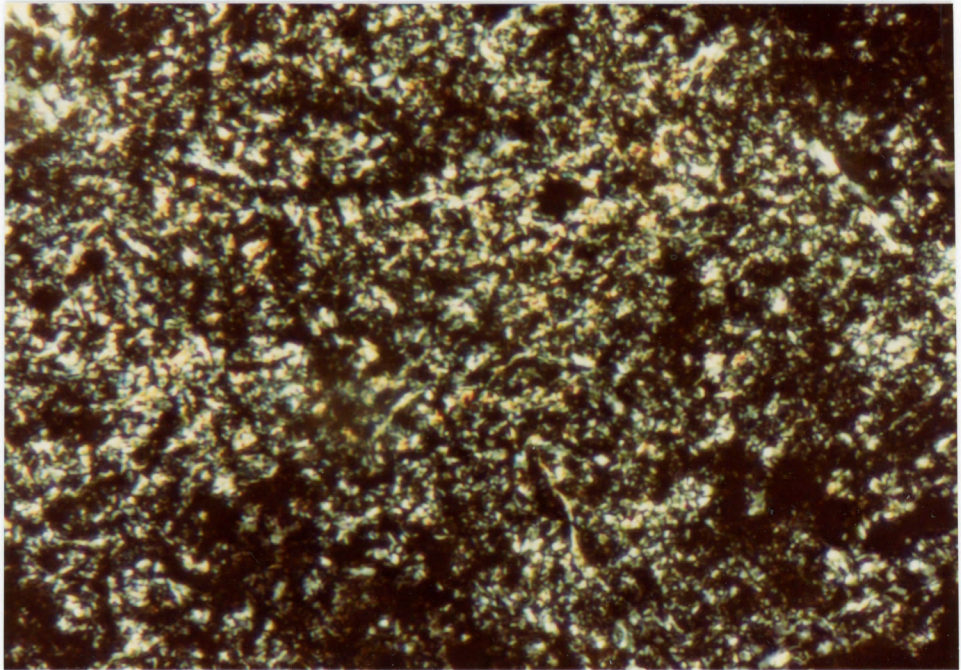
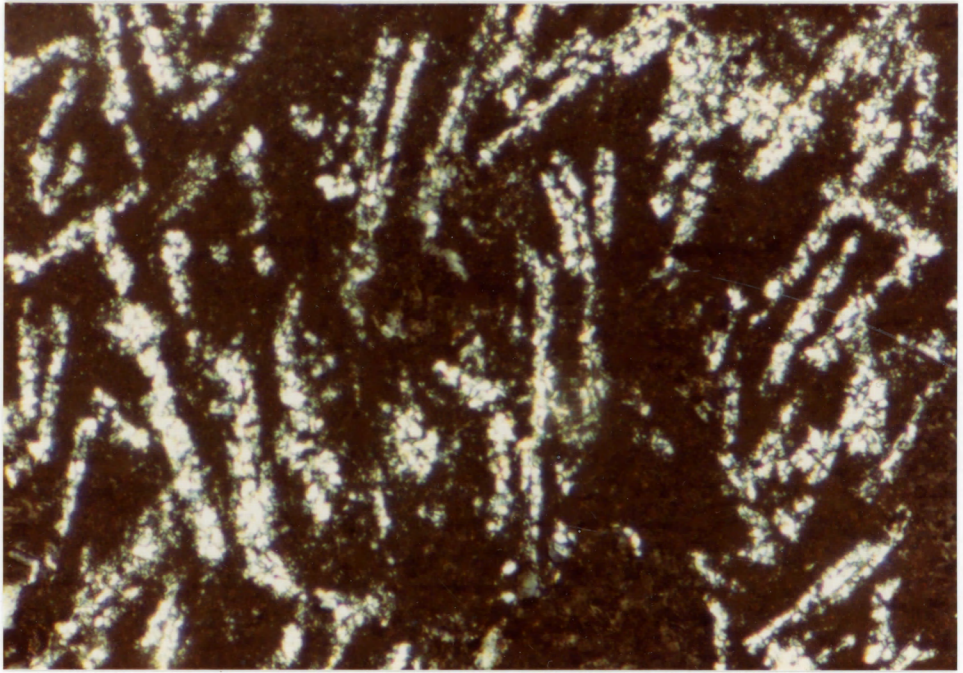


PLATE 4: CY-2A 243.05 m. Pervasively altered basalt with plagioclase microlites completely pseudomorphed by illite. Relict intersertal texture is preserved. Magnification: 10 X 1.6 X 8. Crossed nicols.

PLATE 5: CY-2A 243.05 m. Pervasively altered basalt with no recognizable relict igneous texture. Plagioclase microlites are completely altered to illite. Magnification: 10 X 2.0 X 8. Crossed nicols.

of ore minerals. Sulphides are a major component (>20% of the matrix in a pervasively mineralized basalt. Samples in which highly mineralized veins and/or vesicles comprise at least 25% of the sample are also classified as pervasively mineralized even though the proportion of ore minerals in the matrix may be less than 20%.

3.2a CY-2 Samples

Eight samples were examined from the upper, most altered section of the CY-2 core. Only one sample is pervasively altered while five are partly altered and the two deepest samples are relatively fresh (table 2). Detailed descriptions of the samples appear in Appendix 1.

(i) Relatively Fresh Basalt (CY-2 92.30 m and 92.85 m): The two relatively fresh samples come from the same pillowed basalt unit in CY-2. They consist of brecciated, glassy basalts with a hyalophitic texture. The major components of the matrix are green and brown smectites and relatively fresh labradorite microlites (plate 1). A minor proportion of the microlites, as well as several phenocrysts, have undergone slight alteration to green, anhedral chlorite which is a subordinate component of the matrix. Scattered, fine-grained, anhedral quartz is a trace component of the matrix. Very fine-grained primary anhedral pyrite, subhedral magnetite grains and euhedral ilmenite laths are disseminated in the matrix. Very fine-grained sphalerite may also be present in CY-2 at 92.85 m.

Table 2: CY-2 Sample Descriptions

The sample numbers represent the depth in meters in the core. M=major component(>20%), S=subordinate component (>10-20%), m=minor component(5-10%), t=trace component(<5%). These symbols apply to the matrix mineralogy. The vein and vesicle minerals are simply written in order of decreasing abundance.

Sample	Description	Core Unit	Texture	% Vesicles	Vesicle Minerals	% Veins	Vein Minerals	Smectite	Chlorite	illite	Calcite	Quartz	Plagioclase	Sphene	Epidote	Hematite	Magnetite	Ilmenite	Pyrite	Sphalerite	Chalcopyrite	Others
24.00	Partly altered basalt	II: pillowed lava	hyalophitic	4	quartz chlorite	<1	quartz	M	M			S	S				m	m	t	t		
48.05	Pervasively altered and partly mineralized basalt	III: pillowed lava	relict hyalophitic	4	quartz	3	chlorite pyrite hematite		S	m		M					m		m			
76.70	Partly altered basalt	V: massive flow	intersertal	5	chlorite quartz calcite	1	hematite	M	M		t	S	M				m		t			
79.63	Partly altered basalt	V: massive flow	intersertal	4	chlorite quartz calcite	1	quartz calcite	S	M		m	S	M				m		t			
82.50	Partly altered basalt	V: massive flow	intersertal			5	hematite quartz chlorite	S	M		m	S	M				m		t			
84.15	Partly altered basalt	V: massive flow	intersertal	8	smectite chlorite quartz pyrite hematite	5	smectite chlorite quartz pyrite	M	M			S	S				m		t			iddingsite, t
92.30	Highly brecciated, relatively fresh, glassy basalt	VI: pillowed lava	hyalophitic	3	chlorite quartz	20	quartz hematite chlorite pyrite	M	S			t	M				t	t				anastase, t
92.85	Somewhat brecciated, relatively fresh, glassy basalt	VI: pillowed lava	hyalophitic	5	chlorite quartz	10	chlorite quartz hematite	M	S			t	M				t	t	t	t		

The vesicles are filled with two phases of chlorite and quartz. Lining the vesicles is an anhedral, olive-green chlorite which is optically indistinguishable from the chlorite in the matrix. This is followed by a layer of quartz and a core of chlorite, or directly by a core of subhedral, bluish-green flakes of chlorite (plate 6). The chlorite in the core has a higher birefringence than the chlorite lining the vesicles. The quartz, where present, occurs as fine, anhedral grains between the two varieties of chlorite.

The fractures comprise a significant portion of the sample (10-20%) and are filled with mixtures of chlorite, quartz, botryoidal hematite, and minor fine-grained pyrite. The hematite also displays colloform textures and appears to be a later phase.

(ii) Partly Altered Basalt (CY-2 24.00 m and 76.70 m to 84.15 m):
Four of the partly altered basalt samples belong to the same massive flow unit and have an intersertal texture while the shallowest sample is a pillowed basalt with a dominantly hyalophitic texture. Chlorite, plagioclase (probably labradorite), and smectite are the dominant matrix minerals, while quartz occurs in subordinate quantities. The plagioclase microlites are partly altered to chlorite and green or brown smectite. Chlorite and calcite are replacement minerals of occasional plagioclase phenocrysts. Chlorite is present as fine-grained, anhedral patches or as very fine-grained subhedral flakes, sometimes arranged in radial structures. Quartz occurs as fine, anhedral, isolated grains or as aggregates which appear to be replacing primary phenocrysts of plagioclase. The primary igneous ore minerals are minor to trace, disseminated,

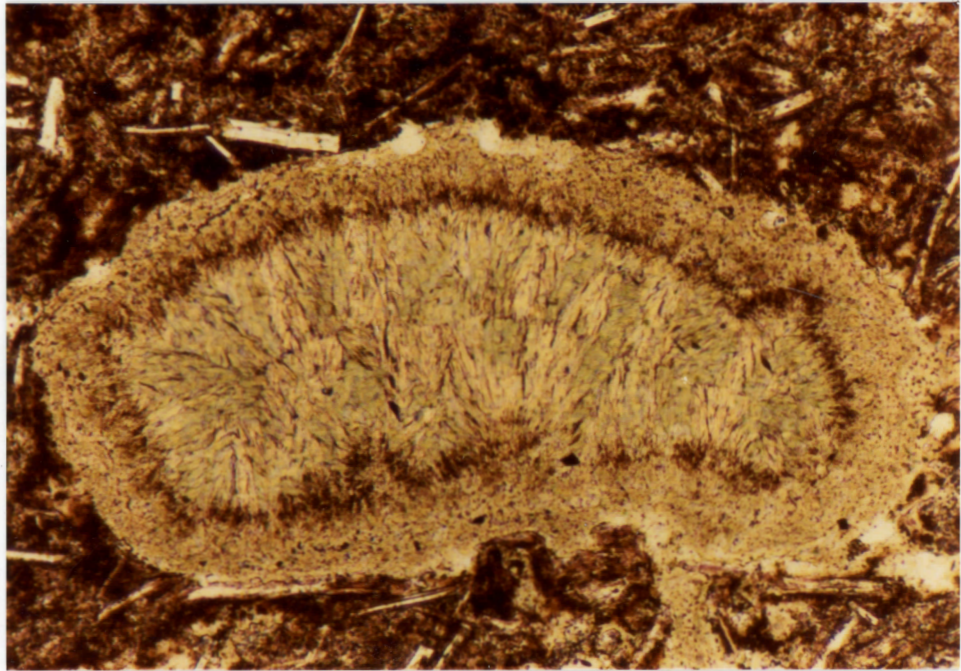


PLATE 6: CY-2 92.85. Two varieties of chlorite in vesicle. Blue-green, relatively Mn-rich flakes of chlorite in core. Olive-green, relatively Mn-poor anhedral chlorite at margin of vesicle. Magnification: 10 X 1.6 X 8.

grained components of the matrix and consist of anhedral pyrite, subhedral and skeletal magnetite, and euhedral ilmenite.

Chlorite, quartz, calcite, and in one sample smectite and secondary pyrite, fill vesicles which comprise minor portions of the sample. Quartz, chlorite, calcite, smectite, and hematite fill small fractures which form an insignificant proportion of the sample.

(iii) Pervasively Altered and Partly Mineralized Basalt
(CY-2 48.05 m):

Only one sample of those studied from Hole CY-2 is pervasively altered and partly mineralized. CY-2 48.05 m consists of pillowed basalt with relict hyalophitic texture. The plagioclase microlites have been completely replaced by chlorite and quartz. Unlike the relatively fresh and partly altered samples, the pervasively altered basalt contains no smectite. The major components of the matrix are quartz and chlorite with quartz comprising about 60% of the matrix and chlorite about 20%. Chlorite occurs as very fine-grained anhedral patches or as subhedral flakes replacing primary pyroxene and/or olivine phenocrysts. Quartz is present as fine, isolated, anhedral grains or as aggregates of quartz grains replacing primary olivine (?) and plagioclase phenocrysts. A minor amount of illite is present as a replacement mineral of plagioclase laths. Very fine-grained primary pyrite and cryptocrystalline magnetite are disseminated in the matrix, while secondary fine-grained pyrite is concentrated in vesiculated areas of the matrix adjacent to veins. The ore minerals comprise a minor proportion of the matrix.

Approximately 4% of the sample consists of vesicles filled with quartz whose grain size increases from the rim towards the core.

Two varieties of chlorite occur as separate phases in the veins. One variety has anomalous blue birefringence and lines the veins while the interior is comprised of chlorite with very dark-grey birefringence. Occasionally, minor secondary pyrite is present in the core. A pyrite and iron-oxide/chlorite vein was observed in the hand sample only.

3.2b CY-2A Samples

The 26 samples examined from the most altered section of hole CY-2A can be grouped into four categories: a short interval (samples 136.70 m and 141.45 m) of relatively fresh basalt, followed by a short section (samples 152.90 m to 161.19 m) of partly to highly altered and highly mineralized basalt. This grades into a long interval (samples 173.66 m to 285.05 m) of pervasively altered and highly to pervasively mineralized basalt which is underlain by another long section (samples 302.35 m to 406.85 m) of highly to pervasively altered and partly mineralized basalt. Abbreviated descriptions of the CY-2A core samples are shown in table 3 while more detailed descriptions appear in Appendix 2.

(i) Relatively Fresh Basalt (CY-2A 136.70 m and 141.45 m):

Although the two samples belong to different lithologies - 136.70 m is a massive glass while 141.45 m is a massive crystalline basalt - they exhibit similar alteration styles in that the dominant alteration minerals are smectites.

Table 3: CY-2A Sample Descriptions

The sample numbers represent the depth in meters in the core. M=major component(>20%), S=subordinate component (>10-20%), m=minor component(5-10%), t=trace component(<5%). These symbols apply to the matrix mineralogy. The vein and vesicle minerals are simply written in order of decreasing abundance.

Sample	Description	Core Unit	Texture	% Vesicles	Vesicle Minerals	% Veins	Vein Minerals	Smectite	Chlorite	Illite	Calcite	Quartz	Plagioclase	Sphene	Epidote	Hematite	Magnetite	Ilmenite	Pyrite	Sphalerite	Chalcopyrite	Others
136.70	Fresh, vesicular, massive glass	VI: massive glass	perlitic fractures	20	smectite gypsum zeolite	8	smectite	M											t			fresh glass, M
141.45	Relatively fresh basalt	VI: massive crystalline basalt	intersertal	5	quartz	8	quartz smectite celadonite	M	m			t	S			t	m	t				celadonite, S
152.90	Partly altered and highly mineralized basalt	VII: massive lava with hydrothermal veins	hyalophitic	8	quartz pyrite sphalerite chalcopyrite chlorite	<1	sphalerite pyrite quartz calcite chalcopyrite	M	M			m	S						m	m	t	
153.10	Partly altered and highly mineralized glassy basalt	VII: massive lava with hydrothermal veins	hyalophitic	8	calcite quartz sphalerite pyrite chalcopyrite	25	quartz sphalerite pyrite calcite laumontite	M	M			m	m						m	m	t	t laumontite in vein
153.25	Partly altered and highly mineralized glassy basalt	VII: massive lava with hydrothermal veins	hyalophitic	20	quartz pyrite sphalerite chlorite	25	quartz sphalerite pyrite	M	M	m	t	t	m						m	m	t	
156.91	Highly altered and mineralized basalt is cut by a large qtz-pyr-calc vein	VIIIa: massive lava	hyalophitic			97	quartz pyrite calcite chlorite	S	M			t	t	m					m	t		

Sample	Description	Core Unit	Texture	% Vesicles	Vesicle Minerals	% Veins	Vein Minerals	Smectite	Chlorite	Illite	Calcite	Quartz	Plagioclase	Sphene	Epidote	Hematite	Magnetite	Ilmenite	Pyrite	Sphalerite	Chalcopyrite	Others	
270.15	Highly altered and mineralized basaltic glass	VIIIb: massive glass	relict hyalophitic	10	quartz pyrite	5	quartz pyrite		M	S		M	t	S	t				m				
272.70	a small qtz.-pyr. vein crosscuts a qtz-hematite-pyrite vein (described in matrix columns since it comprises 92% of sample)	VIIIb: massive lava				8	quartz pyrite hematite calcite		t	t		M			t	M			S				gypsum, t
277.40	Pervasively altered basalt	VIIIb: massive lava	relict hyalophitic	5	quartz chlorite pyrite	<1	quartz pyrite		S	M		M		S	t				t				
282.45	Highly altered and partly mineralized olivine-phyric basalt	IX: post-mineralization dike	porphyritic hyalophitic	<1	quartz calcite			M	M	m	m	t	m		t		m		m				actino- lite(?), t
285.05	Pervasively altered and mineralized basaltic glass is cut by a large qtz-hem-pyr vein which is in turn cut by a pyrite vein	X: massive glass	no relict igneous texture	10	chlorite pyrite	>38	quartz pyrite hematite sphale- ite		M	M				M					m				anatase, m
302.35	Pervasively altered basalt	XI: altered dike	relict hyalophitic	<1	quartz illite chlorite pyrite	1	calcite illite pyrite		M	m	t	M	t	m	t				t	t			anatase, t
332.85	Highly altered and partly mineralized basalt	XI: altered dike	relict hyalophitic	2	quartz chlorite pyrite	1	pyrite chlorite	m	M	m	t	m	S	S	t				m				
350.45	Highly altered and partly mineralized basalt	XI: post-mineralization dike	relict intersertal	3	quartz chlorite calcite	2	chlorite calcite pyrite	M	M		m	m	t	m	t		m		m				

Sample	Description	Core Unit	Texture	% Vesicles	Vesicle Minerals	% Veins	Vein Minerals	Smectite	Chlorite	Illite	Calcite	Quartz	Plagioclase	Sphene	Epidote	Hematite	Magnetite	Ilmenite	Pyrite	Sphalerite	Chalcopyrite	Other
368.02	Pervasively altered basalt	XII: post-mineralization dike	hyalophitic					S	M	m	t	m	m		t		m		t			
386.40	Pervasively altered and partly mineralized basalt	XIII: altered dike	hyalophitic	4	quartz				M			S	S	m	m				t	t		
404.40	Pervasively altered hyaloclastite breccia	XIV: glass	highly fractured	25	quartz chlorite	15	quartz chlorite pyrite sphalerite		M			m	m						m	t	t	
406.85	Highly altered, partly mineralized, and highly fractured basaltic glass	XIV: pillowed lava	relict hyalophitic	<1	quartz pyrite	5	quartz pyrite chlorite smectite		M			m	t	M	m				m	m		

The fresh, vesicular basaltic glass in CY-2A 136.70 m is altered only around the vesicles which comprise approximately 20% of the sample (plate 7). Tan-yellow to rust-yellow smectite(s) fill the hairline fractures which make up approximately 8% of the sample. The same clay mineral, or mixture of clay minerals, fills most of the vesicles and forms a colloform ring around all of them. Minor vesicle-filling minerals are fine-grained, colourless, euhedral gypsum laths and a beige-brown zeolite mineral. Trace, anhedral, very fine-grained primary pyrite is scattered throughout the fresh glass. The fractures in the glass are dominantly perlitic, formed by cooling and subsequent contraction of the glass. The sample has evidently undergone little, if any, brecciation and is therefore described as a massive glass.

CY-2A 141.45 m is texturally similar to the relatively fresh basalts in hole CY-2, however it differs mineralogically in that it contains only minor amounts of chlorite. The dominant alteration minerals are green and brown smectites. Bright, forest-green spicules of celadonite fill interstices between labradorite microlites and comprise a subordinate proportion of the matrix. The generally unaltered, subhedral to euhedral labradorite microlites also comprise a subordinate proportion of the matrix. Green chlorite is a minor component, present as fine-grained subhedral laths to very fine, anhedral grains. Trace anhedral quartz grains are scattered in the matrix while trace amounts of anhedral hematite are concentrated adjacent to veins and vesicles. Magnetite, and lesser ilmenite, are minor, disseminated components of the matrix and are cryptocrystalline to fine-grained.

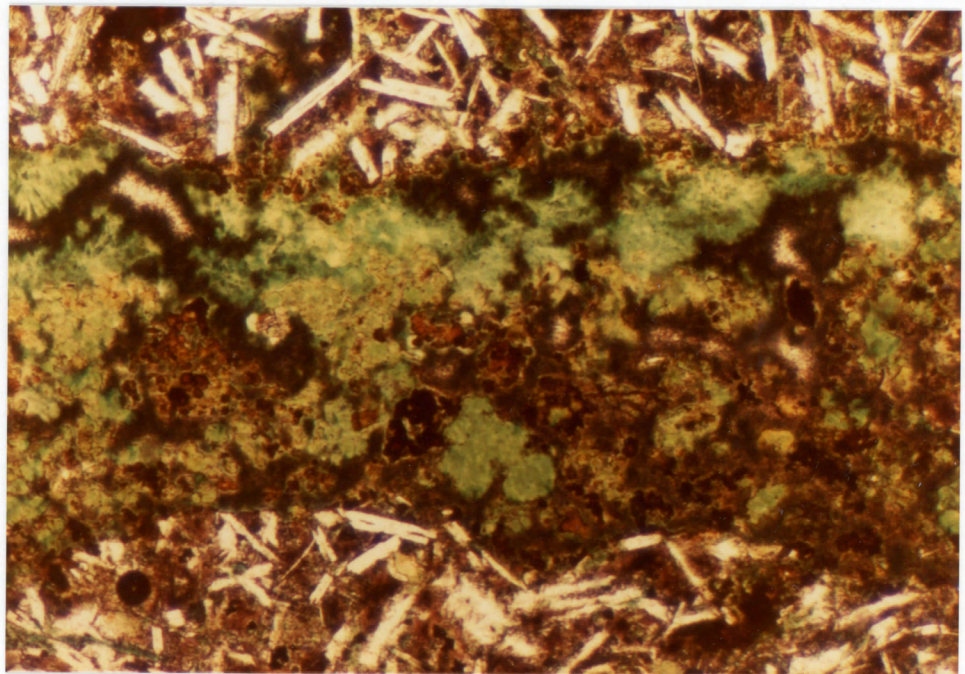
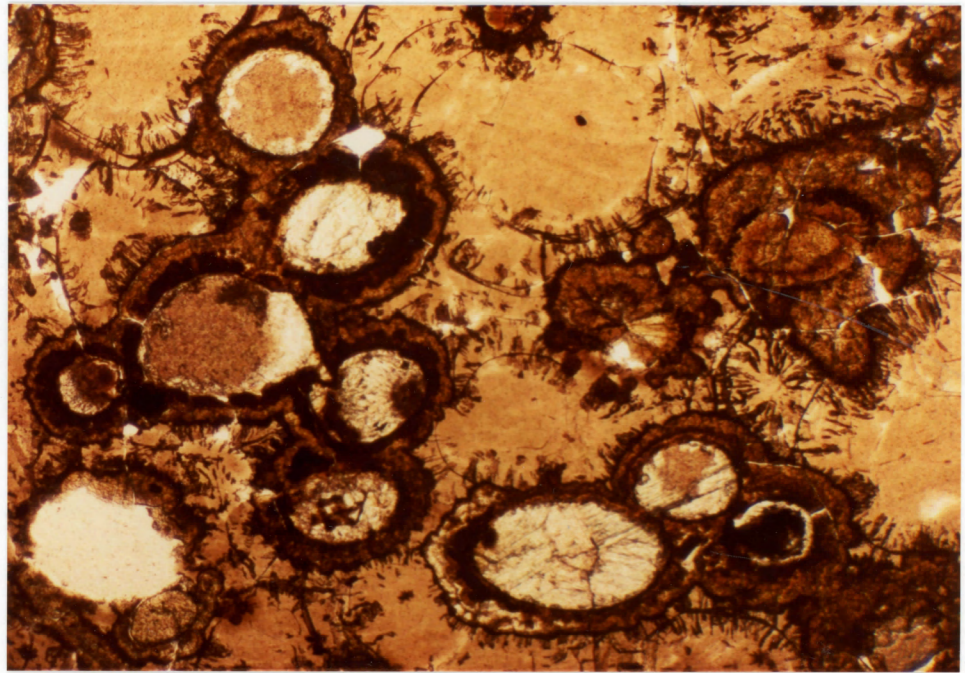


PLATE 7. CY-2A 136.70 m. Fresh, vesicular, massive glass with perlitic fractures. The clear, lath-shaped vesicle-filling mineral is probably gypsum. The brown amorphous mineral in the large vesicle on the left is a zeolite mineral. The more common orange-brown mineral in the vesicles, and forming the colloform ring around most vesicles is smectite(s).
Magnification: 2.5 X 1.25 X 8.

PLATE 8: CY-2A 141.45 m. Dark-green spicules of celadonite, brown and light green smectite fill a vein in a relatively fresh basalt.
Magnification: 2.5 X 2 X 8.

The veins are filled primarily with brown and green smectite, lesser celadonite, and locally quartz (plate 8). The vesicles are filled entirely with quartz. Up to four generations of quartz, distinguished by their different textures, may fill a single vesicle.

(ii) Partly to Highly Altered and Highly Mineralized Basalt (CY-2A 152.90 m to 161.19 m):

Five of the six samples included in this category belong to massive lava units while the sixth, CY-2A 161.19, is a massive glass. These samples are characterized by hyalophitic or relict hyalophitic textures and contain significant proportions of secondary ore minerals. The ore minerals are disseminated in the matrix or concentrated in veins and vesicles.

The matrix is dominated by chlorite which can vary in colour from almost colourless, to green, to brown. Beige to dark brown smectite comprises subordinate to major proportions of the matrix, however in one sample, 159.37 m, it was not present at all. Colourless to orange-brown illite occurs in minor to subordinate amounts in three of the samples where it is concentrated adjacent to the veins and vesicles. Fine-grained, anhedral quartz can vary in proportion from a trace to a subordinate component. Trace to subordinate amounts of primary plagioclase microlites are partly to highly altered to chlorite and/or smectite and/or illite. Minor amounts of cryptocrystalline, brown, equant grains of sphene are present in two of the samples. The secondary ore minerals in decreasing proportion

are anhedral to euhedral pyrite, subhedral to euhedral honey-yellow sphalerite, and anhedral chalcopyrite. They are very-fine to fine-grained and disseminated.

The vein-filling minerals are quartz, pyrite, sphalerite, calcite, chalcopyrite and, in sample 153.10, trace, medium-grained euhedral laumontite (?) laths. Generally, quartz is the dominant vein-filling mineral with sphalerite and pyrite present as subordinate components. Calcite usually forms a minor proportion of the veins but is present in significant amounts in two of the six samples. Chalcopyrite, where present, is a minor to trace vein mineral.

The vesicles contain fine-grained flakes of chlorite in addition to all vein-filling minerals but laumontite. Quartz is again the dominant mineral while the order of abundance of chlorite, pyrite, sphalerite, calcite, and chalcopyrite in the vesicles varies between samples.

The sphalerite in the veins and vesicles has a variable iron content as characterized by the colour. The dominant, honey-yellow sphalerite contains less iron than does the rust-brown sphalerite.

(iii) Pervasively Altered and Highly to Pervasively Mineralized Basalt (CY-2A 173.66 m to 285.05 m with the exception of 282.45 m):

The ten samples included in this category belong to alternating units of massive glass and massive lava. Six of the samples have no recognizable igneous textures while four samples display relict hyalophitic textures. Small areas in two of the samples display relict intersertal textures.

Very fine-grained flakes of subhedral illite, as well as cryptocrystalline, brown, equant grains of sphene are ubiquitous in these samples and present in subordinate to major proportions. Quartz is commonly a dominant matrix mineral although in three of the samples it is present only in trace to minor amounts. Colourless to pale green, anhedral, fine-grained patches of chlorite occur either in trace, or in subordinate to major proportions. Secondary, very fine- to fine-grained pyrite is disseminated in the matrix and in most samples, comprises minor to subordinate amounts of the matrix. Epidote first appears in CY-2A at 270.15 m as a trace component and is present in this proportion to the base of this interval. Primary plagioclase microlites have been completely replaced by illite and lesser quartz and pyrite (plates 4 and 5).

Quartz and pyrite are the most common, dominant, vein-filling minerals. Significant proportions of anhedral and botryoidal hematite, in addition to quartz and pyrite in the veins of three samples forms the large "jasper-quartz-pyrite" veins which penetrate the pervasively altered basalt (plate 9). In some samples, smaller, 100% pyrite veins crosscut the jasper-quartz-pyrite veins and represent an even later phase of mineralization. Chlorite, calcite, gypsum and sphalerite are occasional vein-filling minerals but are present only in trace amounts. Sphalerite occurs as cryptocrystalline, droplet-like inclusions in the pyrite.

Variable proportions of quartz, pyrite, chlorite, calcite and illite fill the vesicles. Quartz is present in all samples and is usually the dominant phase.

(iv) Highly to Pervasively Altered and Partly Mineralized Basalt (CY-2A 282.45 m, and 302.35 m to 406.85 m):

The eight samples included in this interval belong mainly to altered dike or post-mineralization dike units, however 404.40 m comes from a glassy unit and 406.85 belongs to a pillowed lava unit. The textures displayed by these samples include hyalophitic, porphyritic hyalophitic (the post-mineralization dike at 282.45 m), relict hyalophitic and relict intersertal. In addition, sample 404.40 m is a hyaloclastite breccia.

Brown or green, subhedral to anhedral chlorite is the dominant matrix component. Anhedral, fine quartz grains are commonly present in minor amounts although two samples contained subordinate and major proportions of quartz. Two types of plagioclase occur in these samples in trace to subordinate amounts. Lesser, anhedral microlites that are highly altered to illite and/or chlorite and/or secondary albite believed to be primary plagioclase microlites while the more dominant, subhedral to euhedral, relatively fresh microlites are secondary albite. Smectite is present in subordinate to major proportions in the post-mineralization dike units, and in minor proportion in one of the altered dike units (perhaps this is also a post-mineralization dike?). Cryptocrystalline, equant brown grains of sphene occur in variable proportion from completely absent to major, however in most samples sphene is a minor component. Minor amounts of very-fine to fine-grained flakes of illite are found in the first five samples of this interval but are absent in the last three samples. Very fine-grained anhedral calcite, and anhedral to euhedral epidote, occur

scattered in the matrix in trace to minor proportions. The highest proportions of epidote are present in the last two samples of the interval indicating increasing temperature conditions and, together with abundant chlorite and albite, the onset of more readily recognizable greenschist facies conditions.

The ore minerals comprise a minor proportion of the samples in this interval and consist of magnetite, primary and secondary pyrite, sphalerite, and trace chalcopyrite. Subhedral and skeletal magnetite is present in minor amounts in the post-mineralization dike units only. Primary, anhedral pyrite is found in variable proportions in the first five samples (including the three post-mineralization dike units) but is absent in the last three. These samples contain a greater proportion of subhedral to euhedral, fine-grained secondary pyrite as well as trace to minor amounts of subhedral to euhedral sphalerite, and in sample 404.40 m, trace, anhedral chalcopyrite. The sphalerite is dominantly honey-yellow in colour although some grains are the brown, more iron-rich variety.

With the exception of sample 404.40 m, veins and vesicles comprise insignificant proportions of the samples in this interval, and are filled with variable amounts of quartz, chlorite, pyrite, calcite and illite. However, quartz is the dominant phase in the vesicles in all cases.

In the hyaloclastite breccia sample (404.40 m), fractures and vesicles make up approximately 35% of the sample (plate 10) and are filled primarily with quartz and chlorite, while pyrite and sphalerite

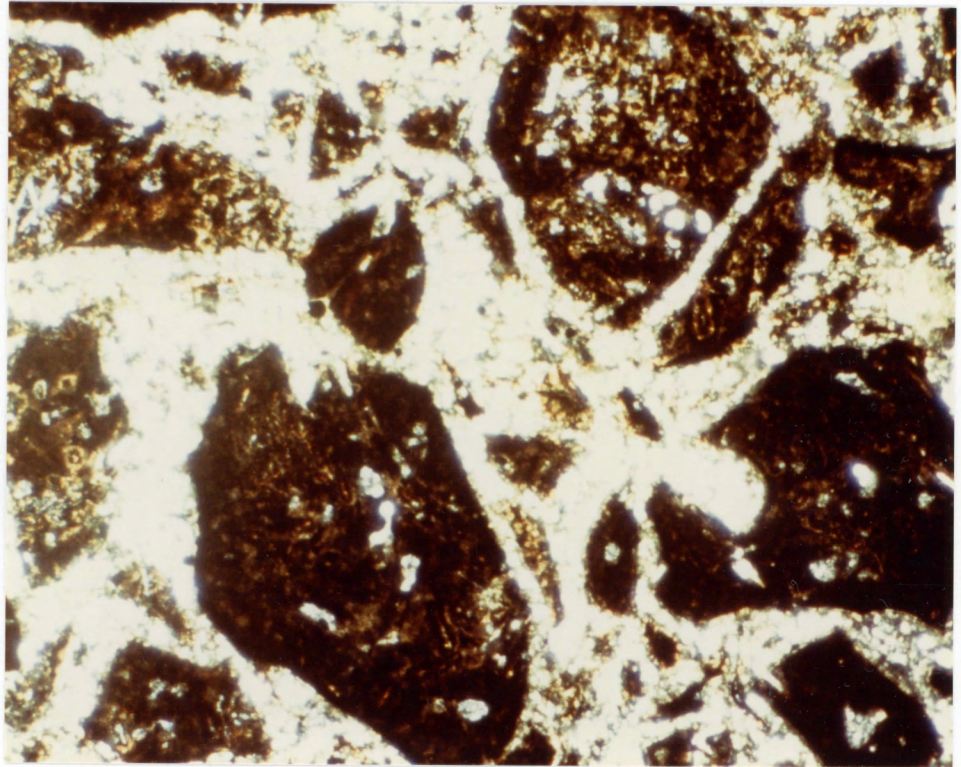
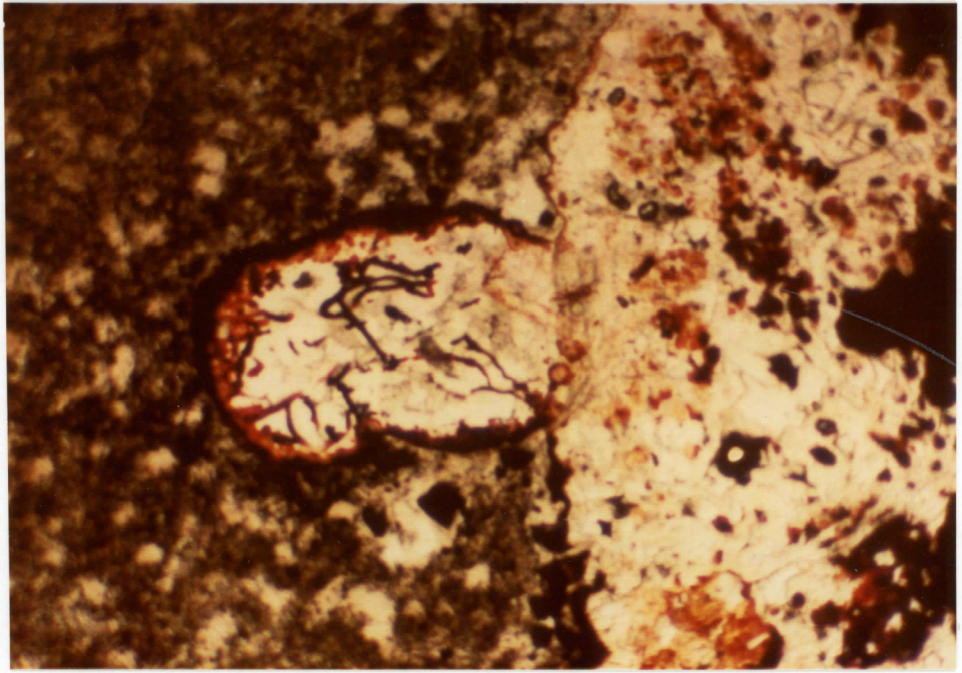


PLATE 9. CY-2A 285.05 m. Quartz-jasper-pyrite vein is projecting into pervasively altered basalt. Magnification: 2.5 X 1.25 X 8.

PLATE 10. CY-2A 404.40 m. Hyaloclastite breccia. Dark brown mineral is chlorite. Fractures are filled with quartz and green chlorite. Magnification: 2.5 X 1.25 X 8. Crossed nicols.

are minor phases. Note the contrast between the highly brecciated appearance of this glass and the unbrecciated form of the massive glass sample (136.70 m) shown in plate 7.

3.3 Ore Mineralogy

Six ore minerals were identified in the drill core samples. In approximate order of decreasing abundance these are: pyrite, hematite, sphalerite, magnetite, chalcopyrite, and ilmenite. The different forms of occurrence of these minerals are described in this section, while their paragenetic sequence is discussed in section 6.2.

(i) Pyrite: Pyrite occurs in a variety of forms ranging from cryptocrystalline to medium-sized and anhedral to euhedral grains. It is found disseminated in the matrix as well as in veins and vesicles. Some forms of pyrite seem to have undergone extensive chemical erosion as evidenced by their anhedral nature and "weathered" appearance (many, small, irregular fractures). This form of pyrite has been interpreted as primary igneous pyrite and occurs in some of the CY-2 samples as well as in CY-2A 136.70 m and the post-mineralization dikes and altered dikes between CY-2A 282.45 m and 368.02 m (plate 11). An alternative explanation to that of primary pyrite for the anhedral, weathered pyrite in the CY-2 samples is that it may have formed by the reduction of seawater sulphate by reaction with ferrous silicates as the seawater began its downward movement. This reaction would have produced disseminated pyrite and magnetite in the rocks at shallow depths near the seafloor (Hutchinson et. al.,

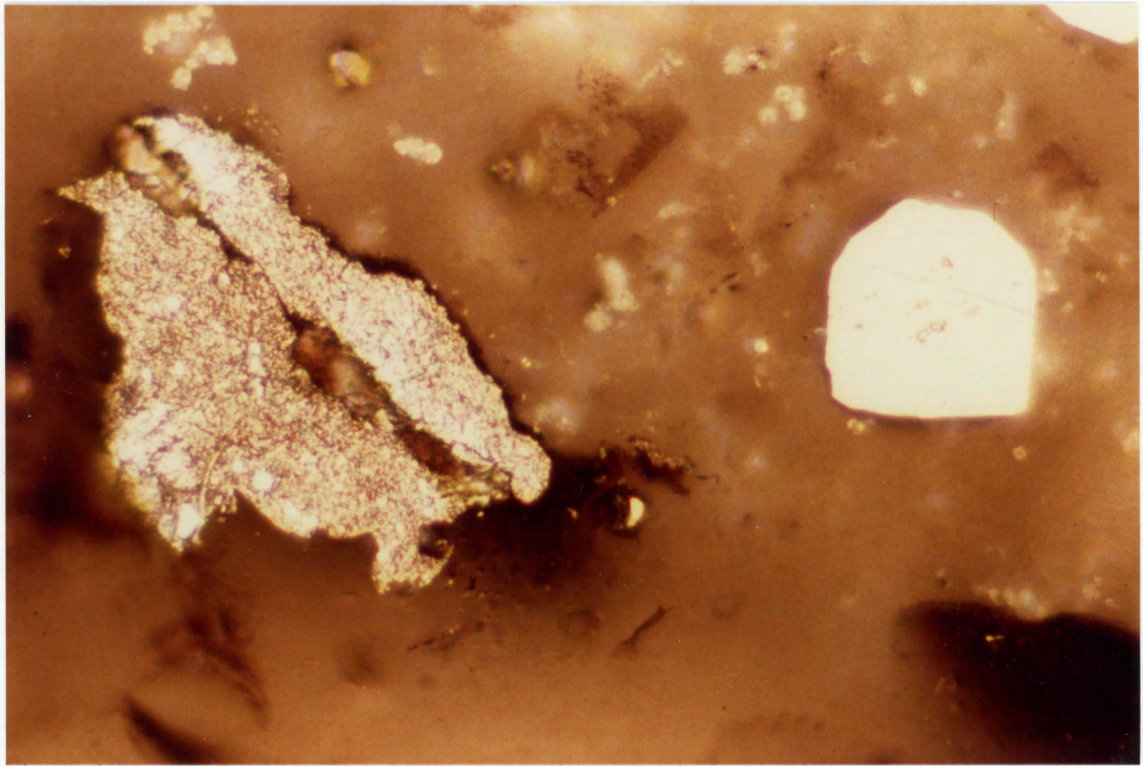


PLATE 11. CY-2A 285.05 m. Primary, anhedral pyrite on left has a weathered appearance due to many small fractures. Secondary, subhedral pyrite on right has a "fresh" appearance. Magnification: 160X.

PLATE 12. CY-2A 285.05 m. Secondary pyrite displays a cataclastic texture caused by high directed pressure in a fault zone.
Magnification: 160X.

1980). The associated occurrence of disseminated magnetite in the CY-2 samples, together with the stratigraphic position of these samples at or near the paleoseafloor (the contact between the L.P.L. and U.P.L.), would support this hypothesis.

The effects of high directed pressure on coarse-grained pyrite from a fault zone (CY-2A 285.05 m) is reflected in the cataclastic texture of this pyrite(plate 12).

Two unusual textures were observed in the pyrite. The first is framboidal pyrite which was found in significant amounts in the veins of sample 153.25 m (about 10% of the pyrite present occurs as framboids) and, less abundantly, in sample 159.7 m (plate 13). The range of diameters of the framboids is small and all are less than 0.1 mm in diameter. They occur in various stages of disintegration from almost pristine with a well-defined boundary, to a virtually empty ring of pyrite, or as fragments of spheres. The framboids appear to have formed earlier than the coarser-grained, anhedral to subhedral pyrite, sphalerite and chalcopyrite crystals that they occur with. At a magnification of 630x, no ordering of the pyrite microcrysts within the framboids is apparent (plate 14). Both organic bacterial origins (Love, 1957), and inorganic processes of formation (Kalliokoski, 1974) have been postulated for these textures. In these samples, the framboids were probably formed by inorganic processes since the physico-chemical conditions in the hydrothermal system at a depth of about 150 m were most likely to be unsuitable for bacterial growth. The occurrence of the framboids in colloidal silica (plate 15) indicate

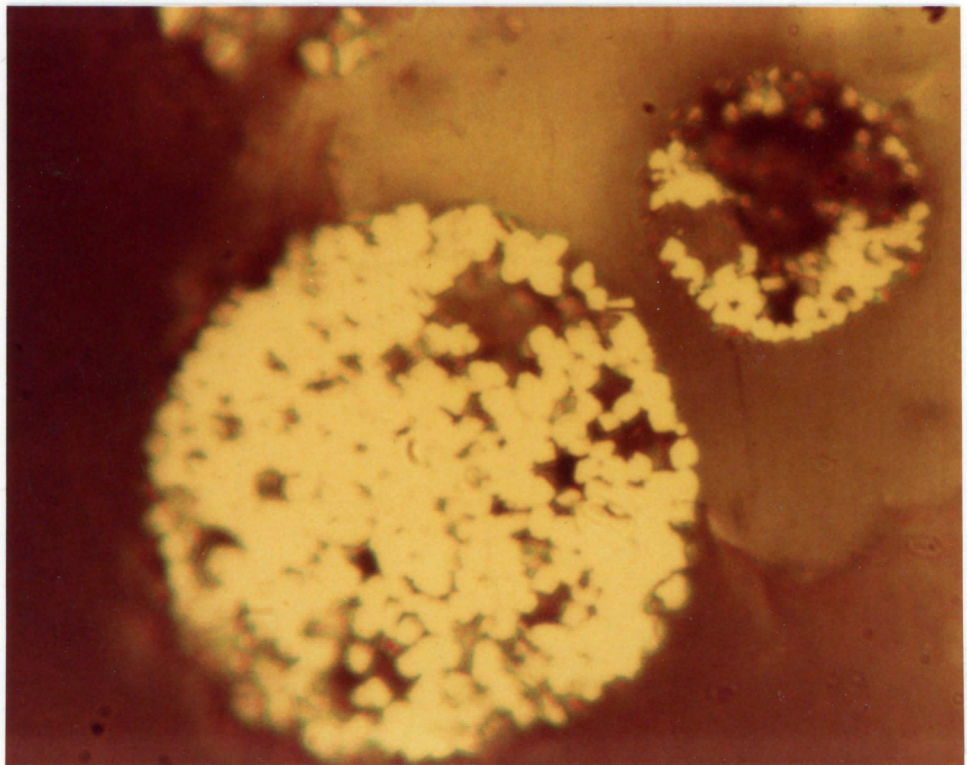
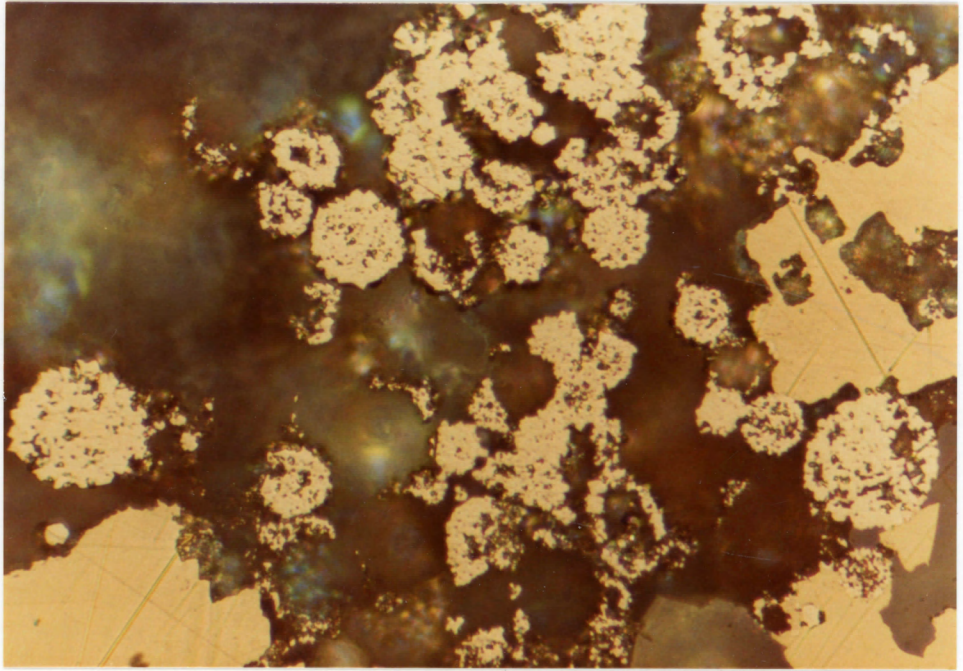


PLATE 13. CY-2A 153.25 m. Pyrite framboids in various stages of disintegration. Later, anhedral pyrite is seen growing around and engulfing a framboid in the lower right-hand corner.
Magnification: 160X.

PLATE 14. CY-2A 153.25 m. Pyrite microcrysts within framboids display a lack of order. Magnification: 630X.

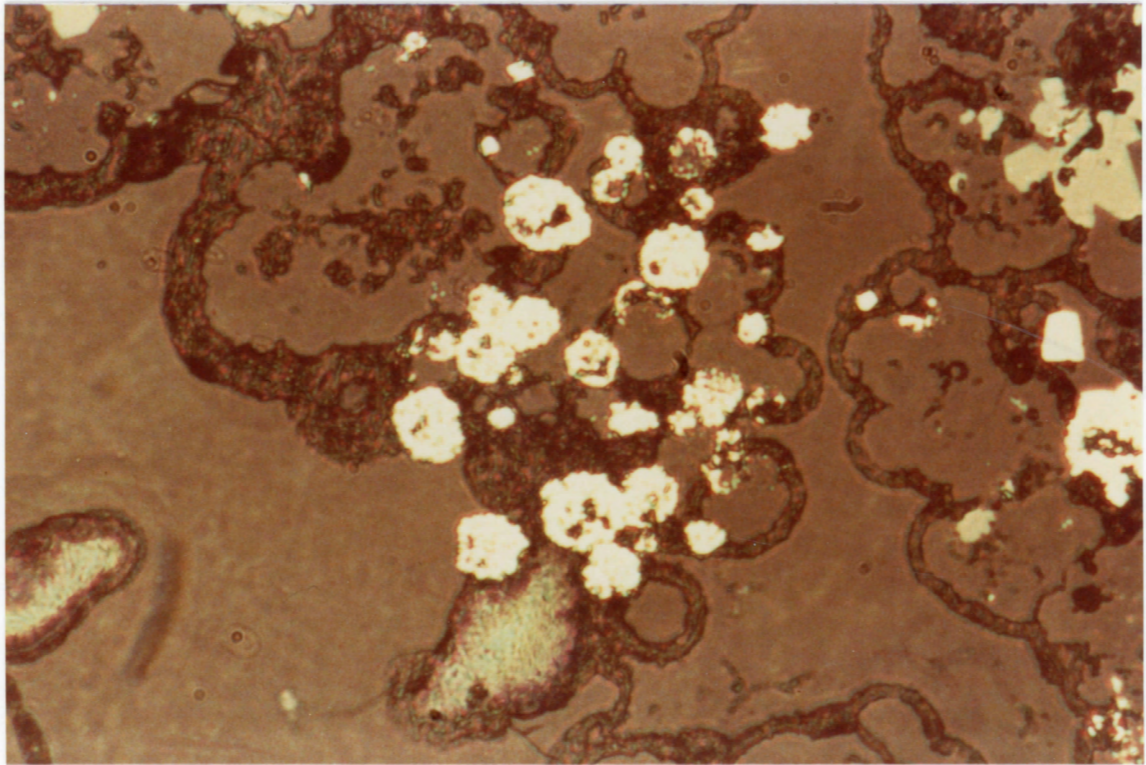


PLATE 15: CY-2A 153.25 m. Pyrite framboids in colloidal silica.

Magnification: 100 X.

that the pyrite probably precipitated out of a supersaturated silica solution and subsequently infilled pre-existing spherical vacuoles formed by entrapped gases. According to Rickard (1970), the spheroidicity can only be formed by pseudomorphism of a pre-existing spherical body at low temperatures ($\leq 200^{\circ}\text{C}$).

The second unusual texture is defined by the presence of circular trails or spherical clusters (up to 0.2 mm in diameter) of inclusions in the cores of subhedral pyrite grains in samples CY-2A 159.37 m, 243.05 m and especially in 193.00 m (plate 16). The fine-grained host pyrite crystals have polygonal boundaries due to crowded conditions of growth. Electron microprobing of these inclusions revealed them to be cryptocrystalline rounded drops of sphalerite of varying regularity (table 12, analysis 7 and plate 17). Two origins are possible for this texture. One is that the drops are dispersions (emulsions) formed by exsolution of sphalerite from pyrite as the temperature fell to a certain level below which solid solution between the two minerals was no longer possible. An alternative interpretation is that the inclusions are residuals from replacement processes. Since exsolutions in pyrite are rare (Ramdohr, 1979), this texture is probably the result of replacement of secondary sphalerite by a later secondary pyrite phase.

(ii) Hematite: Hematite is generally found in veins and occurs in three forms. The most common form is anhedral patches of hematite, usually associated with quartz. Where hematite is present in approximately equal proportions with quartz, the association of the two minerals is commonly referred to as jasper (plate 9).

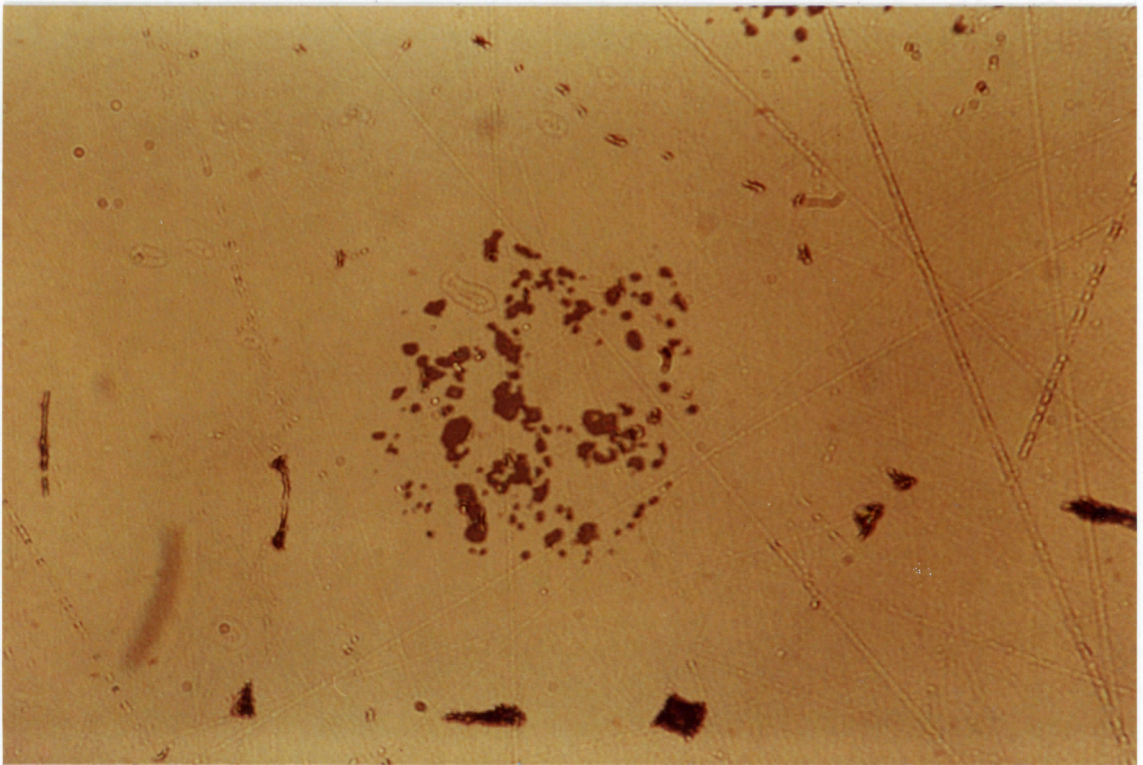
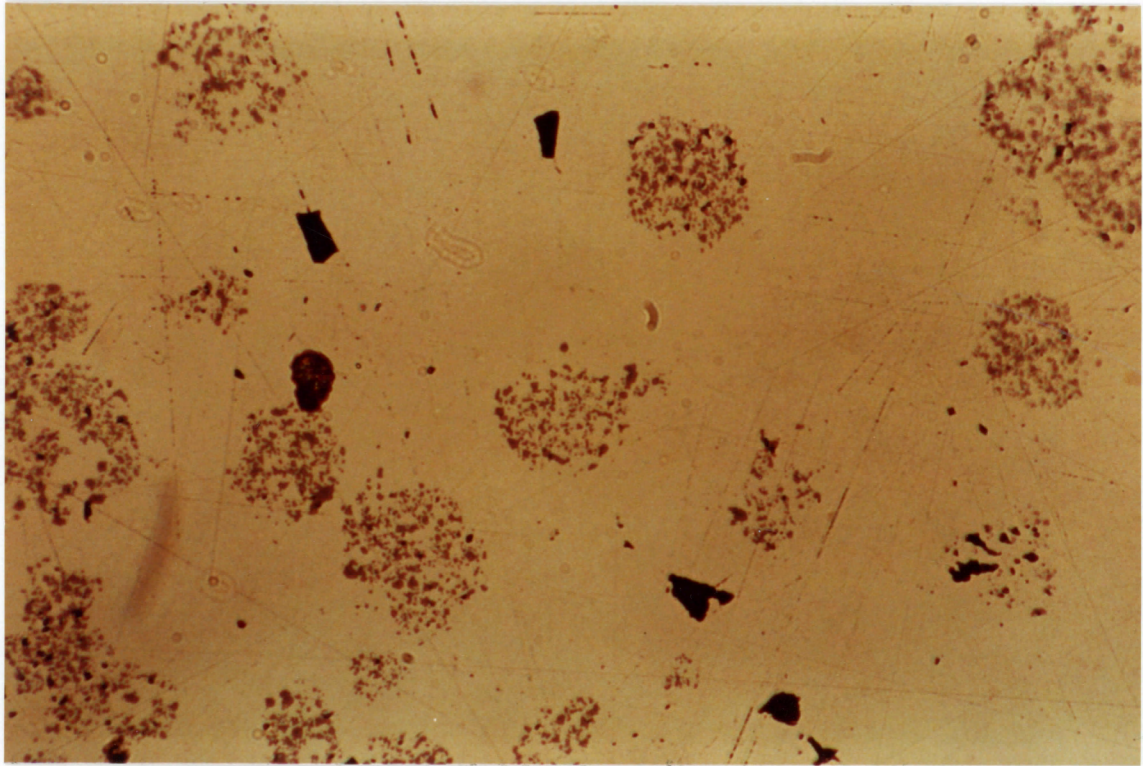


PLATE 16. CY-2A 193.00 m. Subspherical clusters of sphalerite inclusions in cores of pyrite grains. Polygonal boundaries of pyrite grains due to crowded conditions of growth are barely discernible. Magnification: 63X.

PLATE 17. CY-2A 193.00 m. Sphalerite inclusions are rounded droplets of varying regularity. Magnification: 200X.

Less commonly, hematite occurs in a series of concentric layers with curvature convex toward the younger surface (i.e. away from the vein wall). These layers define a colloform texture (plate 18).

Sometimes hematite is found as clusters of rounded, hollow, very fine-grained shells defining a botryoidal or pellet texture (plate 19). Some pellets were observed enclosing pyrite grains which are usually found with hematite in veins. The botryoidal and colloform textures are closely related and often occur together.

(iii) Sphalerite: Most sphalerite observed was honey-yellow in colour. Lesser amounts of rust-brown sphalerite are present with the darker colour indicating a higher iron content. The iron-rich variety of sphalerite (mole % FeS is greater than about 10%) thought to occur in the CY-2A core by members of the ICRDG was not found. Sphalerite is commonly present as subhedral to euhedral, very-fine to medium-sized grains. Euhedral, zoned sphalerite with a honey-yellow core poorer in iron, and a rust-brown rim richer in iron was found in two samples (table 12, analyses 3,4 and plate 20).

In sample CY-2A 152.9, the sphalerite present in the altered margin of a vein is consistently richer in iron than the sphalerite occurring within the vein (plate 21). This feature may reflect a change in the chemistry of the solutions from which the sphalerite grains precipitated, or may represent a later leaching of FeS from the sphalerite grains occurring within the vein. The iron-leaching solutions would not have come in contact with the sphalerite grains occurring within the altered margin.

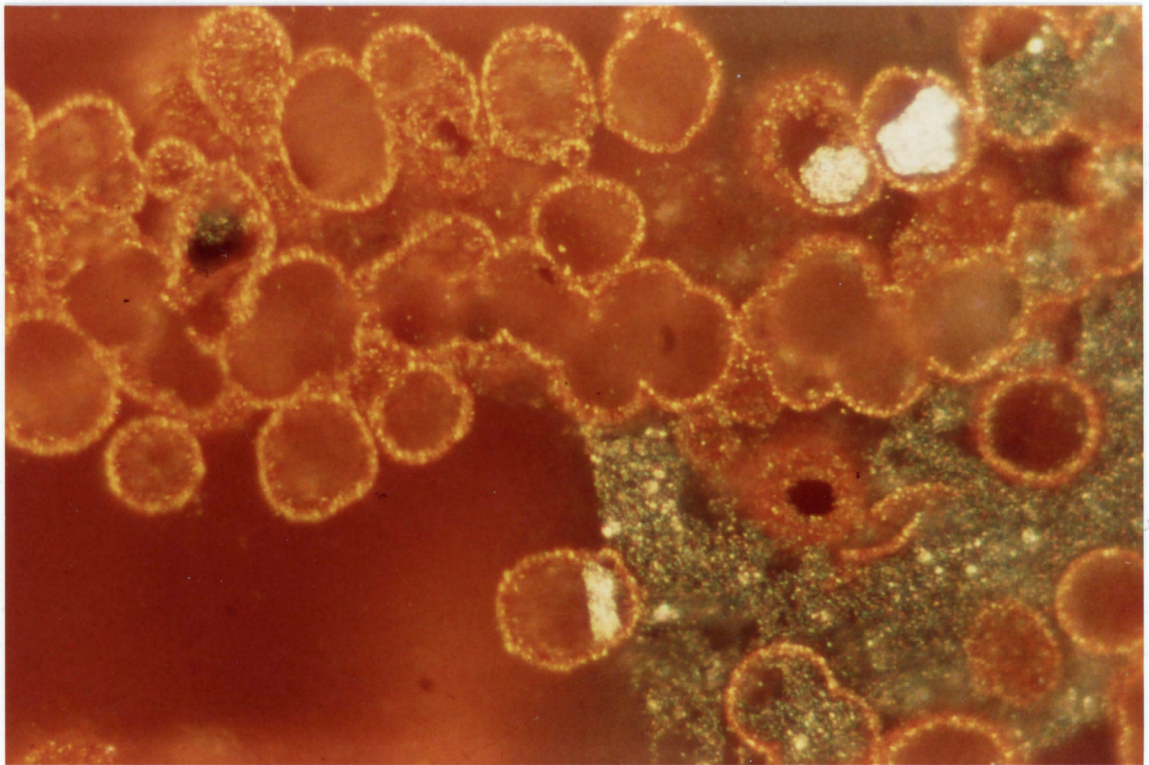
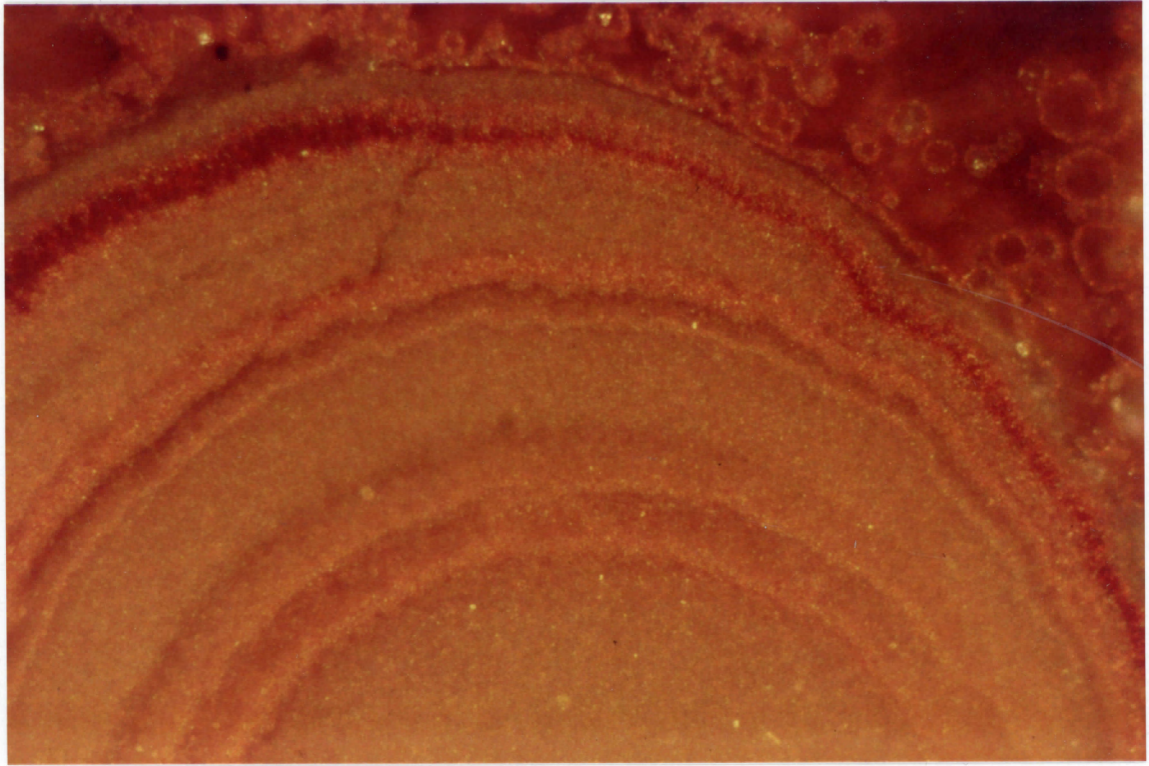


PLATE 18. CY-2 92.30 m. Colloform banding in hematite. Magnification: 160X.

PLATE 19. CY-2 92.30 m. Botryoidal hematite. Occasional pyrite grains enclosed by hematite. Magnification: 200X.

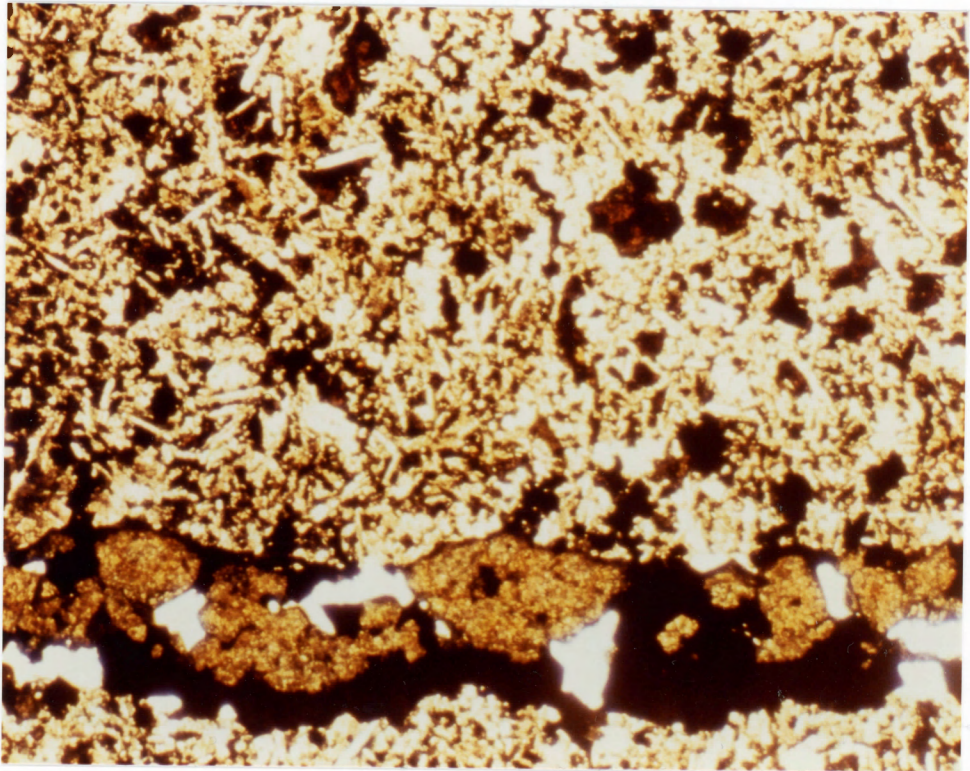
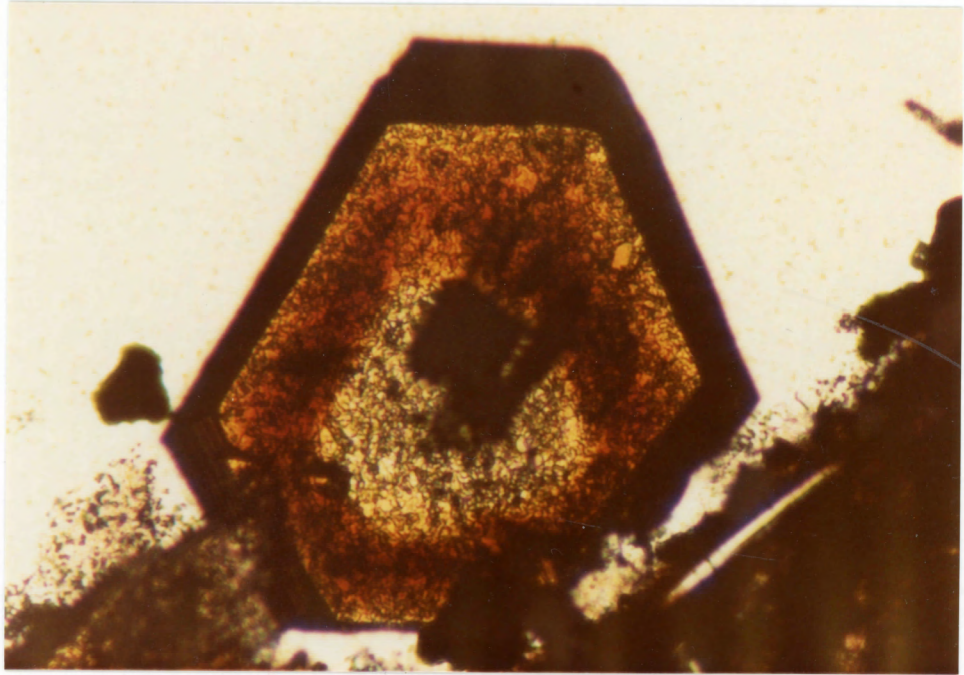


PLATE 20. CY-2A 153.25 m. Zoned sphalerite with a honey-yellow, relatively iron-poor core and a rust-brown, relatively iron-rich rim. Magnification: 63X.

PLATE 21. CY-2A 153.25 m. Honey-yellow, relatively iron-poor sphalerite in vein. Rust-brown, relatively iron-rich sphalerite in altered margin of vein. Magnification: 2.5 X 1.6 X 8.

(iv) Magnetite: Magnetite occurs in few samples as subhedral to skeletal (plate 22), very-fine to fine-grained crystals. Its partly to highly altered nature indicates increasing disequilibrium with the conditions which produced the alteration in the basalts, and points to a primary origin for the magnetite. However, as previously discussed, some of the magnetite in the CY-2 samples, together with pyrite, may have been formed by downward penetrating seawater carrying sulphate as it reacted with ferrous silicates in the basalt.

(v) Chalcopyrite: Minor to trace proportions of chalcopyrite were observed in a few samples. Chalcopyrite is present as very-fine to fine, anhedral grains, often intergrown with pyrite. It occurs disseminated in the matrix as well as within veins.

(vi) Ilmenite: The identification of ilmenite was based on petrographic studies alone. The cryptocrystalline to very fine-grained nature of the mineral in these samples makes simple petrographic identifications of ilmenite unreliable. The identification of ilmenite was based on its low reflectivity, anisotropy, lath-like habit, and common association with magnetite. The cryptocrystalline to very fine-grained microlites generally occur disseminated in the matrix, although in sample CY-2 92.30 m the ilmenite laths were observed fringing a vesicle and apparently collected within a hematite-pyrite colloidal liquid.

CHAPTER 4

X-RAY DIFFRACTION ANALYSES

Whole rock X-ray diffraction analyses were carried out on five samples from Hole CY-2 and 17 samples from Hole CY-2A. The results of these analyses appear in tables 4 and 5.

The mineral identifications made by X-ray diffraction generally confirmed the petrographic identifications.

In some cases minerals which had not been previously distinguished under the microscope, for example the colourless chlorite in CY-2A 207.00 m, 270.15 m, and 277.40 m, or had been misidentified petrographically, for example the thick, amorphous, brown chlorite which had been mistaken for smectite in CY-2A 404.40 m, were properly identified by X-ray diffraction patterns. These identifications were then correlated petrographically with samples which had not been analyzed by X-ray diffraction methods.

The smectite mineral in CY-2 92.30 m and CY-2A 161.19 m was identified as nontronite. The chlorite in CY-2A 92.30 m and CY-2A 159.37 m, 161.19 m, 270.15 m, 302.35 m and 404.40 m was identified as ripidolite. The plagioclase in samples CY-2 92.30 m and CY-2A 141.45 m was identified as labradorite whereas the plagioclase in CY-2A 332.45 m and 404.40 m was identified as albite. The labradorite is primary while the albite is secondary.

TABLE 4: Whole Rock X-ray Diffraction Analyses of Samples from CY-2

○ = 70% of sample ○ = 30-70% of sample ○ = 10-30% of sample ○ = 5-10% of sample

Sample	Smectite	Chlorite	Illite	Calcite	Quartz	Plagioclase	Sphene	Pyrite	Others
24.00	○	○			○	○			
48.05		○	○		○				magnetite ○
79.63	○	○			○	○			
84.15		○			○	○			magnetite ○
92.30	○ to ○ ¹	○ ²			○	○ ³			

TABLE 5: Whole Rock X-ray Diffraction Analyses of Samples from CY-2A

○ = 70% of sample ○ = 30-70% of sample ○ = 10-30% of sample ○ = 5-10% of sample

Sample	Smectite	Chlorite	Illite	Calcite	Quartz	Plagioclase	Sphene	Pyrite	Others
136.70	○								
141.45						○ ³			celadonite ○
156.91	○			○	○			○	
159.37		○ ²	○		○			○	
161.19	○ ¹	○ ²	○		○	○	○	○	
183.50			○					○	
193.00			○		○			○	
207.00		○	○		○			○	
243.05			○		○		○	○	
270.15		○ ²	○		○			○	
277.40		○	○		○		○		
282.45	○	○			○	○			
302.35		○ ²	○		○		○		
332.45	○	○	○		○	○ ⁴			
386.40		○			○	○	○		
404.40		○ ²			○	○			
406.85		○			○		○		

1. smectite identified as nontronite.
2. chlorite identified as ripidolite.
3. plagioclase identified as labradorite.
4. plagioclase identified as albite.

The abundances of the individual minerals within a sample estimated from the X-ray diffraction patterns generally conform with the abundances estimated petrographically. However whole-rock X-ray diffraction analyses of samples in which more clays were believed to exist revealed the presence of much less, if any, clay. The best example of this discrepancy is sample CY-2A 141.45 m. It is obvious from the hand sample, thin-section and more conclusively, from the microprobe analysis of this sample, that smectite is present. The X-ray pattern however, revealed no smectite peaks. Clay separation by settling was attempted for some of these samples, followed by another X-ray diffraction analysis. In some of these patterns the clay peaks which had already been observed were enhanced during the second analysis. In most cases, the pattern did not change and in no case did new peaks appear after the clays had been separated. This points to the conclusion that either a) settling times were too short and not enough clay material had been obtained, or b) that separation by simple settling in a water column is not adequate and other techniques must be employed.

It appears that reliable identification of clay and mica minerals, together with an accurate determination of their relative abundances by X-ray diffraction methods, requires a combination of several analyses run before and after treatment of the samples with heat and organic liquids. Time limitations prevented the undertaking of such conclusive procedures in this study.

CHAPTER 5

MICROPROBE STUDIES

Electron microprobe analyses were carried out on one sample from Hole CY-2 and eight samples from Hole CY-2A. The clay, chlorite, mica, carbonate and sulphide minerals were analyzed in order to identify some of these very fine-grained minerals directly. The results appear in tables 5 to 13 and represent averages of at least three analyses for each mineral.

The very fine-grained, and often intermixed, nature of the clays, micas and chlorites, together with their hydrous composition, produced highly variable results for what appeared under the microscope to be different grains of the same mineral.

The fact that clay and chlorite standards are not available at Dalhousie, and therefore other minerals were used as standards, also contributed to the variability of the results. The low totals (i.e. much less than 100%) for the chlorites, clays, micas and calcite are due to the presence of volatiles in these minerals which are burned off by the electron beam. Chlorites have between 11% and 13% water in their structure, smectites between 15% and 23% water, illites between 6% and 12% water, and celadonite between 9% and 14% water (note that these are weight percentages). Calcite contains approximately 45wt.% CO₂ (Deer et.al.,1962). A few analyses included in the tables have an even lower total than can be accounted for by the presence

Table 5: Chemical Analyses of Smectite Minerals

	<u>1</u>	<u>2</u>	<u>3</u>	<u>4</u>	<u>5</u>
SiO ₂	40.71	34.49	45.36	46.07	37.38
TiO ₂	1.69	1.38	0.82	-	1.04
Al ₂ O ₃	4.80	0.35	16.55	17.20	23.31
FeO	26.28	31.40	14.10	7.84	1.82
MnO	0.33	0.28	0.25	0.43	0.06
MgO	1.88	0.12	5.04	7.27	1.30
CaO	1.23	0.26	4.97	1.57	0.20
Na ₂ O	1.30	-	2.78	2.41	0.36
K ₂ O	2.40	-	0.31	2.44	4.70
P ₂ O ₅	0.35	-	-	0.20	-
V ₂ O ₅	-	-	0.20	-	-
TOTAL	80.97	68.28	90.38	85.43	70.41

1. Green nontronite in CY-2A 141.45 m.
2. Brown nontronite mixed with Fe-oxide in CY-2A 141.45 m.
3. Dark brown nontronite in CY-2A 153.25 m.
4. Montmorillonite in CY-2A 161.19 m.
5. A smectite-group mineral in CY-2A 173.66 m.

Table 6: Chemical Analyses of Chlorite Minerals

	1	2	3	4	5	6	7	8	9	10
SiO ₂	24.74	28.22	32.60	28.99	28.50	27.13	27.59	36.21	27.13	26.78
TiO ₂	-	-	1.91	1.92	-	-	-	0.11	-	-
Al ₂ O ₃	13.57	16.28	20.44	19.34	19.35	20.58	19.32	27.57	21.95	20.22
FeO	19.86	27.03	13.30	16.86	25.64	22.09	26.08	6.15	16.59	25.40
MnO	2.44	5.64	0.56	0.72	0.70	0.86	0.97	0.17	1.52	1.29
MgO	9.88	10.64	13.11	16.24	14.49	16.50	15.65	7.13	19.67	14.36
CaO	0.81	0.30	0.19	0.08	0.08	0.16	-	0.08	-	0.05
Na ₂ O	-	-	0.11	0.17	-	-	-	0.40	-	-
K ₂ O	-	-	1.24	0.29	-	-	0.06	4.34	-	-
V ₂ O ₅	-	0.21	-	-	0.41	-	-	0.26	0.26	0.08
TOTAL	71.30	88.32	83.46	84.61	89.17	87.32	89.67	82.42	87.12	88.18

1. Ripidolite in matrix of CY-2 92.85 m.
2. Ripidolite in vesicles of CY-2 92.85 m.
3. Impure brown ripidolite in matrix of CY-2A 159.37 m.
4. Orange-brown clinochlore adjacent to vesicles of CY-2A 159.37 m.
5. Green ripidolite in vesicles of CY-2A 159.37 m.
6. Ripidolite in matrix of CY-2A 173.66 m.
7. Ripidolite in vesicles of CY-2A 173.66 m.
8. Mixed chlorite/illite in matrix of CY-2A 285.05 m.
9. Ripidolite in vesicles of CY-2A 285.05 m.
10. Ripidolite in matrix of CY-2A 302.35 m.

Table 7: Chemical Analyses of Celadonite and Illite Minerals

	<u>1</u>	<u>2</u>	<u>3</u>	<u>4</u>
SiO ₂	52.17	67.27	41.69	48.45
TiO ₂	0.14	1.28	-	-
Al ₂ O ₃	3.02	15.60	29.38	33.05
FeO	19.83	1.27	9.95	1.91
MnO	0.18	-	0.41	-
MgO	4.78	-	6.69	1.21
CaO	0.24	5.01	0.27	0.20
Na ₂ O	-	3.62	0.73	0.75
K ₂ O	6.62	0.28	3.75	6.15
V ₂ O ₅	0.14	-	-	-
TOTAL	87.12	94.33	92.87	91.72

1. Celadonite in CY-2A 141.45 m.
2. Orange-brown illite adjacent to veins and vesicles of CY-2A 153.25 m.
3. Fe-enriched illite in CY-2A 173.66 m.
4. Al-enriched illite in CY-2A 173.66 m.

Table 8: Chemical Analyses of Calcite

	<u>1</u>	<u>2</u>
FeO	0.36	-
MnO	5.80	1.37
MgO	0.27	-
CaO	48.48	53.33
TOTAL	54.91	54.70

1. Calcite in CY-2A 153.25 m.
2. Calcite in CY-2A 302.35 m.

Table 9: Chemical Analyses of Plagioclase

	<u>1</u>	<u>2</u>
SiO ₂	54.23	54.82
Al ₂ O ₃	29.71	28.37
FeO	0.72	1.04
CaO	12.54	12.53
Na ₂ O	4.55	4.26
K ₂ O	-	0.12
<hr/>		
TOTAL	101.75	101.14

1. Labradorite in CY-2 92.85 m.
2. Labradorite in CY-2A 141.45 m.

Table 10: Chemical Analyses of Sphene and Anatase

	<u>1</u>	<u>2</u>
SiO ₂	29.90	12.04
TiO ₂	36.05	63.28
Al ₂ O ₃	1.86	7.85
FeO	0.69	2.39
MgO	-	2.51
CaO	28.90	0.27
K ₂ O	-	1.10
P ₂ O ₅	0.27	-
<hr/>		
TOTAL	97.67	89.44

1. Sphene in CY-2A 302.35 m.
2. Impure anatase in CY-2A 285.05 m.

Table 11: Chemical Analyses of Pyrite

	<u>1</u>	<u>2</u>	<u>3</u>
S	53.22	53.31	53.76
Fe	46.13	46.44	45.70
Zn	00.17	-	-
<hr/>			
TOTAL	99.52	99.75	100.46

1. Pyrite in CY-2A 153.25 m.
2. Pyrite in CY-2A 193.00 m.
3. Pyrite in CY-2A 285.05 m.

Table 12: Chemical Analyses of Sphalerite

	<u>1</u>	<u>2</u>	<u>3</u>	<u>4</u>	<u>5</u>	<u>6</u>	<u>7</u>
S	32.71	32.86	33.09	33.41	33.13	32.75	45.29
Fe	2.11	1.83	4.03	0.93	2.00	1.86	28.53
Zn	65.25	65.42	63.21	68.58	64.91	65.27	26.02
<hr/>							
TOTAL	100.07	100.11	100.33	102.92	100.04	99.88	99.84

1. Sphalerite in matrix of CY-2A 153.25 m.
2. Sphalerite in veins of CY-2A 153.25 m.
3. Iron-rich rim of zoned sphalerite in vesicles of CY-2A 153.25 m.
4. Iron-poor core of zoned sphalerite in vesicles of CY-2A 153.25 m.
5. Sphalerite in CY-2A 159.37 m.
6. Sphalerite in CY-2A 161.19 m.
7. Sphalerite inclusions in pyrite of CY-2A 193.00 m.

Table 13: Chemical Analysis of Chalcopyrite in CY-2A 153.25 m

S	35.15
Fe	29.68
Cu	33.35
Zn	0.42
<hr/>	
TOTAL	98.60

of volatiles (for example, table 1, analyses 2 and 5). The lack of proper standards may be the cause of this.

Despite these drawbacks, the reliable identification of several minerals could be made. Nontronite is the brown and green smectite mineral in CY-2A 141.45 m and 153.25 m. Montmorillonite occurs in CY-2A 161.19 m, while the clay in CY-2A 173.66 m could only be identified as a smectite mineral. From table 5 it is apparent that the clay compositions have a wide range. Al_2O_3 , FeO, MgO, and CaO vary to the greatest degree between the different smectites.

Ripidolite appears to be the dominant chlorite mineral with only one other variety, orange-brown clinochlore, present in CY-2A 159.37 m (table 6). Analysis 8 can only be explained in terms of a mixed-layer chlorite/illite present in the matrix of CY-2A 285.05 m. Although the MnO values of all the chlorites are generally higher than MnO values reported for chlorites from hydrothermally altered basalt samples by D.S.D.P. scientists, there is a significant proportion of MnO in the matrix and especially in the vesicle chlorites in CY-2 92.85 m. In these minerals, Mn has replaced Mg in the chlorite structure (Deer et. al., 1962). The MnO content of the chlorite increases with depth in the CY-2A samples, and in all samples the MnO content of the vesicle chlorites is greater than the MnO content of the matrix chlorites (figure 6). Experimental studies of Hajash (1975, 1977) show that, at 500°C and a water/rock ratio of 50, 100% of the Mn goes into solution. Direct observation on discharge systems has shown Mn concentrations up to 1400 ppm (Spooner, 1977). From these studies one would not expect to find

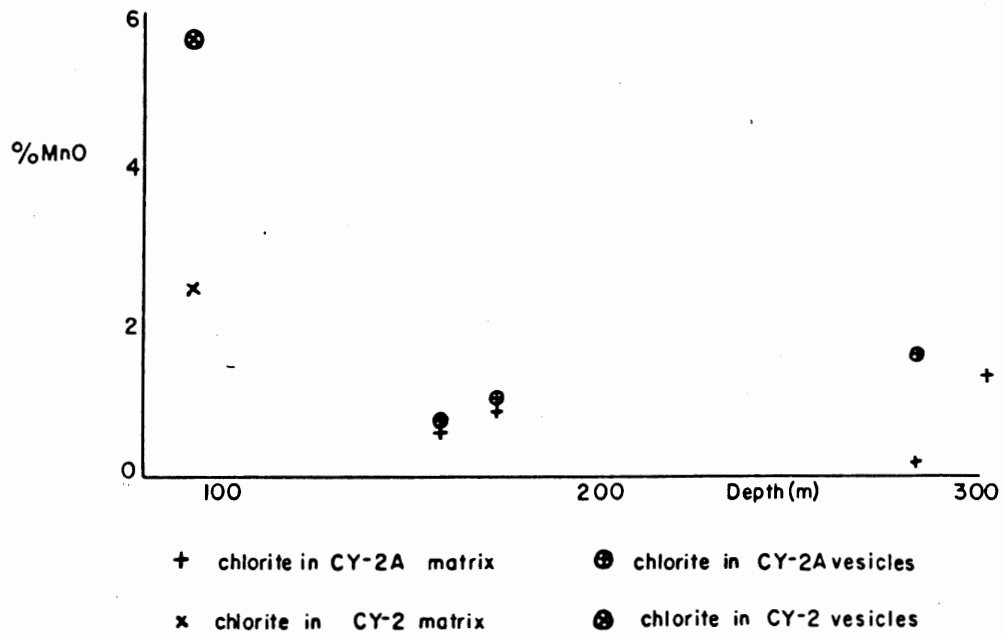


FIGURE 6. Percent MnO in chlorites of CY-2 and CY-2A versus depth.

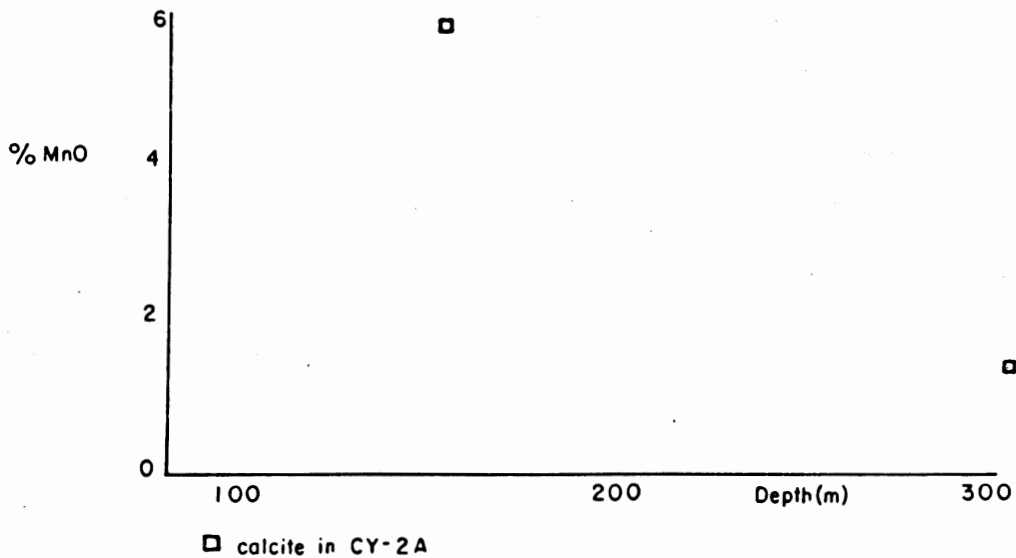


FIGURE 7. Percent MnO in calcite from CY-2A versus depth.

chlorites enriched in MnO within the samples from the Agrokippa paleohydrothermal system. The anomalous MnO concentrations may be a result of later downward seepage of seawater, which is now enriched in MnO in the area of the hydrothermal vent. The fact that the highest values of MnO are found in the chlorites of CY-2 92.85 m, the sample closest to the paleoseafloor and therefore in contact with the greatest volumes of downward seeping seawater, supports this hypothesis. However the increasing concentration of MnO in the chlorites of the CY-2A samples with depth contradicts this idea. Perhaps the fact that less and less MnO is incorporated in the chlorite structure as the hydrothermal fluid rises accounts for the observed high concentration of MnO in the fluid that is vented on the seafloor. In any case, the behaviour of Mn in a hydrothermal system is apparently not a simple matter of total leaching of Mn from the basalts and subsequent venting of all the Mn on the seafloor.

The analyses of calcite also yielded unusually high MnO values (table 8), however in the case of calcite, the proportion of MnO in sample CY-2A 153.25 m is significantly higher than the percentage of MnO in CY-2A 302.35 m (figure 7).

Celadonite was analyzed in CY-2A 141.45 m, and three reliable illite analyses were obtained from CY-2A 153.25 m and CY-2A 173.66 m (table 7). Again, the most noteworthy characteristic of these analyses is the great variation in composition, especially in the concentrations of SiO_2 , Al_2O_3 , FeO, MgO and K_2O between the minerals.

The plagioclase in CY-2 92.85 m and CY-2A 141.45 m was identified as labradorite (table 9).

The Ti-minerals sphene and anatase were analyzed in CY-2A 302.35 m and 285.05 m, respectively (table 10).

The analyses of pyrite in CY-2A 153.25 m, 193.00 m, and 285.05 m show it to remain remarkably constant in composition between these levels in the core (table 11).

Numerous sphalerite analyses were carried out (table 12) in order to apply the sphalerite geobarometer, however this technique could not be used due to the lack of pyrrhotite in these samples. Analyses 1 and 2 show that there is no significant difference in the chemical composition between the sphalerite occurring in the matrix and the sphalerite occurring in the veins of CY-2A 153.25 m, with the exception of a slightly higher Fe content in the matrix sphalerite. Analyses 3 and 4 represent the iron-rich rim and iron-poor core of a zoned sphalerite (plate 20), respectively. Attempts were made to obtain a pure analysis of the sphalerite droplets within the pyrite in CY-2A 193.00 m (analysis 7). Although contamination by pyrite could not be avoided, it is obvious that the inclusions are in fact sphalerite.

A chalcopyrite analysis was obtained from CY-2A 153.25 m, and confirms its presence in the CY-2A core (table 13).

CHAPTER 6

DISCUSSION

6.1 Downhole Distribution of Primary and Secondary Minerals

(a) CY-2 Core: The downhole distribution of primary plagioclase, pyrite, magnetite and ilmenite, as well as secondary minerals and lithology in the samples studied from Hole CY-2 is shown in figure 8.

Secondary smectite minerals are a major component of the rock at the top of the interval, are absent in the sample which has undergone argillic alteration, and reappear at a depth of about 60 m as a major component. Near the base of the interval smectite is seen to be a subordinate component of the lower, partly altered samples and the relatively fresh basalts (85 m to 93 m). In the argillized interval smectite has been replaced by illite.

Celadonite is not present in the samples examined from Hole CY-2.

Chlorite is a major component of the rocks throughout the interval represented by the samples from CY-2, with the exception of the argillized zone around 45 m and the relatively fresh basalts at the base of the interval (90 m to 93 m) in which chlorite is a subordinate component.

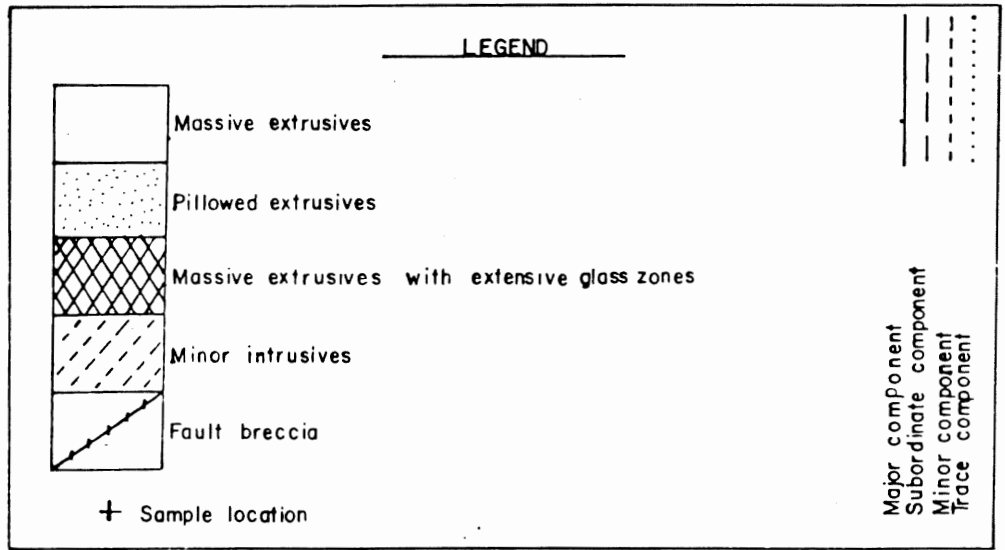
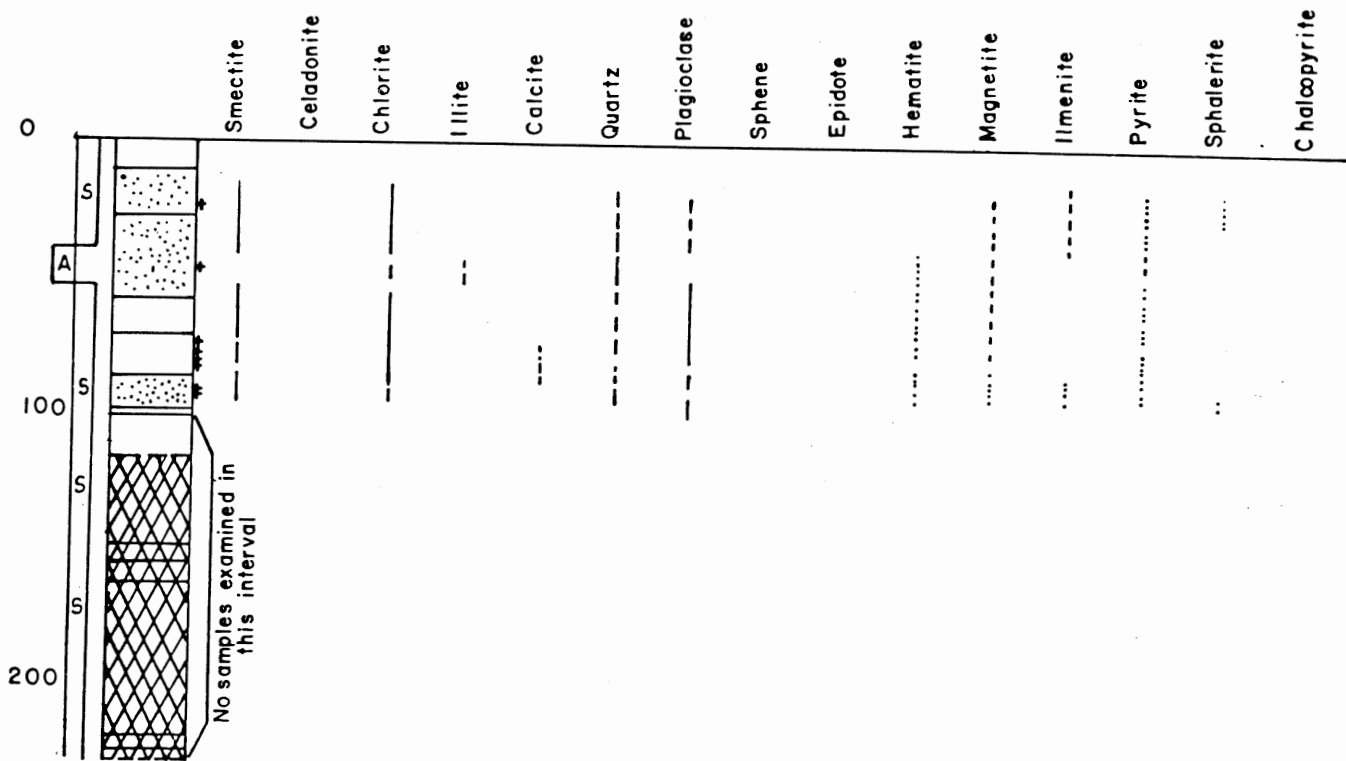


FIGURE 8. Downhole distribution of primary plagioclase, pyrite, magnetite, and ilmenite, as well as secondary minerals and lithology of the CY-2 drill core.

Illite occurs as a minor component in the argillized interval around 45 m only.

Secondary calcite appears at about 75 m as a trace component, and increases in proportion to a minor component until 83 m.

Secondary quartz is ubiquitous in the samples but reaches its greatest concentration in the argillized zone around 45 m and its lowest concentration as a trace component in the relatively fresh basalts at about 90 m. In the remainder of the interval it is found as a subordinate component.

Primary plagioclase occurs in subordinate proportions between approximately 20 m and 40 m. It is absent in the argillized interval around 45 m, and reappears as a major component in the partly altered basalts between approximately 60 m and 85 m. In the remainder of the interval characterized by the occurrence of relatively fresh basalts it forms a subordinate component of the rocks.

Sphene and epidote are absent in the CY-2 samples.

Hematite appears as a trace component at about 40 m and continues to be present in this proportion to the base of the interval.

Magnetite, which may be primary or secondary as discussed in Section 3.3(iv), is present as a minor component between approximately 20 m and 80 m. For the rest of the interval it occurs as a trace component.

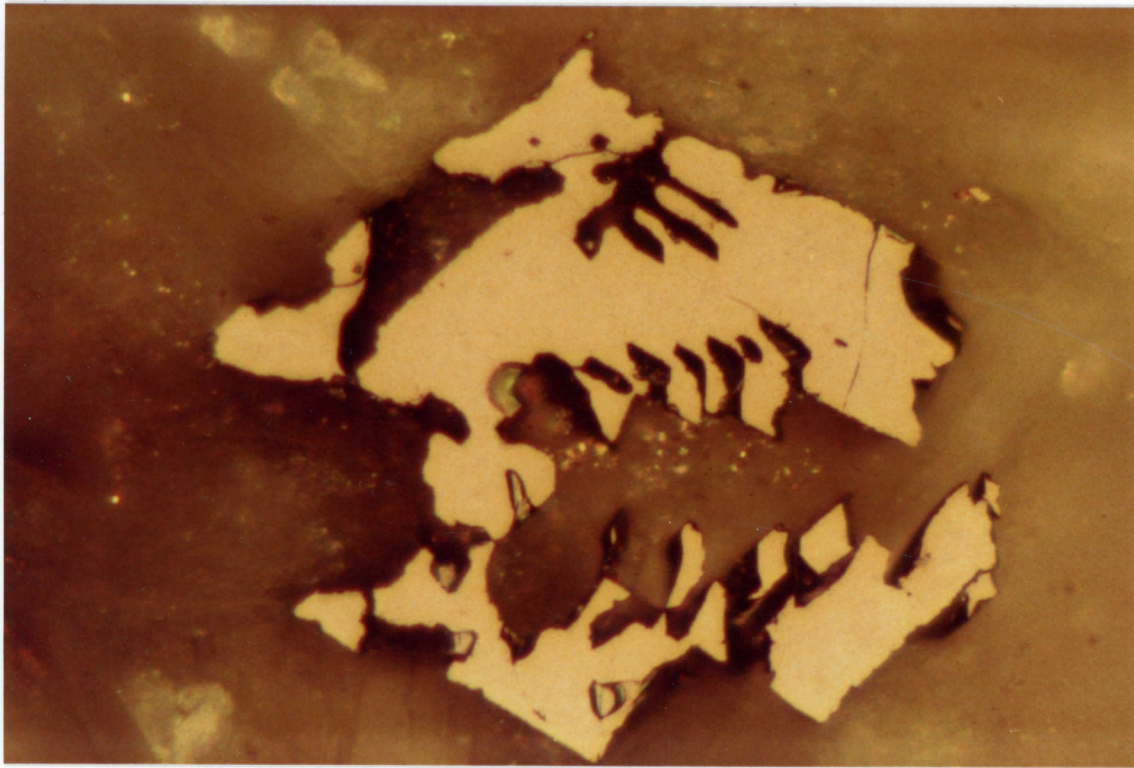


PLATE 22: CY-2 76.70 m. Skeletal magnetite grain. Magnification: 250 X.

Primary ilmenite was observed at the top of the interval between 20 m and 40 m comprising a minor proportion of the sample, and again at the base of the interval between about 90 m and 93 m, where it occurs as a trace component.

Pyrite is ubiquitous in the interval represented by the samples. It is a trace component of the matrix throughout the section with the exception of the argillized zone around 45 m where it comprises a minor proportion of the sample. This increase in concentration is due to the introduction of significant amounts of secondary pyrite in hydrothermal veins.

Sphalerite appears twice in the interval examined and always as a trace component. It was observed between about 20 m and 30 m and again between 90 m and 93 m.

Chalcopyrite is not present in the samples examined from Hole CY-2.

(b) CY-2A Core: The downhole distribution of primary plagioclase, pyrite, magnetite and ilmenite, as well as secondary minerals and lithology in the samples studied from Hole CY-2A is shown in figure 9.

Smectite minerals comprise a dominant proportion of the samples between approximately 135 m and 154 m. They continue to be present in subordinate proportion to about 174 m, and gradually decrease in concentration until they are completely absent at 180 m. An anomalous presence of smectite within the argillized zone was observed at 207 m

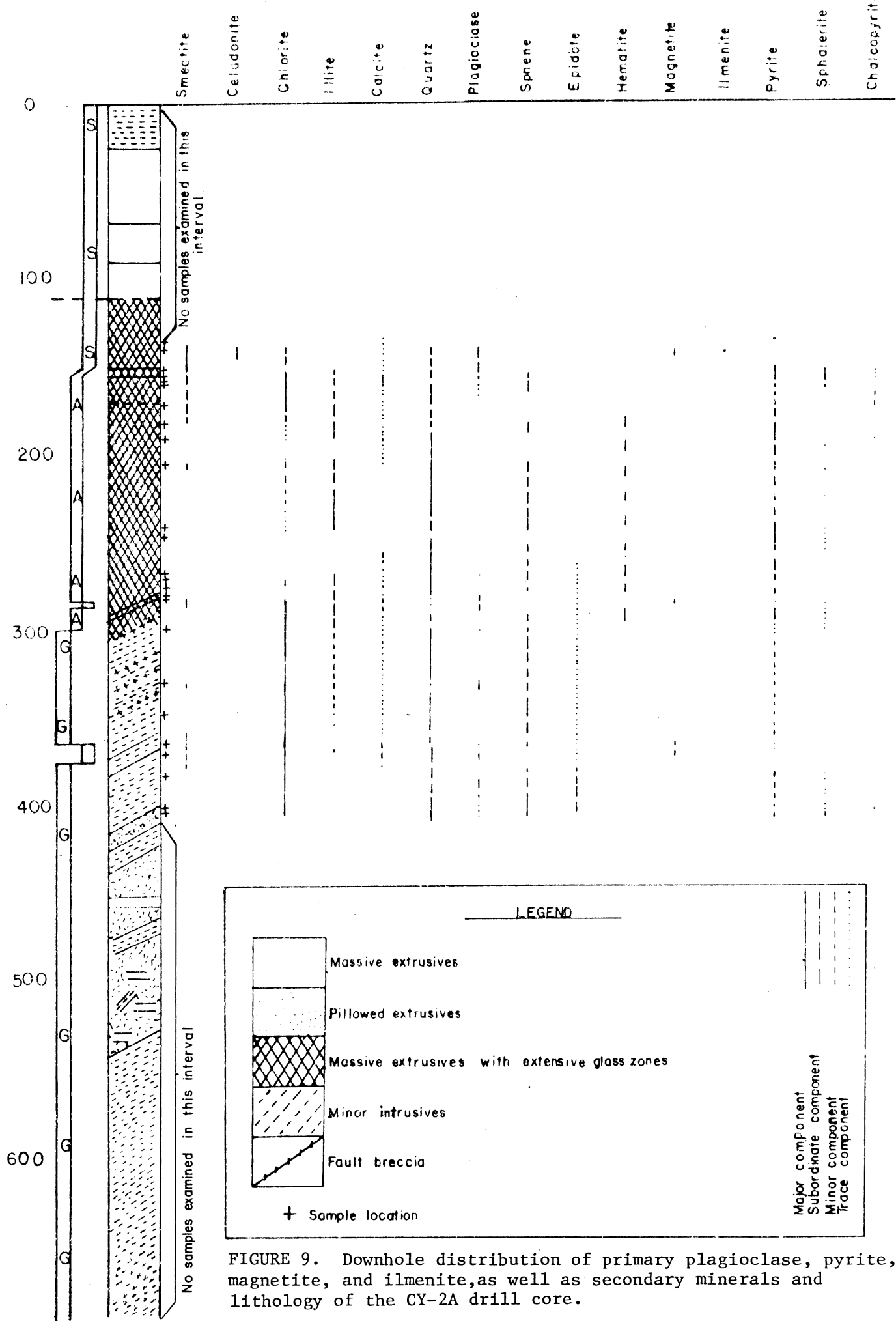


FIGURE 9. Downhole distribution of primary plagioclase, pyrite, magnetite, and ilmenite, as well as secondary minerals and lithology of the CY-2A drill core.

where it occurs as a minor component. Throughout the remainder of the section it is found only locally as a minor component within an altered dike sample, and as a subordinate to major component within the post-mineralization dikes.

Celadonite was observed in only one sample, CY-2A 141.45 m, where it occurs as a subordinate component.

Chlorite is found throughout most of the section but is concentrated at the top of the interval between approximately 140 m and 175 m in the less altered samples, and again at the lower end of the interval between 280 and 407 m in the samples which have undergone alteration in greenschist facies conditions. Chlorite is absent or present in trace to minor, and locally subordinate, proportion between 175 m and 280 m in the interval of intense argillic alteration.

Illite is found throughout most of the interval. It first appears in minor proportion at 158 m and increases in concentration to 184 m where it occurs as a major component. Illite is absent in the massive ore unit around 193.00 m, and also in the jasper-pyrite veins which occur locally in the interval of argillic alteration. It is, however, present in subordinate to major proportions throughout the remainder of the argillized zone. Illite is absent or present in minor amounts in the samples between 285 m and 370 m. Illite was not observed below 370 m.

Secondary calcite occurs as a trace component between 135 m and 152 m. At the top of the mineralization at 153 m it increases in abundance to become a minor component and attains its highest concentration at 157 m, where it forms a major proportion of a large vein. Between 158 m and 210 m calcite is present only in trace amounts. Calcite is absent between 210 m and 260 m in the argillized interval, but appears again as a trace component between 260 m and 370 m. Locally in this interval calcite is present in minor proportions within the post-mineralization dikes. Calcite is absent between 370 m and the base of the interval at 407 m.

Quartz is ubiquitous below about 137 m in the interval represented by the samples. It occurs as a minor to subordinate component in the less altered basalts between approximately 140 m and 156 m. Below this level in the argillized interval, quartz generally comprises a major proportion of the matrix. Its concentration decreases in the greenschist alteration zone to a subordinate component, however quartz occurs locally as a trace to minor component within the post-mineralization dikes and the altered dike unit at 332.85 m.

Primary plagioclase, identified as labradorite in sample 141.45 m, is present as a minor to subordinate component between 140 m and 165 m. In the argillized interval between 165 m and 302 m plagioclase is absent or present locally in trace amounts. In the remainder of the core plagioclase, present as two varieties, comprises trace to subordinate proportions of the sample. The plagioclase in this interval consists of lesser, highly altered, primary plagioclase microlites together with dominant, subhedral to euhedral, secondary albite.

Sphene occurs irregularly throughout the section. It first appears as a minor component at 156.91 m, but increases to subordinate and major proportions where it occurs locally within the remainder of the interval. Sphene is noticeably absent or present in minor amounts within the post-mineralization dikes.

Epidote is absent in the upper part of the interval but is present as a trace component between approximately 275 m and 375 m. For the rest of the sequence to 407 m, epidote occurs as a minor proportion of the sample.

Secondary hematite is a major component of the jasper-pyrite veins which occur locally within the argillized zone between approximately 180 m and 300 m.

Magnetite of likely primary origin was found occurring in the relatively fresh basalt at the top of the interval, and again in the post-mineralization dikes. In all cases magnetite comprises a trace to minor proportion of the matrix.

Primary ilmenite was observed only in the sample at 141.45 m, where it occurred as a trace component.

Pyrite is ubiquitous in the interval represented by the samples. It is concentrated in the highly mineralized zone between 153 m and 300 m where it occurs as a subordinate to major component. It is present in trace to minor proportions in the remainder of the interval.

Sphalerite is present in the greatest concentration at the beginning of the mineralized sequence between 152 m and 155 m where it comprises a major proportion of the sample. Between 155 m and approximately 162 m it is found as a minor component. Sphalerite was observed occurring in trace amounts locally within the argillized zone and at the base of the unit between 386.40 m and 405 m. The last meter of the section studied contained a minor proportion of sphalerite.

Chalcopyrite is limited in occurrence within the CY-2A samples examined. It is present as a trace to minor component around 153 m, and again between 160 m and 175 m. The only other samples in which chalcopyrite was observed are 193.00 m and 404.40 m. At both levels chalcopyrite was present only in trace amounts.

6.2 Paragenetic Sequence of the Secondary Minerals

(a) Paragenesis of the Clays, Chlorites and Micas in CY-2 and CY-2A:

The paragenetic sequence of this group of secondary alteration minerals in CY-2 and CY-2A is shown in figure 10 and appears to be as follows:

green	→	green	→	green	→	illite	→	brown	→	green
to		and		chlorite		and		and		chlorite
brown		brown		in veins		clear		green		in veins
smectite		chlorite		and		chlorite,		chlorite		and
		in matrix		vesicles		primarily		in matrix		vesicles
						in matrix				

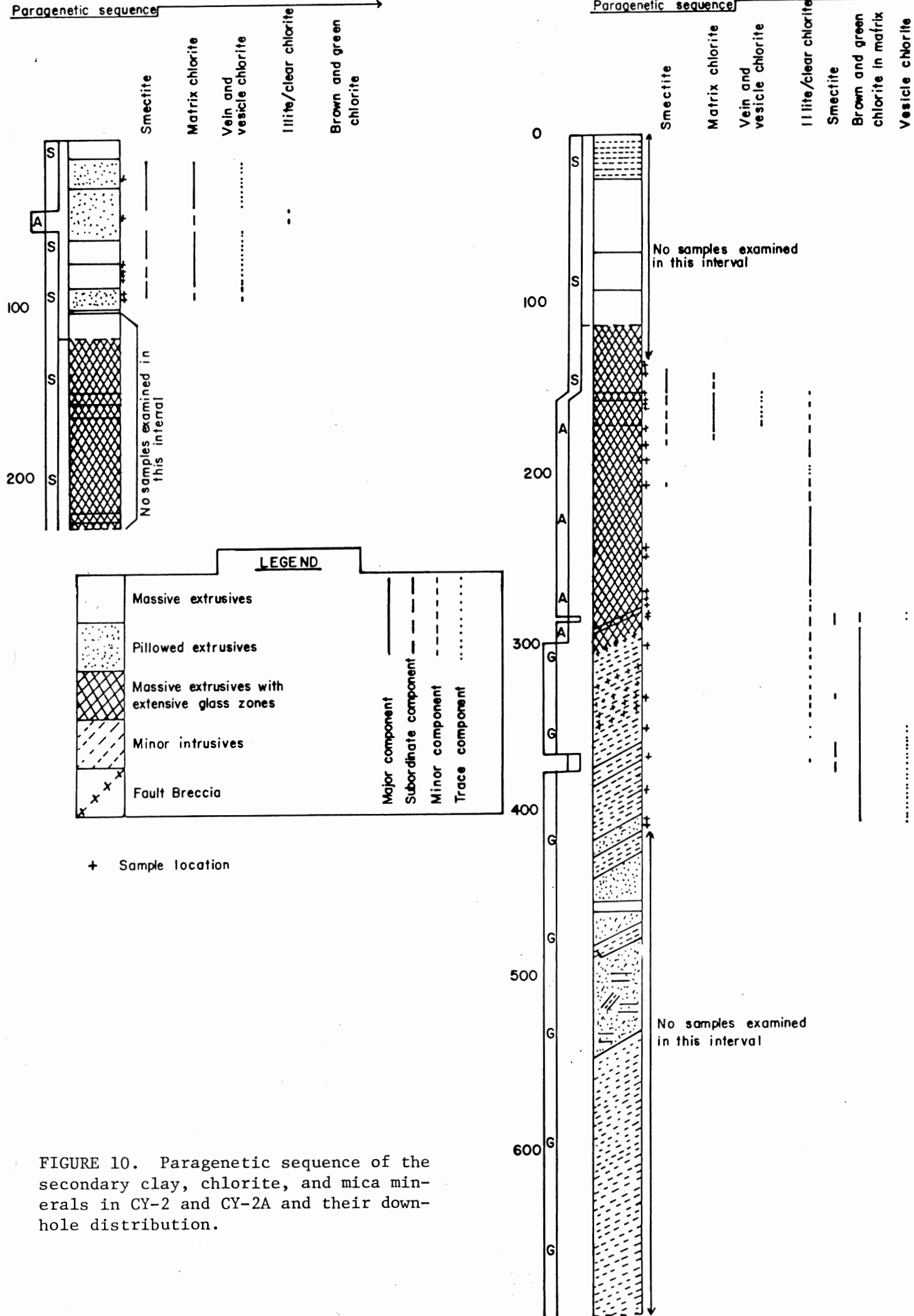


FIGURE 10. Paragenetic sequence of the secondary clay, chlorite, and mica minerals in CY-2 and CY-2A and their down-hole distribution.

The paragenetic sequence within the post-mineralization dikes is:

brown smectite → green and olive → green chlorite
 in matrix chlorite in in vesicles
 matrix and veins

The distribution of the different phases in samples from CY-2 is similar to their distribution in samples from CY-2A that have undergone similar styles of alteration.

In CY-2, green to brown smectite occurs in interstices of the matrix as a dominant component between 20 m and 40 m, and again from approximately 50 m to 70 m. In the remainder of the core it is present as a subordinate component.

In CY-2, green matrix chlorite formed after the smectite occurs throughout the studied interval as a major component, with the exception of the argillized zone between 40 m and 50 m where it is a pale green, subordinate component, and the base of the interval between 90 m and 93 m where it also occurs in subordinate proportions.

The darker, more bluish-green chlorite formed in the veins and vesicles of the CY-2 samples after the formation of the matrix chlorite, is found throughout the section as a trace component, and at the base as a minor component, with the exception of the argillized interval between 40 m and 50 m where this phase of chlorite is absent.

Minor proportions of illite were observed only in the argillized zone of CY-2.

In CY-2A, early formed smectite occurs at the top of the interval between 135 m and 175 m as a major to subordinate component. Below this depth it continues to be present as a minor component for a few metres, and then is entirely absent.

Green and brown chlorite, formed after the smectite, occurs as a minor to major component in the same interval as the smectite.

The green chlorite in the vesicles was observed between 154 m and 175 m forming a trace proportion of the sample. This interval coincides with the section in which the matrix chlorite is a major component.

Illite was first observed as a minor component adjacent to the veins and vesicles around 153 m. It continues to be present in this proportion until 174 m where it increases in abundance to a subordinate component. Between 174 m and 300 m illite, and locally clear chlorite, occur in subordinate to major proportions. Below 300 m, this alteration phase decreases in concentration until it is no longer present at about 360 m.

A later phase of brown smectite occurs deeper in the core within the post-mineralization dikes where it comprises subordinate to major proportions of the samples.

The late brown and green chlorite occurring in the matrix first appears at about 280 m as a subordinate component. At 290 m it increases in proportion to a major component, and continues to be present at this concentration to the base of the interval at 407 m.

The latest phase of chlorite is the green variety which occurs in the veins and vesicles of the samples near the base of the interval as a trace component. It first appears in the post-mineralization dike at 282.45 m, and then again between 349 m and 407 m.

b) Paragenesis of the Ore Minerals in CY-2 and CY-2A:

The paragenetic sequence of the ore minerals in CY-2 and CY-2A is shown in figure 11 and appears to be as follows:

magnetite	→	secondary	→	secondary	→	pyrite +	→	sphalerite	→	later
+ pyrite		pyrite +		sphalerite		hematite				secondary
+ ilmenite		hematite								pyrite
are		in CY-2								
probably		<u>or</u>								
primary		secondary								
		pyrite +								
		chalcopyrite								
		in CY-2A								

The downhole distribution of the ore minerals in CY-2 is as follows. Primary magnetite, pyrite and ilmenite occur as minor disseminations throughout the interval represented by the samples, however at the base of the sequence between 83 m and 93 m they are present in trace amounts.

Secondary pyrite and hematite first appeared in and adjacent to the veins in the argillized zone as minor components. They occur again between approximately 76 m and 97 m in trace to minor proportions of the samples, but concentrated in the veins.

Traces of honey-yellow sphalerite were observed disseminated in the matrix in the interval between 20 m and 40 m and again at the base of the sequence between 90 m and 93 m. This phase of sphalerite was never observed in contact with the secondary pyrite and hematite and so its exact position in the paragenetic sequence is uncertain.

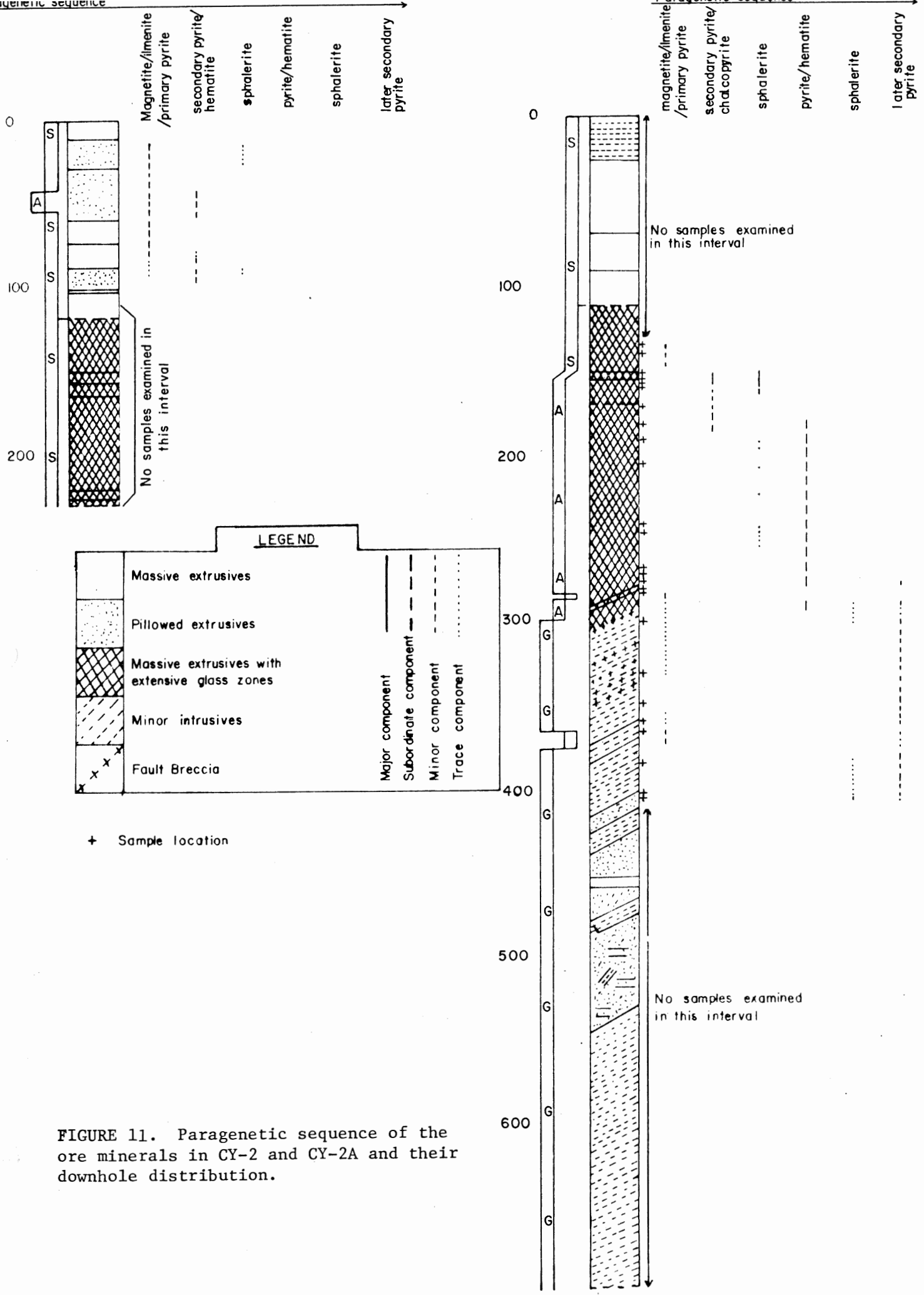


FIGURE 11. Paragenetic sequence of the ore minerals in CY-2 and CY-2A and their downhole distribution.

The paragenesis of the ore minerals and their downhole distribution in CY-2A is more complex, reflecting the intense hydrothermal mineralization of these samples.

What appear to be primary magnetite, ilmenite and pyrite were found at the top of the interval between 135 m and 145 m within the relatively fresh basalts, and again near the base of the sequence between 282 m and 335 m, and between 354 m and 374 m within the altered and post-mineralization dikes. The primary ore minerals occur in trace to minor proportions.

In contrast to CY-2, the first phase of secondary pyrite occurs with chalcopyrite rather than with hematite. These minerals first appear at the top of the mineralized sequence at 153 m as major components of the samples. They occur intergrown and therefore appear to have formed at the same time (plate 23). Between 160 m and 189 m they are present in minor to subordinate proportion, and do not occur again in the remainder of the section. Pyrite and chalcopyrite are concentrated in the veins and vesicles of the samples but are also present as finer-grained disseminations in the matrix.

The first phase of sphalerite crystallized after the formation of pyrite and chalcopyrite as evidenced by the growth of sphalerite around pyrite grains and its projection into pyrite (plate 24). It first appears at the top of the mineralized zone at 153 m as a major component. Between 160 m and 166 m the sphalerite grains are present in subordinate amounts. Sphalerite is concentrated in the veins and

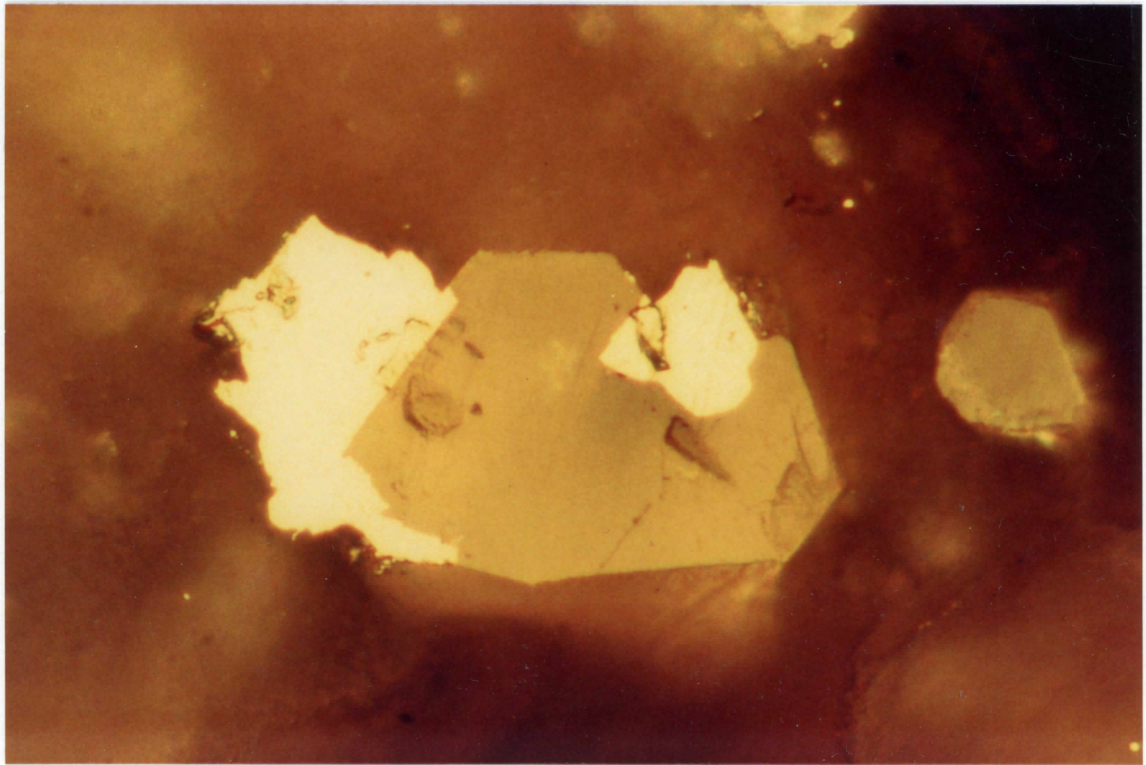
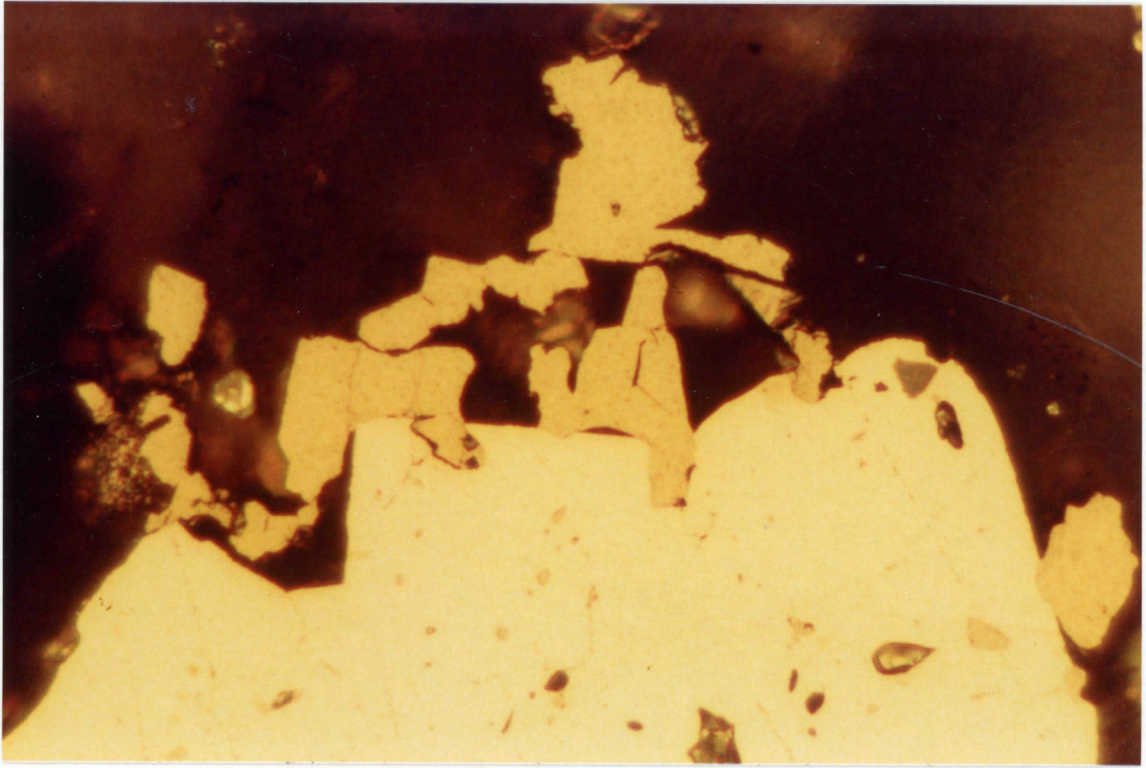


PLATE 23. CY-2A 153.25 m. Intergrown yellow pyrite and orange chalcopyrite.
Note projections of chalcopyrite into pyrite and inclusion of
chalcopyrite in pyrite in lower right. Magnification: 250X.

PLATE 24. CY-2A 153.25 m. Grey, subhedral sphalerite is growing around
and projecting into yellow pyrite. Magnification: 250X.

vesicles, but was also observed disseminated in the matrix. Cryptocrystalline, droplet-like inclusions of sphalerite were observed in the cores of pyrite grains locally in the interval between 190 m and 257 m. These inclusions are believed to be relics of the replacement of sphalerite grains by a later pyrite phase.

A later phase of secondary pyrite is present between 180 m and 290 m in subordinate, and usually in major, proportions. Locally it occurs with abundant hematite within the jasper-pyrite veins. In some samples, for example the "massive ore" samples, the pyrite may form up to 60% of the sample.

Sphalerite appears again in trace proportions as very fine grains in vesicles and veins between 285 m and 303 m, and again between 383 m and 405 m. At the very base of the interval its concentration increases to minor amounts.

A third phase of secondary pyrite is known to exist because veins of 100% pyrite are seen to cross-cut jasper-pyrite veins. In addition, pyrite was observed forming around the later phase of sphalerite and projecting into the sphalerite grains. This latest phase of pyrite occurs between 285 m and 407 m as a trace to minor component however it is absent, or present in only trace amounts, within the post-mineralization dikes.

6.3 Probable Relative Temperatures of Alteration of a Number of Samples from Different Levels in the Cores

The positions of the CY-2 and CY-2A cores with respect to the paleohydrothermal system which produced the Agrokipia A and B massive sulphide deposits are illustrated in figure 12. CY-2A intersected highly altered and mineralized basalts and therefore probably the mineralized stockwork zone of the Agrokipia B deposit. Most of the samples recovered by CY-2 are relatively fresh to partly altered and therefore probably come from the weaker mineralized zone of the Agrokipia A deposit. Figure 12 is highly simplified and does not take structural relationships between the cores and the regional geology into account.

The probable relative temperatures of alteration of samples from four levels are considered. Sample A is a typical partly altered basalt sample from CY-2. This sample would be affected by relatively low temperatures at its position near the paleoseafloor, producing a smectite + green chlorite + quartz + hematite alteration mineral assemblage.

The downward penetrating seawater became increasingly saline and hotter with depth as it moved towards the present Agrokipia B stockwork zone.

Sample B is a highly altered basalt sample in which alteration occurred under conventional greenschist facies conditions. Of the samples examined, this sample would have been exposed to the highest temperatures, resulting in a chlorite + epidote + albite + pyrite + sphalerite alteration mineral assemblage.

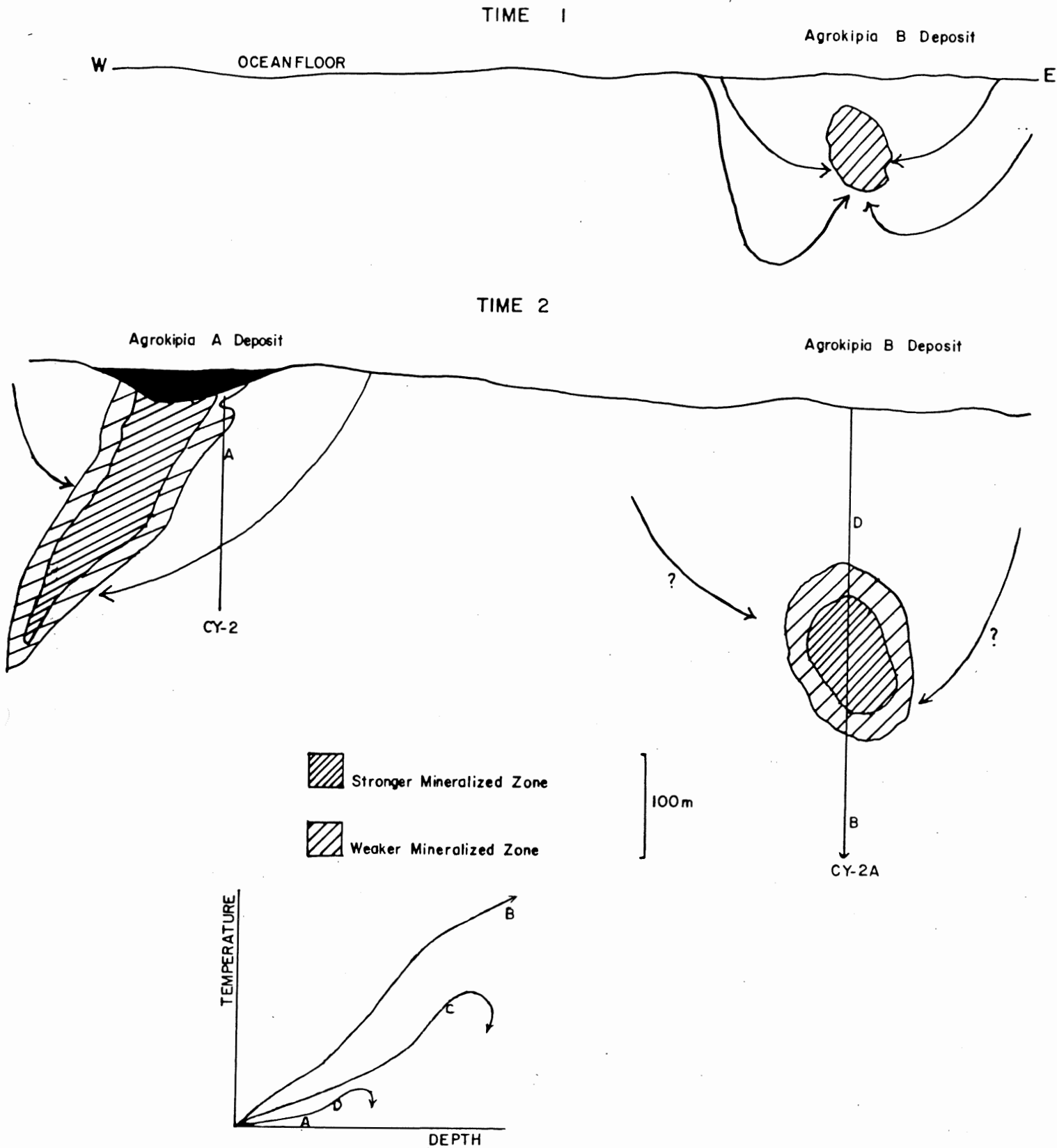


Figure 12: Schematic diagrams illustrating the formation of the Agrokipia B deposit at Time 1, followed by the deposition of Agrokipia A at a later time, T2. The convective system which formed Agrokipia B may or may not have still been active at Time 2. The position of the CY-2 and CY-2A cores relative to the deposits is shown in the second diagram. The probable relative temperatures of alteration of sample A from CY-2, and samples B, C, and D from CY-2A are depicted in the graph below.

As the mineralizing solution rose in the channels its temperature gradually decreased due in part to mixing with increasing volumes of downward seeping seawater.

Sample C, coming from the argillized zone, was affected by temperatures lower than those affecting Sample B. The alteration mineral assemblage in this sample is illite + quartz + sphene + pyrite + hematite.

Sample D is a partly altered basalt containing abundant smectite and chlorite. Sample D would have been exposed to even lower temperatures than Sample C, but probably slightly higher temperatures than those affecting Sample A because of the position of D near the paleohydrothermal system.

CHAPTER 7

SUMMARY

The thirty-four drill core samples studied from Holes CY-2 and CY-2A can be classified into four groups with regard to their alteration and mineralization characteristics. A stable secondary mineral assemblage is associated with each group. The four groups are:

1. Relatively fresh to partly altered basalt (all CY-2 samples, with the exception of CY-2 48.05 m, as well as CY-2A 136.70 m and 141.45 m)
Assemblage: abundant smectite + green chlorite + minor quartz + hematite
2. Partly to highly altered and highly mineralized basalt (CY-2A 152.90 m to 161.19 m)
Assemblage: green and brown chlorite + smectite + pyrite + sphalerite + chalcopyrite
3. Pervasively altered and highly to pervasively mineralized basalt (CY-2 48.05 m and CY-2A 173.66 m to 285.05 m, with the exception of 282.45 m)
Assemblage: illite + quartz + sphene + pyrite + hematite
4. Highly to pervasively altered and partly mineralized basalt (CY-2A 282.45 m, and 302.35 m to 406.85 m)
Assemblage: abundant green and brown chlorite + albite + epidote + pyrite + sphalerite

The temperatures and pressures of formation increase from assemblage 1 to assemblage 4. Except for sample CY-2 48.05, it appears that Hole CY-2 did not penetrate hydrothermally altered basalts while the 150 m to 300 m interval in Hole CY-2A represents the most intense hydrothermal activity.

Suggestions for Future Work

1. A comparison of whole rock chemical analyses of the altered basalt samples with analyses of fresh basalt samples would be useful in the determination of the bulk chemical changes produced by hydrothermal alteration.
2. Complete chemical analyses obtained by electron microprobe transects from the matrix of a sample to the altered margin of a vein and into the vein itself would also aid in the determination of the exact nature of the chemical exchange between the hydrothermal solutions and the basalt.
3. Reliable identification of all the secondary sheet silicate minerals through separation procedures, followed by application of thermal and organic liquid treatments between X-ray diffraction analyses, is required.
4. The role of the massive glass sections in the formation of the ore deposits may be determined by means of a detailed examination of their structural and chemical relationship to adjacent lithologies.

5. What is the significance of the Mn-rich chlorites and calcites? Determination of the continuous variation of Mn with depth is required to answer this question. Perhaps all the manganese is not vented at the seafloor as was previously believed.

6. A detailed search of the literature dealing with observed and experimental determinations of the conditions of formation of the secondary minerals present in the CY-2 and CY-2A cores should be carried out. Limits can then be placed on the physical and chemical parameters that prevailed during the life of the hydrothermal system, and their variation with depth.

REFERENCES

- Adamides, N.G. (1975): Geological history of the Limni concession, Cyprus in the light of the plate tectonics hypothesis. Trans. Inst. Min. Met., 84, B17-23.
- Bear, L.M. (1960): The geology and mineral resources of the Akaki-Lythrodondha area. Cyprus Geol. Surv. Dept. Mem., 3, 122 p.
- Bear, L.M. (1963): The mineral resources and mining industry of Cyprus. Cyprus Geol. Surv. Dept. Bul., 1, 184 p.
- Castaneda, G., Palaganas, U., Wang, B. (1982): Geological study of the Agrokipia "A" pit and vicinity. Unpublished report resulting from Cyprus Crustal Study Project, 19 p.
- Constantinou, G. (1980): Metallogenesis associated with Troodos ophiolite: in Panayiotou, A., ed., Ophiolites, Proceedings International Ophiolite Symposium, Cyprus, 1979, p. 663-674.
- Constantinou, G. and Govett, G.J.S. (1973): Geology, geochemistry and genesis of Cyprus sulphide deposits. Econ. Geol., 68, p. 843-858.
- Deer, W.A., Howie, R.A. and Zussman, J. (1962): Rock-forming minerals, sheet silicates, V. 3, Longman, London, 270 p.
- Deer, W.A., Howie, R.A. and Zussman, J. (1966): An introduction to the rock-forming minerals, Longman, London, 528 p.
- Francheteau J., Needham, H.D., Choukroune, P., Juteau, T., Seguret, M., Ballard, R.D., Fox, P.J., Normark, W., Carranza, A., and Cordoba, D. (1979): Massive deep-sea sulfide ore deposits discovered by submersible on the East Pacific Rise: Project RITA, 21°N. Nature, 277, p. 523-528.
- Gass, I.G. and Masson-Smith, D. (1963): The geology and gravity anomalies of the Troodos massif, Cyprus. Roy. Soc. London Phil. Trans., A255, p. 417-467.
- Hajash, A. (1975): Hydrothermal processes along mid-ocean ridges: an experimental investigation. Contrib. Min. Pet., 53, p. 205-226.
- Hajash, A. (1977): Experimental sea water/basalt interactions: effects of water/rock ratio and temperature gradient. Geol. Soc. Am. Ann. Meeting Abstracts, p. 1002.

- Hutchinson, R.W., Fyfe, W.S., and Kerrich, R. (1980): Deep fluid penetration and ore deposition. Minerals Sci. Engng., 12, no. 3, p. 107-120.
- International Crustal Research Drilling Group (1983): Drilling investigations of the Agropia paleohydrothermal system, Cyprus. Nature, in press.
- Kalliokoski, J. (1974): Pyrite framboids: animal, vegetable or mineral? Geology, 2, no. 1, p. 26-27.
- Love, L.G. (1957): Micro-organisms and the presence of syngenetic pyrite. Geol. Soc. London Quart. Jour., 113, p. 429-440.
- Ramdohr, P. (1979): The ore minerals and their intergrowths. Pergamon Press, Oxford. 1174 p.
- Rickhard, D.T. (1970): The origin of framboids. Lithos, 3, p. 269-293.
- Robertson, A.H.F. (1977): Tertiary uplift of the Troodos massif, Cyprus. Geol. Soc. Amer. Bull., 88, 1763-1772.
- Searle, D.L. (1972): Mode of occurrence of the cupriferous pyrite deposits of Cyprus. Trans. Inst. Min. Met., 81, B89-97.
- Spooner, E.T.C. (1977): Hydrodynamic model for the origin of the ophiolitic cupriferous pyritic ore deposits of Cyprus: in Volcanic processes in ore genesis., Inst. Mining Metallurg., London, United Kingdom, p. 58-71.
- Spooner, E.T.C., Bray, C.J., and Chapman, H.J. (1977): A seawater source for the hydrothermal fluid which formed the ophiolitic cupriferous pyrite ore deposits of the Troodos massif, Cyprus [abstr]. Geol. Soc. Lond. J., 134, p. 395.
- Spooner, E.T.C., Chapman, H.J., and Smewing, J.D. (1977): Strontium isotopic contamination and oxidation during ocean floor hydrothermal metamorphism of the ophiolitic rocks of the Troodos massif, Cyprus. Geochim. Cosmochim. Acta, 41, no. 7, p. 873-890.
- de Vaumas, E. (1959): The principle geomorphological regions of Cyprus. Cyprus Geol. Surv. Dept. Ann. Rept. for 1958, p. 38-42.
- de Vaumas, E. (1961): Further contributions to the geomorphology of Cyprus. Cyprus Geol. Surv. Dept. Ann. Rept. for 1960, p. 24-34.

Appendix 1: CY-2 Sample Descriptions

M=major component(>20%), S=subordinate component(>10-20%), m=minor component(5-10%), t=trace component(<5%).

Sample (depth in m)	Rock Type, Texture and Core Unit	Matix Mineralogy			Vesicles			Veins			Ore Minerals		
		Mineral	Proportion of Matrix	Description	(%) of sample	Diam- eter(mm)	Description	% of sample	Width (mm)	Description	% of ore minerals	Description	
24.00	Partly altered basalt. Both intersertal and hyalophitic textures present in patches but the hyalophitic texture is dominant. Unit II: pillowed lava	chlorite	M	very fine-grained anhedral patches or flakes arranged in radial structures; replacement mineral of primary phenocrysts.	4	0.3-2.0	partly to completely filled with quartz. Grain size of quartz increases from wall to core. Some have a narrow quartz lining and a large chlorite core.	<1	0.4-0.9	2 quartz veinlets; 2 empty fractures	47	cryptocrystalline, subhedral to anhedral magnetite occurs as disseminations	
		quartz	S	fine, single, anhedral grains in interstitial spaces; replacement mineral of primary phenocrysts							47	cryptocrystalline, subhedral, ilmenite laths	
		plagioclase	S	microlites are partly altered to chlorite and smectite.							3	scattered, very-fine-grained subhedral to anhedral pyrite.	
		smectite	M	brownish-olive; occurs in irregular patches in association with chlorite							3	subhedral, honey-gold sphaerite occurs in a vesicle and veinlet.	
		ore minerals	m	very fine-grained and disseminated									
48.05	Pervasively altered and partly mineralized basalt. Relict hyalophitic texture. Unit III: pillowed lava	chlorite	S	very fine-grained anhedral patches or flakes; replacement mineral of primary phenocrysts (pyroxene and/or olivine?)	4	0.4-0.6	quartz-filling; grain size of quartz increases from wall to core of vesicle.	3	0.4 and 1.0 mm	the 2 veins are slightly anastomosing with poorly defined boundaries. One variety of chlorite lines the veins and another comprises the core ± minor py.	60	magnetite occurs as anhedral, cryptocrystalline disseminations	
		quartz	M	fine, single, anhedral grains; replacement mineral of primary phenocrysts (olivine and plagioclase?)							40	pyrite occurs in two forms 1) primary very fine-grained, disseminated, pyrite is generally subhedral. 2) secondary fine-grained pyrite occurs in veins, and in matrix adjacent to veins, as subhedral grains.	
		plagioclase	none	microlites completely replaced by chlorite and quartz									
		illite	m	occurs replacing plagioclase as very fine-grained flakes									
		ore minerals	m	fine-grained and disseminated as well as concentrated in vesiculated areas of matrix.					1-1.5	one pyrite + one hematite + chlorite vein in handsample.			

Sample (depth in m)	Rock Type, Texture and Core Unit	Matrix		Mineralogy	Vesicles		Veins		Ore	Minerals		
		Mineral	Proportion of Matrix	Description	(%) of sample	Diameter (mm)	Description	% of sample	Width (mm)	Description	% of ore minerals	Description
82.50	Partly altered basalt. Intersertal texture Unit V: massive flow	chlorite	M	subhedral, fine-grained flakes; replacement mineral of primary phenocrysts; occurs in the phenocryst cores and is rimmed by hematite				5	0.1-20	3 types of veins 1 Hematite vein and veinlet 2 chlorite- lined, quartz- filled 3 chlorite veinlets; All veins and veinlets are subparallel.	60	magnetite is cryptocrystalline to fine-grained and anhedral to subhedral. Larger grains are skeletal. Occurs with pyrite and before hematite
		quartz	m	fine-grained, anhedral scattered grains and slightly larger grains fill small cavities (<0.3mm) in matrix							36	anhedral and colloidal hematite
		plagioclase	M	microlites are slightly altered to chlorite and lesser smectite							10	primary pyrite is subhedral to anhedral and very fine- to fine- grained; occurs as disseminations.
		smectite	S	reddish-brown to darker brown, closely associated with chlorite								
		hematite	t	occurs adjacent to hematite vein in matrix.								
		calcite	t	medium-grained, anhedral, replacement mineral								
		ore minerals	t	fine-grained and disseminated								
84.15	Partly altered basalt. Well-defined intersertal texture. Unit V: massive flow	chlorite	M	subhedral, fine-grained flakes;	8	1.2-3.5	Vesicles are filled with dark green smectite containing minor quartz grains and plagioclase microlites. Patchy occurrences of brown smectite within green smectite.	5	0.9-1.5	anastomosing veins are inter- rupted by large vesicles. The veins have a very dark green smectite matrix within which are minor random quartz grains and plagioclase micro- lites as well as small chlorite ± minor quartz vesicles. Also, small patches of pyrite are present.	60	pyrite occurs mainly as secondary, fine- grained, subhedral pyrite in veins and vesicles; minor, prim- ary, disseminated cryptocrystalline pyrite in matrix.
		quartz	S	anhedral, fine-grained isolated grains								
		plagioclase	S	microlites are partly altered to chlorite and smectite.								
		smectite	M	very dark-green smectite								
		iddingsite(?)	t	anhedral, reddish-brown, very fine-grained								
		ore minerals	m	very fine-grained and disseminated							40	cryptocrystalline, subhedral magnetite and possibly ilmenite (fine microlites are present)
						<0.2- 2	Smaller vesicles within larger vesicles have a narrow quartz lining (5%) and a chlorite (90%) plus pyrite (5%) core.				t	hematite in vesicles is anhedral

Sample (depth in m)	Rock Type, Texture and Core Unit	Matrix		Mineralogy Description	Vesicles		Veins		Ore Minerals						
		Mineral	Proportion of Matrix		(%) of sample	Diameter (mm)	Description	% of sample	Width (mm)	Description	% of ore minerals	Description			
92.30	Highly brecciated, relatively fresh, glassy basalt Hyalophitic texture. Unit VI: pillowed lava.	chlorite	S	anhedral, yellowish olive-green chlorite is ubiquitous in matrix.	3	0.3- 2.5	subangular to elliptic; filled with quartz or lined with chlorite followed by quartz and a core of chlorite. Some vesicles are circled with a single layer of anatase. (80% chlorite, 20% quartz)	20	0.3- 3.0	Complex fracture pattern; frac- tures are filled with quartz, botroidal hematite and chlorite (70% quartz, 20% hematite, 10% chlorite). Occa- sional minor pyrite.	70	hematite occurs largely in the vein with botroidal and colloform textures			
		plagioclase	M	euhedral microlites are quite fresh. Several medium-grained phenocrysts are partly altered to chlorite.									20	pyrite occurs as very fine-grained, anhedral grains in vein with hematite;	pyrite sometimes found within pellets of hematite
		smectite	M	cloudy greenish-brown smectite occurs in association with chlorite.									5	magnetite occurs as anhedral, very fine grains collected in a pyrite-hematite colloidal liquid; also occurs disseminated in matrix	
		anatase	m	very fine-grained, brown min- eral ubiquitous in matrix.									5	ilmenite microlites occur arranged around vesicles and disseminated	
		quartz	t	occasional, fine-grained, anhedral.											
		ore minerals	m	cryptocrystalline and dissem- inated				< 0.4	Numerous chlorite-filled veinlets						
92.85	Somewhat brecc- iated, relatively fresh, glassy basalt. Hyalophitic texture approaching inter- sertal in small patches. Unit VI: pillowed lava.	chlorite	S	anhedral, yellowish, olive-green chlorite is fine-grained.	5	0.3-1	vesicles are lined with chlorite, fol- lowed by quartz and a core of chlorite	10	< 0.5- 5 ave. = 2mm	veins are filled with a mixture of chlorite, quartz and hematite	50	hematite occurs in the same forms as in C-2 92.30			
		plagioclase	M	microlites and several phenocrysts are slightly altered to chlorite.									15	pyrite occurs as fine, anhedral grains scattered in the matrix -	
		quartz	t	occasional, fine-grained, anhedral quartz and medium-grained phenocrysts											
		smectite	M	both brown smectite and greenish-brown smectite occur in separate patches in the sample. Some smectite-free patches also.									35	may be primary cryptocrystalline anhedral grains of sphalerite (?) and magnetite, as well as microlites of ilmenite.	
		ore minerals	m	several irregularly scattered grains are very fine-grained. Numerous, cryptocrystalline, disseminated grains.											

Sample (depth in m)	Rock Type, Texture and Core Unit	Matrix		Mineralogy	Vesicles		Veins		Ore	Minerals					
		Mineral	Proportion of Matrix	Description	(%) of sample	Diameter (mm)	Description	% of sample	Width (mm)	Description	% of ore minerals	Description			
152.90	Partly altered and highly mineralized basalt Hyalophitic texture Unit VII: massive lava with hydro-thermal veins.	chlorite	M	occurs in anhedral, very fine-grained patches and as subhedral flakes arranged in radial structures	8	ave. ~ 1.0	vesicles are irregular in shape and size; generally empty or partly lined with quartz ± sulphides ± chlorite; one vesicle is almost filled with calcite. 4 mm in length elliptical cavity joins vein and contains 3 generations of quartz.	< 1	0.1-0.7 ave. = 0.4	vein is filled with mixed sphalerite, pyrite, quartz, chalcopyrite and calcite (in order of decreasing abundance). The vein has a 5 mm wide alteration zone with sharp boundaries. < 0.2 several calcite-filled fractures		sphalerite in the altered margin has a higher iron-content than the sphalerite in the vein itself. Sphalerite is probably dominant over pyrite (this is an estimate because there is no polished section for this sample).			
		quartz plagioclase	m S	fine-grained, anhedral, isolated grains fine-grained, subhedral microlites partly altered to smectite and chlorite											
		smectite	M, but less than chlorite	greenish brown smectite is mixed with chlorite throughout the sample except in altered margin of vein where chlorite appears to be absent and only minor brown smectite is present.											
		ore minerals	S	fine-grained and disseminated											
153.10	Partly altered and highly mineralized glassy basalt. Hyalophitic texture Unit VII: massive lava with hydro-thermal veins.	quartz plagioclase	m m	fine-grained, anhedral isolated grains euhedral to subhedral microlites are slightly altered to smectite.	8	0.2-4.0 ave. = 1.5	elliptical to spherical vesicles are lined with sphalerite plus pyrite and filled with 1 to 3 generations of quartz or have an empty core.	25	0.5-1.0	veins are filled with quartz, sphalerite and pyrite in variable proportion as well as minor calcite. Medium grained euhedral laths of laumontite (?) occur in quartz of largest vein. Altered margin of vein is 0-3 mm wide; maximum extent adjacent to sulphide concentrations in vein.		sphalerite is more abundant than pyrite in veins and vesicles. It ranges from very fine to medium-grained and is generally subhedral; sphalerite is either pure honey-yellow or zoned with a yellow core and a narrow rust-brown rim. Pyrite is subordinate and very-fine to fine-grained. Again there is no polished section for this sample.			
		smectite/ chlorite	M	mixed dark brown smectite and chlorite with smectite dominant over chlorite; chlorite and dark brown smectite grade into orange-brown illite adjacent to veins.											
		opaques	?	impossible to distinguish from smectite without a polished section ∴ exact proportion of ore minerals is unknown but some were observed.											

Sample (depth in m)	Rock Type, Texture and Core Unit	Matrix		Mineralogy	Vesicles		Veins		Ore	Minerals		
		Mineral	Proportion of Matrix	Description	(%) of sample	Diameter (mm)	Description	% of sample	Width (mm)	Description	% of ore minerals	Description
159.37	Highly altered and mineralized basalt is cut by large quartz-pyrite-minor sphalerite vein. Relict hyalophitic texture is present in a small patch of the section. Unit VIIIa: massive lava.	illite	S	orange-brown illite with low birefringence is dominant adjacent to veins.				60	20	anastomosing vein inter-fingers with glass; contains quartz, pyrite and traces of yellow sphalerite	90	pyrite is primarily euhedral with minor subhedral to anhedral pyrite. Sphalerite inclusions similar to those in CY-2A 193.00m occur in some pyrite.
		chlorite	M	tan, orange-brown chlorite is dominant away from veins								
		plagioclase	E	microlites are highly altered to chlorite								
		ore minerals	E	fine-grained, disseminated. Greater concentrations adjacent to veins					0.6-20	2 quartz-pyrite veins. 70% fine to medium-grained quartz and 30% very fine to fine-grained pyrite in veins	10	honey-yellow sphalerite in large vein is very fine to fine-grained and subhedral to euhedral
161.19	Partly altered and mineralized glassy basalt. Hyalophitic texture. Unit VIIIa: massive glass	chlorite	M	pale-green, very fine-grained flakes	8	ave. = 4 mm	vesicles partly filled with quartz plus minor sphalerite ± pyrite in core. Quartz is fine to medium-grained.	<1	0.1-0.5	anastomosing vein is filled with quartz plus yellow sphalerite and minor pyrite. Bleached zone adjacent to vein is only visible at hand sample scale and is variable in width (~3.5m) and is characterized by alternating white and grey bands parallel to the vein.	45	sphalerite has 2 modal sizes: 1) coarse-grained and subhedral occurring in cores of vesicles 2) majority of sphalerite is fine-grained, anhedral and occurs in vein
		quartz	S	isolated, fine-grained, anhedral								
		plagioclase	S	subhedral to anhedral plagioclase laths are partly replaced by chlorite.								
		smectite	S	cloudy, light-brown smectite occurs adjacent to veins and vesicles and in a vein-like strip in the matrix, illite dominates over smectite		ave. = 1	Smaller vesicles usually have a quartz lining followed by a peripheral ring of chlorite and an inner core of quartz. One of the smaller vesicles has two generations of quartz.					
		illite	m									
		sphene	m	very fine-grained aggregates of cryptocrystalline, equant grains.								
		ore minerals	m	fine-grained, anhedral to subhedral disseminated ore minerals.								
											55	pyrite is fine to medium-grained and primarily subhedral occurring in vein and vesicle cores as well as in matrix
											E	chalcopyrite occurs as minute inclusions in a sphalerite grain.

Sample (depth in m)	Rock Type, Texture and Core Unit	Matrix		Mineralogy Description	Vesicles		Veins		Ore Minerals			
		Mineral	Proportion of Matrix		(%) of sample	Diameter (mm)	Description	% of sample	Width (mm)	Description	% of ore minerals	Description
173.66	Pervasively altered and partly mineralized basalt Relict hyalophitic texture Unit VIII b: massive lava	chlorite	M	very fine-grained, web-like patches of chlorite are mixed with smectite	20	0.1-3mm	irregularly shaped and sized vesicles and cavities are filled with quartz. 15% of the vesicles have up to 25% chlorite in addition to quartz.	<1	<0.2	mineralized fractures are filled with chalcopyrite	60	pyrite ranges from anhedral to euhedral but most is sub- hedral; grain size from very fine to coarse-grained but most is medium-grained. Occurs disseminated in matrix. Mostly secondary pyrite.
		quartz	S	fine-grained, anhedral, isolated grains.								
		plagioclase	none	completely altered to quartz, chlorite and primarily illite								
		smectite	S	dark brown cloudy smectite is ubiquitous in sample								
		illite	S	very fine-grained flaky aggregates replacing plagioclase and mixed with smectite								
		anatase(?)	m	reddish-brown, very fine-grained, anhedral								
		ore minerals	m	fine-grained and disseminated								
183.50	Pervasively altered and mineralized basaltic glass. No relict igneous texture is recog- nizable in most of the sample, however relict intersertal texture is recognizable in a small patch of basalt (~8% of section) Unit VIII b: massive glass	quartz	m	generally fine-grained, anhedral grains	<1	4x1	elliptical, quartz- filled vesicle occurs within patch of basalt displaying relict intersertal texture; Quartz is medium- grained.	35	≤1mm	clumps of pyrite occur in anas- tomosing trails having the appearance of a vein but no definite vein boundaries or continuous mineralization.	100	dominantly secondary pyrite with trace, fractured, anhedral, primary pyrite. 2 Modal sizes 1) very fine- to fine- grained subhedral to euhedral pyrite in vesiculated areas and as disseminations 2) fine to medium- grained subhedral to euhedral pyrite in 'veins'.
		sphene	S	brown, cryptocrystalline, rounded grains are concentrated in irregular trails and patches.								
		chlorite	t	occurs as very fine-grained, web-like patches in less altered rock.								
		illite	M	very fine-grained and flaky; concentrated adjacent to sulphides in veins								
		plagioclase ore minerals	none M	completely altered to illite fine to medium-grained and concentrated in vesiculated areas near veins								

Sample (depth in m)	Rock Type, Texture and Core Unit	Matix		Mineralogy	Vesicles		Veins		Ore	Minerals		
		Mineral	Proportion of Matrix	Description	(%) of sample	Diameter (mm)	Description	% of sample	Width (mm)	Description	% of ore minerals	Description
193.00	Vuggy pyrite-quartz-minor chlorite vein. Unit VIII b: massive ore				15		cavities are highly irregular in size and shape and are subangular.	100	?	quartz is sub-to anhedral and fine-grained. 80% of pyrite is aggregated into variably sized clumps while 20% of pyrite occurs as single grains within quartz. Ratio of quartz: pyrite: chlorite is 45:45:10. Trace amounts of medium to coarse-grained gypsum laths are present.	99	pyrite is medium to coarse-grained and subhedral to anhedral. Most grains have polygonal boundaries due to crowded conditions of growth. A circular aggregate of sphalerite inclusions occurs in the cores of most pyrite grains
207.00	Pervasively altered and highly mineralized basalt. Relict hyalophitic texture is virtually obliterated. Unit VIII b: massive lava.	quartz plagioclase illite smectite chlorite sphene ore minerals	M none S m M S S	fine, anhedral, scattered grains completely altered to cryptocrystalline illite occurs throughout the section but dominates over smectite in alteration zone adjacent to vein minor smectite in altered margin of oldest vein but more abundant in the rest of the section very fine-grained, colourless, irregularly-shaped grains, low B.F. cryptocrystalline, equant grains are more common away from vein. fine-grained and disseminated.	6 30	0.6-6 ave.=1 ~0.5	spherical to elliptical vesicles are partly to completely filled with quartz and trace calcite. irregularly shaped cavities 75% of which are filled with quartz.	5	0.4 and 0.5	2 subparallel veins are present older quartz-pyrite vein (40% quartz, 60% pyrite) Most of the pyrite is concentrated along the vein margins. Altered margin bordering vein is ~3.5 mm wide Z younger fracture is partly filled with pyrite	100	pyrite is primarily secondary, subhedral to euhedral, very-fine to fine-grained cubes; occurs in veins, vesiculated areas of matrix and disseminated in the matrix. Trace primary, anhedral pyrite is altering to chlorite and smectite(?).

Sample (depth in m)	Rock Type, Texture and Core Unit	Matrix		Mineralogy Description	Vesicles		Veins			Ore Minerals				
		Mineral	Proportion of Matrix		(%) of sample	Diameter (mm)	Description	% of sample	Width (mm)	Description	% of ore minerals	Description		
243.05	Pervasively altered and highly mineral- ized basaltic glass No relict igneous textures apparent in 80% of matrix however a 5mm wide "strip" in the section displays relict intersertal texture. There is a gradational contact between the two textural types. Unit VIIIb: massive glass	quartz sphene illite plagioclase ore minerals	m M M none S	scattered, fine, anhedral grains of quartz are altering to illite. cryptocrystalline equant grains are concentrated adjacent to vesicles very fine-grained flakes completely altered to illite medium-grained ore minerals are concentrated in vesiculated areas of matrix.	35	1 2-7	80% of the vesicles are spherical and filled either with medium-grained quartz or fine- grained illite ± minor quartz or pyrite. Several larger, elliptical vesicles are filled with medium- grained quartz with an occasional pyrite core subangular, irregularly shaped and sized cavities.	1	1	quartz-pyrite vein visible in handsamp!	99.9 0.1	pyrite is primarily secondary with trace, primary, anhedral, fractured pyrite. Most pyrite is fine to medium-grained and subhedral to anhedral. Secondary pyrite has embayed boundaries sphalerite (?) inclusions in some pyrite as in C4-2A 193.00		
248.70	Quartz-pyrite- hematite vein. Vuggy texture Unit VIIIb: massive lava				10			100	?	pyrite and quartz are major com- ponents of the vein while hem- atite is subord- inate. Quartz is fine-grained and subhedral. The hematite associated with the quartz is fine-grained and anhedral. Trace epidote inclusions in the pyrite			75 25 t	medium to coarse- grained pyrite is anhedral due to crowded growth conditions. Most grains have embayed boundaries. Some trace, anhedral, fine-grained, fractured primary pyrite. botroidal hematite present; never in contact with pyrite since always separated by quartz. cryptocrystalline sph- alerite (?) inclusions in pyrite as in C4-2A 193.00

Sample (depth in m)	Rock Type, Texture and Core Unit	Matrix		Mineralogy	Vesicles		Veins		Ore	Minerals
		Mineral	Proportion of Matrix	Description	(%) of sample	Dia- meter mm	Description	% of sample	Width (mm)	Description

270.15 Highly altered and mineralized basaltic glass
Relict hyalophitic texture
Unit VIIIb: massive glass

quartz	M	fine-grained, anhedral, quartz
illite	S	very fine-grained flakes
sphene	S	brown, cryptocrystalline, equant grains are more concentrated in patches near vesicles
chlorite	M	very fine-grained, irregularly-shaped grains; colourless and low B.F.
epidote	t	very fine, rounded equant grains with high relief and high B.F.
plagioclase	t	highly altered to illite
ore minerals	m	fine-grained and disseminated but concentrated adjacent to veins.

10	<0.5-2	irregularly shaped vesicles are filled with medium-grained quartz and occasional cores of pyrite.
----	--------	---

5	1-3	several veins are filled with a quartz-pyrite mixture with quartz usually lining the vein while pyrite fills the core.
---	-----	--

100		pyrite is subhedral to euhedral and fine-grained (no polished section for this sample)
-----	--	--

272.70 Quartz-pyrite vein crosscuts a quartz-hematite-minor pyrite vein. The older vein comprises 92% of the section and is described under the "Matrix Mineralogy" column.
Unit VIIIb: massive lava.

mixed quartz	M (80%)	Quartz is very-fine to medium grained. Larger grains display oscillatory extinction. Hematite is generally anhedral
hematite		
pyrite	S (20%)	fine-grained and disseminated in quartz-hematite mixture.
illite	t	very fine-grained flakes surround pyrite
epidote	t	very fine-grained inclusions in pyrite
gypsum	t	fine-grained subhedral laths occur scattered within quartz
chlorite	t	aggregates of very fine-grained flakes are scattered within quartz

--	--	--

8	<0.1-0.5	hairline fractures
	1-6	anastomosing veins filled with quartz (65%), pyrite (30%), hematite (5%) and traces of calcite occur in one vein.

100		pyrite is subhedral to euhedral and fine-grained (no polished section for this sample).
-----	--	---

Sample (depth in m)	Rock Type, Texture and Core Unit	Matrix Mineralogy			Vesicles			Veins			Ore Minerals	
		Mineral	Proportion of Matrix	Description	(%) of sample	Diameter (mm)	Description	% of sample	Width (mm)	Description	% of ore minerals	Description
277.40	Pervasively altered basalt. Relict hyalophitic texture Unit VIIIb: massive lava	chlorite	S	very fine-grained, anhedral	5	0.9-4	variably shaped	<1	0.5-2	veins are only	100	90% secondary pyrite, 10% primary pyrite.
		quartz	M	fine-grained and anhedral		ave.=3	and sized ves-			visible in the		Secondary pyrite is
		plagioclase	none	completely altered to quartz and illite.			icles are filled			hand sample.		Fine-grained and
		illite	M	very fine-grained and flaky			with quartz, chlorite,			Veins are lined		subhedral to euhed-
		sphene	S	very fine-grained isolated grains or clusters; more concentrated around vesicles.			a second quartz			with quartz		ral. Primary pyrite
		epidote	t	cryptocrystalline, equant, grains with high relief and high birefringence.			phase, and pyrite			and have a		is anhedral, fine-
		ore minerals	t	very fine-grained and disseminated			in order from			core of pyrite.		grained and highly fractured.
							the margin to					
							the core. Quartz					
							is the major					
							component in the					
							vesicles while					
							the other minerals					
							are subordinate.					
282.45	Highly altered and partly mineralized olivine-phyric basalt. Porphyritic hyalo- phitic texture. Unit IXb: post- mineralization dike.	chlorite	M	very fine-grained flakes	<1	1	irregularly				50	fine-grained, subhed-
		quartz	t	fine-grained and anhedral			shaped, quartz-					to anhedral
		plagioclase	m	minor subhedral, fresh albite microlites; majority are anhedral and altered to illite and smectite			lined and				50	skeletal magnetite
		epidote	t	subhedral, fine-grained epidote is replacing a plagioclase phenocryst.			partly calcite-					fine-grained,
		illite	m	very fine-grained flakes.			filled vesicle.					highly fractured,
		actinolite(?)	t	very fine-grained, subhedral								anhedral primary
		smectite	M	olive-brown smectite is mixed w. chlorite								pyrite. Primary
		altered olivine	S	very coarse-grained (5-10 mm), subhedral to euhedral phenocrysts have been completely altered to calcite/smectite and are highly oxidized along fractures								pyrite occurs intergrown with magnetite.
		ore minerals	m	fine-grained and disseminated.								Apparently no secondary pyrite.

Sample (depth in m)	Rock Type, Texture and Core Unit	Matix		Mineralogy	Vesicles		Veins		Ore Minerals			
		Mineral	Proportion of Matix	Description	(%) of sample	Diam- eter (mm)	Description	% of sample	Width (mm)	Description	% of ore minerals	Description
285.05	Pervasively altered and mineralized basaltic glass has no relict igneous textures and is cut by a large quartz-hematite-pyrite vein which is in turn cut by a smaller pyrite vein Unit X: massive glass	chlorite/illite mixture	M	anhedral, fine-grained or subhedral flakes	10	0.5-6	irregularly sized and shaped; smaller vesicles are filled with chlorite; larger vesicles are lined with chlorite and in addition some are partly to completely filled with coarse pyrite	<1	<0.4	quartz-filled veinlet ends in a partly quartz-filled, pyrite- and hematite-lined vesicle.	95	Secondary pyrite is subhedral to euhedral, fine-grained and disseminated. About 10% of the pyrite is primary and anhedral. The pyrite in the vein is highly brecciated due to its presence in a fault zone.
		sphene	M	brown sphene thickens around vesicles, patchy distribution in matrix								
		anatase	m	reddish-brown, very fine-grained, anhedral grains								
		ore minerals	m	very fine to fine-grained; disseminated and in small aggregates				>30	?	hematite-quartz pyrite vein projects into altered basalt. Pyrite is embayed and fractured	5	sphalerite is very fine-grained and anhedral. It occurs in small aggregates in the quartz-hematite-pyrite vein
302.35	Pervasively altered basalt Relict hyalophitic texture Unit XI: altered dike	chlorite	M	anhedral, fine-grained	<1	1.1	poorly defined vesicles are filled primarily with quartz and minor illite, chlorite, and pyrite.	1	ave=0.5 max=1.5	several cross-cutting veinlets in hand sample but only one in thin section; partly filled with calcite, illite and pyrite. Approximately 40% of the vein is empty.	90	90% of the pyrite is secondary and occurs as fine to medium anhedral grains with embayed boundaries. 10% of pyrite is primary and anhedral. sphalerite occurs as inclusions in pyrite and as small, fine-grained clusters in the matrix; sphalerite is anhedral.
		quartz	M	fine to medium-grained quartz is aggregated into poorly defined clumps (0.5-1 mm in diameter)								
		plagioclase	t	almost completely altered to chlorite and illite								
		sphene	m	brown, cryptocrystalline anhedral grains								
		illite	m	fine-grained flakes in matrix and a replacement mineral of plagioclase phenocrysts								
		calcite	t	very fine-grained calcite is scattered in matrix and is a replacement mineral of plagioclase phenocrysts								
		epidote	t	cryptocrystalline, high relief, equant grains								
anabase	t	brown, very fine-grained rounded grains										
ore minerals	t	coarse end of fine-grained scale; disseminated in matrix.										

Sample (depth in m)	Rock Type, Texture and Core Unit	Matrix		Mineralogy	Vesicles		Veins		Ore Minerals					
		Mineral	Proportion of Matrix	Description	(%) of sample	Diameter (mm)	Description	% of sample	Width (mm)	Description	% of ore minerals	Description		
332.85	Highly altered and partly mineralized basalt Relict hyalophitic texture. Unit XI: altered dike	quartz	m	anhedral, fine-grained	2	0.8	This is diameter of well-defined vesicles but there are also irregularly shaped and sized cavities, all are filled with quartz, spherulitic chlorite and occasional minor pyrite.	1	~0.4	pyrite occurs in fractures with minor spherulitic brown chlorite.	100	pyrite is 60% secondary and 40% primary. One variety dominates in one part of the slide while the other type dominates elsewhere. Secondary pyrite is very-fine to fine-grained and disseminated as well as occurring in clusters. Primary pyrite is anhedral and fractured.		
		plagioclase	S	minor primary plagioclase is highly altered to illite while the more dominant euhedral microlites are secondary albite.										
		smectite	m	brown smectite associated with sphene										
		chlorite	M	very fine-grained flakes										
		sphene	S	cryptocrystalline, equant grains										
		epidote	t	cryptocrystalline, equant, high B.F. grains in illite dominated area										
		calcite	t	anhedral, fine-grained; replaces plagioclase										
		illite	m	occurs in small area where chlorite is not present.										
		ore minerals	m	fine to very-fine-grained; disseminated										
350.45	Highly altered and partly mineralized basalt Relict intersertal texture Unit XI: altered, post-mineralization dike.	chlorite	M	very-fine-grained flakes	~3	0.3-1.5 ave=0.9	vesicles are filled with mixtures of chlorite, calcite and quartz with proportions varying from one vesicle to the next.	2	0.4-1.0	3 anastomosing veins observed in handsample with poorly defined borders; filled with calcite and chlorite. One veinlet had a pink oxidized zone at its margins. The other two veins contained pyrite in addition to calcite and chlorite.	60	fine-grained, sub-hedral to anhedral skeletal magnetite is disseminated in matrix 40 fine to medium-grained, subhedral to euhedral secondary pyrite occurs in and adjacent to veins Trace, primary, anhedral, fractured pyrite.		
		quartz	m	fine-grained, anhedral quartz is altering to chlorite.										
		plagioclase	t	fine-grained microlites are highly altered to chlorite + smectite										
		smectite	M	abundant brown smectite thins adjacent to a vein which is seen only in the handsample (bleached margin)										
		sphene	m	cryptocrystalline equant grains; difficult to distinguish from smectite.										
		calcite	m	fine, anhedral grains										
		epidote	t	very fine-grained, euhedral crystals are cross-sections of elongate, green epidote crystals										
		ore minerals	m	fine-grained and disseminated.										

Sample (depth in m)	Rock Type, Texture and Core Unit	Matix		Mineralogy	Vesicles		Veins		Ore	Minerals				
		Mineral	Proportion of Matrix	Description	(%) of sample	Diameter (mm)	Description	% of sample	Width (mm)	Description	% of ore minerals	Description		
404.40	Pervasively altered hyaloclastite breccia Highly fractured texture Unit XIV: glass	quartz	m	fine-grained, anhedral microlites are relatively fresh, secondary albite. brown chlorite has replaced glass; thickens around vesicles. Anomalous brown birefringence and radiating structure of fibers. fine-grained; concentrated in vesiculated areas of matrix	25	0.5	from spherical to elliptical in shape; filled with 70% quartz and 30% chlorite as well as trace pyrite. Minor chlorite in the core occurs after quartz, which formed after the chlorite lining.	15	<0.4	fractures are filled with the same minerals which are in the vesicles. Chlorite, rather than quartz dominates in the fractures	98	very fine to fine- grained, subhedral to euhedral pyrite occurs in fractures and vesiculated areas of matrix. Also some pyrite in vesicles.		
		plagioclase	m										2	very fine-grained anhedral sphalerite with pyrite in fractures
		chlorite	M (80%)										E	anhedral chalcopyrite is intergrown with pyrite.
		ore minerals	m										60	sphalerite occurs primarily as crypto- crystalline, subhedral to anhedral disseminations in the matrix; Honey-yellow colour. Minor fine-grained sphalerite occurs in vesicle and is being overgrown by pyrite. One apparently Fe-rich grain pyrite occurs mostly as very-fine to fine-grained, subhedral to euhedral grains in veins and vesicles. Minor cryptocrystalline disseminations in matrix
406.85	Highly altered, partly mineralized basaltic glass. Highly fractured and relict hyalo- phitic texture Unit XIV: pillowed lava	chlorite	M	very fine-grained, subhedral fibres.	<1	0.5-4	variably sized vesicles are lined with quartz and filled with pyrite. Proportion of pyrite to quartz is variable	5	<5-7	fractures and veins are filled with a quartz- chlorite- smectite-pyrite mixture. Quartz is the dominant mineral (50%). Very small fractures are partly filled with pyrite.	40			
		quartz	m	fine-grained, anhedral, isolated grains										
		plagioclase	E	microlites are almost completely altered to chlorite and sphene										
		sphene	M	cryptocrystalline equant grains are ubiquitous in matrix but less concentrated adjacent to veins producing "bleached" effect.										
		epidote	m	scattered, anhedral, very- fine grains										
ore minerals	m	fine-grained ore minerals occur in vesiculated areas adjacent to veins only.												